

PARAMETERS INFLUENCING ASSEMBLY OF YEAST CELLS ON SURFACES
FROM A DRYING DROPLET

by
Ertuğ Avcı

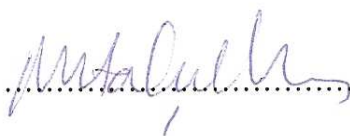
Submitted to the Institute of Graduate Studies in
Science and Engineering in partial fulfillment of
the requirements for the degree of
Master of Science
in
Biotechnology

Yeditepe University
2010

PARAMETERS INFLUENCING ASSEMBLY OF YEAST CELLS ON SURFACES
FROM A DRYING DROPLET

APPROVED BY:

Assoc. Prof. Mustafa Çulha
(Thesis Supervisor)

.....

Assist. Prof. Andrew Harvey

.....

Assist. Prof. Seyda Bucak

.....

DATE OF APPROVAL: 22.07.2010

ACKNOWLEDGEMENTS

I am heartily thankful to my supervisor, Assoc. Prof. Mustafa ulha, whose encouragement, supervision and support from the preliminary to the concluding level enabled me to develop an understanding of the subject. It was him who gave me the valuable opportunity to join his lab and paved my way to become a scientist. Special thanks go to Mehmet Kahraman for his teaching me many things about nanobiotechnology.

I am also extremely happy to meet the people in Nanobiotechnology Group. In particular, I would like to thank İsmail Sayın, Kemal Oğuz Keserođlu, and İlknur Sur for their friendship and never ending encouragement during these two years.

My deepest gratitude goes to my family for their unflagging love and support throughout my life; this thesis is simply impossible without them. Finally, I want to express my gratitude to Yeditepe University for the financial support during my master education.

ABSTRACT

PARAMETERS INFLUENCING ASSEMBLY OF YEAST CELLS ON SURFACES FROM A DRYING DROPLET

Deposition of cells on surfaces in a controllable and patterned way is of critical importance for biotechnological and biomedical applications. There are several approaches used for patterning and assembling cells uniformly on surfaces, and among them, droplet templating stands out with its simplicity and no requirement for complex instrumentation.

In this study, a uniform assembly of yeast cells on hydrophilic and hydrophobic surfaces from a drying droplet is investigated using *Saccharomyces cerevisiae* as model organism. The experimental parameters such as pH of the suspension, droplet size, and number of yeast cells are explored for preparation of uniform cellular assemblies for possible biomedical and biotechnological applications. As compared to the previously reported approaches such as ‘convective assembly’, it is found that the drop casting can be as effective as previously reported techniques.

ÖZET

MAYA HÜCRELERİNİN KURUYAN BİR DAMLACIKTAN YÜZEYLERDE DİZİLİMİNİ ETKİLEYEN PARAMETRELER

Hücrelerin yüzeylerde kontrollü ve örüntülü olarak dizilimi biyoteknolojik ve biyomedikal uygulamalar açısından kritik öneme sahiptir. Hücrelerin yüzeylerde dizilimi ve örüntülenmesi için çeşitli yaklaşımlar vardır ve bunların arasında damlacık yoluyla örüntüleme, basitliği ve kompleks aletler gerektirmemesiyle öne çıkmaktadır.

Bu çalışmada, *Saccharomyces cerevisiae* hücrelerinin model organizma olarak kullanılmasıyla, maya hücrelerinin kuruyan bir damlacıktan hidrofilik ve hidrofobik yüzeylerde düzenli bir şekilde dizilimi incelenmiştir. Süspansiyonun pH değeri, damlacık büyüklüğü ve maya hücrelerinin sayısı gibi deneysel parametreler bu düzenli dizilimlerin muhtemel biyomedikal ve biyoteknolojik uygulamalarda kullanımları için araştırılmıştır. ‘Konvektif dizilim’ gibi önceden bildirilmiş tekniklerle karşılaştırıldığında damlacık yoluyla dizilim ve örüntülemenin en az onlar kadar etkili ve işe yarar olduğu bulunmuştur.

TABLE OF CONTENTS

ACKNOWLEDGEMENTS	iii
ABSTRACT	iv
ÖZET	v
TABLE OF CONTENTS	vi
LIST OF FIGURES.....	viii
LIST OF SYMBOLS / ABBREVIATIONS	xiv
1. INTRODUCTION.....	1
1.1. TECHNIQUES USED FOR CELL DEPOSITON AND PATTERNING	1
1.1.1. Dielectrophoresis.....	1
1.1.2. Micropatterning.....	4
1.1.2.1. Photolithography	5
1.1.2.2. Soft lithography.....	6
1.1.3. Convective Assembly.....	8
1.1.4. Droplet Templating	9
2. MATERIALS and METHODS.....	13
2.1. PREPARATION OF HYDROPHILIC AND HYDROPHOBIC SURFACES	13
2.2. PREPARATION OF YEAST CELL SUSPENSIONS.....	14
2.3. DEPOSITION OF CELL COATINGS.....	15
2.3.1. Droplet Templating	15
2.3.2. Convective Asembly	15
2.4. COATING CHARACTERIZATION	17
3. RESULTS and DISCUSSION	18
3.1. pH EFFECT	19
3.2. EFFECTS of SURFACE HYDROPHOBICITY and HYDROPHILICITY on the BEHAVIOUR of CELL COATING	35
3.2.1. Effects of Surface Hydrophobicity.....	36
3.2.2. Effects of Surface Hydrophilicity	43
3.3. CONVECTIVE ASSEMBLY.....	60
4. CONCLUSION and RECOMMENDATIONS.....	62
4.1. CONCLUSION.....	62

4.2. RECOMMENDATIONS 63
REFERENCES..... 64

LIST OF FIGURES

Figure 1.1.	Schematic illustrating dielectrophoresis (DEP) resulted from electroic force	1
Figure 1.2.	Photograph of dielectrophoretically formed microbial assembly in the form of adjacent layers. The layers are A: <i>S. cerevisiae</i> ; B: <i>M. luteus</i> ; C: <i>E. coli</i>	2
Figure 1.3.	Optical micrographs of chains assembled from live cells using ac electric fields (a) Yeast (<i>S. cerevisiae</i>) cell chains under 15Vmm^{-1} and a 50 Hz electric field. (Inset) The viability of the cells is preserved in the electric field after 2 h as indicated by the compartmentalized appearance of the cell interior. (b) NIH/3T3 mouse fibroblast cells under 10V mm^{-1} and a 10 kHz electric field. (Inset) The blue color indicates a dead cell. Most cells remain viable during the assembly process for up to 1h	3
Figure 1.4.	Micropatterning using photoresist lithography	6
Figure 1.5.	Schematic procedure for patterning using soft lithography related techniques. (A) Microcontact printing, (B) Microfluidic patterning, and (C) Stencil patterning.....	7
Figure 1.6.	Schematic of the drying region of a thin wetting film being dragged at a rate, v_w , on a substrate	8

Figure 1.7.	(A) When the contact line is not pinned, droplet interface moves from the solid line to the dashed line, and the contact line moves from A to B (a). However, if the contact line is pinned, then the motion from A to B is prevented by an outflow to replenish the liquid removed from the edge (b). (B) Bright-field image of evaporation pattern from droplet of <i>Saccharomyces cerevisiae</i>	10
Figure 1.8.	The three convective mechanisms in a drying droplet	11
Figure 2.1.	The images of peeled PDMS (A), PDMS peeled glass slide (B), scalpel blade (C)	14
Figure 2.2.	Active dried yeast in granulated form	14
Figure 2.3.	Convective assembly setup.....	16
Figure 2.4.	Schematic of the convective assembly process. The top slide remains in place while the bottom slide is moved to the left	16
Figure 3.1.	Photographs of water droplets on a slide prepared by PDMS cast and peel (A) and on a regular glass slide (B)	18
Figure 3.2.	AFM images of regular glass slide (A) and glass slide prepared by PDMS cast and peel (B)	19
Figure 3.3	General components of yeast cell walls	20
Figure 3.4.	Patterns obtained from evaporative deposition of 4 μ l of stock suspensions at five different pH values. The scale bars correspond to 500 μ m	22

Figure 3.5.	Patterns obtained from evaporative deposition of 4 μl of 1:2 diluted suspensions at five different pH values. The scale bars correspond to 500 μm	23
Figure 3.6.	Patterns obtained from evaporative deposition of 4 μl of 1:4 diluted suspensions at five different pH values. The scale bars correspond to 500 μm	24
Figure 3.7.	Patterns obtained from evaporative deposition of 4 μl of 1:8 diluted suspensions at five different pH values. The scale bars correspond to 500 μm	25
Figure 3.8.	Patterns obtained from evaporative deposition of 4 μl of 1:16 diluted suspensions at five different pH values. The scale bars correspond to 500 μm	26
Figure 3.9.	Patterns obtained from evaporative deposition of 4 μl of 1:32 diluted suspensions at five different pH values. The scale bars correspond to 500 μm	27
Figure 3.10.	Patterns obtained from evaporative deposition of 4 μl of 1:64 diluted suspensions at five different pH values. The scale bars correspond to 500 μm	28
Figure 3.11.	Patterns obtained from evaporative deposition of 4 μl of 1:128 diluted suspensions at five different pH values. The scale bars correspond to 500 μm	29
Figure 3.12.	Patterns obtained from evaporative deposition of 4 μl of 1:256 diluted suspensions at five different pH values. The scale bars correspond to 500 μm	30
Figure 3.13.	Two modes of drying.....	31

Figure 3.14. SEM image of a part of the deposition pattern obtained with 32 times diluted form of the stock solution at pH 2.....	33
Figure 3.15. SEM image of a part of the deposition pattern obtained with 64 times diluted form of the stock solution at pH 2.....	34
Figure 3.16. SEM image of a part of the deposition pattern obtained with 128 times diluted form of the stock solution at pH 2.....	35
Figure 3.17. Deposition patterns obtained from evaporation of 200 μl of suspensions. The scale bars correspond to 2 mm.....	37
Figure 3.18. Deposition patterns obtained from evaporation of 100 μl of suspensions. The scale bars correspond to 2 mm.....	38
Figure 3.19. Deposition patterns obtained from evaporation of 50 μl of suspensions. The scale bars correspond to 1 mm.....	39
Figure 3.20. Deposition patterns obtained from evaporation of 10 μl of suspensions. The scale bars correspond to 500 μm	40
Figure 3.21. Deposition patterns obtained from evaporation of 5 μl of suspensions. The scale bars correspond to 500 μm	41
Figure 3.22. Deposition patterns obtained from evaporation of 1 μl of suspensions. The scale bars correspond to 500 μm	42
Figure 3.23. Patterns obtained from evaporative deposition of 5 μl of stock suspensions at five different pH values. The scale bars correspond to 1 mm.....	44

Figure 3.24. Patterns obtained from evaporative deposition of 5 μ l of 1:2 diluted suspensions at five different pH values. The scale bars correspond to 1 mm.....	45
Figure 3.25. Patterns obtained from evaporative deposition of 5 μ l of 1:4 diluted suspensions at five different pH values. The scale bars correspond to 1 mm.....	46
Figure 3.26. Patterns obtained from evaporative deposition of 5 μ l of 1:8 diluted suspensions at five different pH values. The scale bars correspond to 1 mm.....	47
Figure 3.27. Patterns obtained from evaporative deposition of 5 μ l of 1:16 diluted suspensions at five different pH values. The scale bars correspond to 1 mm.....	48
Figure 3.28. Patterns obtained from evaporative deposition of 5 μ l of 1:32 diluted suspensions at five different pH values. The scale bars correspond to 1 mm.....	49
Figure 3.29. Patterns obtained from evaporative deposition of 5 μ l of 1:64 diluted suspensions at five different pH values. The scale bars correspond to 1 mm.....	50
Figure 3.30. Patterns obtained from evaporative deposition of 5 μ l of 1:128 diluted suspensions at five different pH values. The scale bars correspond to 1 mm.....	51
Figure 3.31. Patterns obtained from evaporative deposition of 50 μ l of stock suspensions at five different pH values. The scale bars correspond to 2 mm	52

Figure 3.32. Patterns obtained from evaporative deposition of 50 μl of 1:2 diluted suspensions at five different pH values. The scale bars correspond to 2 mm.....	53
Figure 3.33. Patterns obtained from evaporative deposition of 50 μl of 1:4 diluted suspensions at five different pH values. The scale bars correspond to 2 mm.....	54
Figure 3.34. Patterns obtained from evaporative deposition of 50 μl of 1:8 diluted suspensions at five different pH values. The scale bars correspond to 2 mm.....	55
Figure 3.35. Patterns obtained from evaporative deposition of 50 μl of 1:16 diluted suspensions at five different pH values. The scale bars correspond to 2 mm.....	56
Figure 3.36. Patterns obtained from evaporative deposition of 50 μl of 1:32 diluted suspensions at five different pH values. The scale bars correspond to 2 mm.....	57
Figure 3.37. Patterns obtained from evaporative deposition of 50 μl of 1:64 diluted suspensions at five different pH values. The scale bars correspond to 2 mm.....	58
Figure 3.38. Patterns obtained from evaporative deposition of 50 μl of 1:128 diluted suspensions at five different pH values. The scale bars correspond to 2 mm.....	59
Figure 3.39. Coatings of the yeast cells by convective assembly at pH 2, 4, 6, 8, and 10.....	61

LIST OF SYMBOLS / ABBREVIATIONS

E	Electric field intensity
∇E_{rms}	Gradient of the electric field intensity
F_{DEP}	Dielectrophoretic force
h	Height of the deposited colloidal crystal
j_e	Evaporation rate
K	Effective polarizability of the particle in the medium
R	Particle radius
v_c	Crystal growth rate
ε	Porosity of the deposited colloidal crystal
ε_m	Dielectric permittivity of the medium
ε_p	Dielectric permittivity of the particle
σ_m	Conductivity of the medium
σ_p	Conductivity of the particles
τ_{MW}	Maxwell-Wagner charge-relaxation time
Φ	Volume fraction of the particles in suspension
ω	Frequency of AC field
AFM	Atomic force microscopy
DEP	Dielectrophoresis
LbL	Layer-by-layer
PEG	Poly(ethylene glycol)
PDMS	Poly(dimethylsiloxane)
SEM	Scanning electron microscopy
SERS	Surface-enhanced Raman scattering

1. INTRODUCTION

Deposition and ordering of cells on surfaces is of importance for numerous technological applications and has captured the interest of scientists for decades. Having a proper understanding and knowledge about cell-cell, cell-biomaterial, and cell-surface interactions is very crucial and a prerequisite for their use in molecular, biomedical, and biotechnological approaches, and to achieve these, a wide variety of deposition and patterning techniques have been developed. In the following parts, some of these techniques are presented.

1.1. TECHNIQUES USED FOR CELL DEPOSITION and PATTERNING

Up to now, a large number of cell deposition techniques have been developed and most of these techniques involve creation of various micropatterned surfaces and dielectrophoresis between microelectrodes. Although droplet templating and convective assembly methods have been used for a variety of applications, the reports about their use as cell deposition techniques are very few. In the following subsections, these four mentioned techniques are briefly outlined.

1.1.1. Dielectrophoresis

Cells in suspensions can be manipulated in electric fields using dielectrophoresis (DEP) [1-7]. DEP is defined as the mobility of dielectric particles in a medium imparted by nonuniform electric fields as seen on Figure 1.1 [9, 10]. The use of alternating current (ac) electric fields in DEP allows controlled organization of particles without causing water electrolysis and electroosmotic effects. When an ac field with frequency of ω is applied across a colloidal suspension, it leads to the polarization of particles. The dipoles induced in the particles interact with the applied electric field, giving rise to DEP. The magnitude of the dielectrophoretic force is proportional to the gradient of the electric field intensity squared (∇E_{rms}^2) and is expressed by the following equation:

$$F_{DEP} = 2\pi\epsilon_m R^3 \operatorname{Re}|K(\omega)| |\nabla E_{rms}|^2 \quad (1.1)$$

where ϵ_m is the dielectric permittivity of the medium, R is the particle radius, E is the electric field intensity, and K is the Clausius-Mossotti function, the effective polarizability of the particle in the medium. The real part of K is given by:

$$\operatorname{Re}|K(\omega)| = \frac{\epsilon_m - \epsilon_p}{\epsilon_m + 2\epsilon_p} + \frac{3(\epsilon_p \sigma_m - \epsilon_m \sigma_p)}{\tau_{MW} (\sigma_m + 2\sigma_p)^2 (1 + \omega^2 \tau_{MW}^2)} \quad (1.2)$$

where ϵ_p is the dielectric permittivity of the particle and $\sigma_{m,p}$ represents the conductivities of the medium and particles, respectively. The $\operatorname{Re}|K(\omega)|$ function changes sign at a crossover frequency of $\omega_c = \tau_{MW}^{-1}$, where $\tau_{MW} = (\epsilon_m + \epsilon_p) / (\sigma_m + 2\sigma_p)$ is the Maxwell-Wagner charge-relaxation time. When $\operatorname{Re}|K(\omega)| > 1$, the particles are attracted to the region of maximum field intensity and the phenomenon is known as positive DEP. Particles with lower polarizability than the medium are repelled from the high-field-intensity areas by negative DEP.

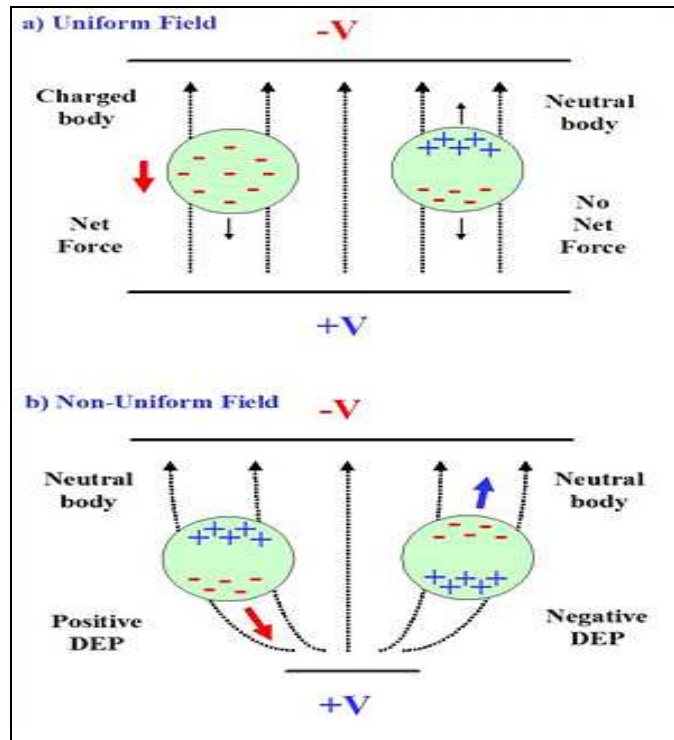


Figure 1.1. Schematic illustrating dielectrophoresis (DEP) resulted from electric force [8]

Microbial cells' electrical properties are frequency dependent. At low frequencies (<10 kHz), the surface charge is the main determinant of the electrical properties of the cell. Around 50 kHz, the cell wall conductivity is the main determinant, while at higher frequencies (around 1 MHz) the electrical properties are a complex function of the cell wall, cell membrane and cell interior properties. At very high frequencies, the low permittivity of the cell's constituent organic materials compared to the high medium permittivity is the main determinant of the dielectrophoretic force. Because the dielectrophoretic force is dependent on the electrical properties of the medium surrounding the cells, the dielectrophoretic force is highly dependent on the medium conductivity. Unless the medium conductivity becomes much larger than the cell wall conductivity, the medium conductivity does not affect the electrical properties of the cells themselves [11, 12]. At moderate pH values, the pH of the medium is unlikely to affect the dielectrophoretic force. In microbiology, the phenomenon of DEP has been exploited for the measurement of the dielectric properties of microbial cells [13-16], the separation of mixtures of microbes into the component species [13, 17] on the basis of differences in their cell wall conductivities, as well as the separation of cells according to their viability [14]. Pohl has described [10] the use of a combination of DEP and electro-orientation to produce tissue-like materials from bacteria containing oriented cells. However, he only used a single species in his experiment. In another work, Alp *et al.* described the use of DEP to attract different microbial species sequentially onto the surface of micro-electrodes to form layered aggregates of microbial cells which mimic the types of microstructures observed in naturally occurring microbial assemblies as shown on Figure 1.2 [2].

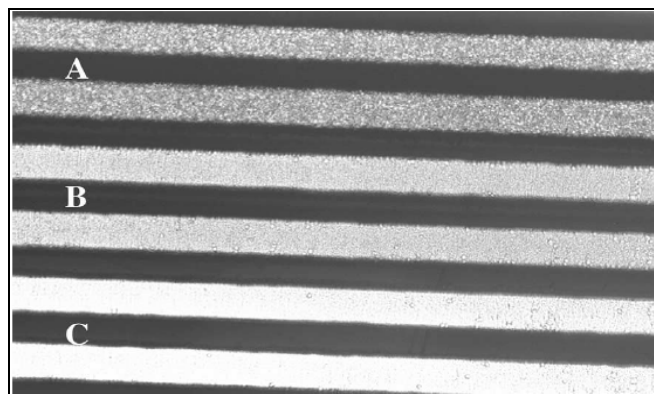


Figure 1.2. Photograph of dielectrophoretically formed microbial assembly in the form of adjacent layers. The layers are A: *S. cerevisiae*; B: *M. luteus*; C: *E. coli* [2]

Furthermore, during DEP process, the dipoles induced in the particles by the ac field also exert attractive forces between particles and cause them to align into chains. By the help of this phenomenon, in a recent work, Gupta *et al.* coassembled live cells and functionalized colloidal particles to yield 1D chains and 2D arrays on a chip as shown on Figure 1.3 [18].

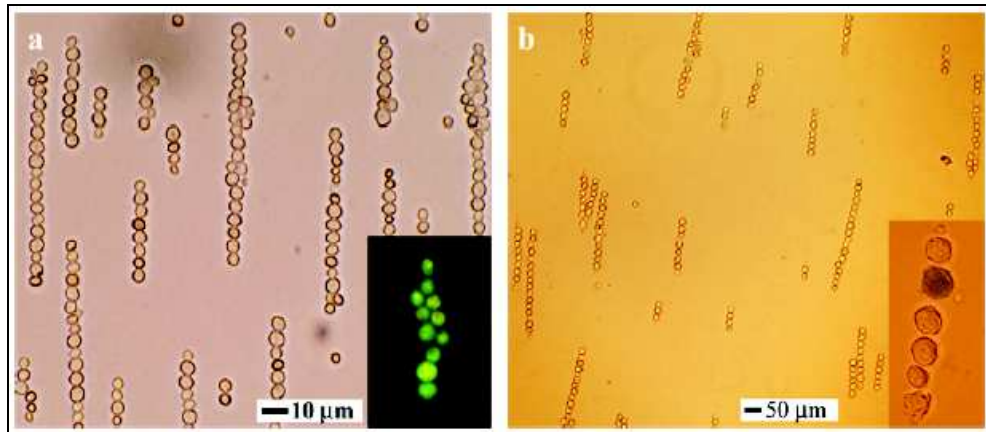


Figure 1.3. Optical micrographs of chains assembled from live cells using ac electric fields (a) Yeast (*S. cerevisiae*) cell chains under 15Vmm^{-1} and a 50 Hz electric field. (Inset) The viability of the cells is preserved in the electric field after 2 h as indicated by the compartmentalized appearance of the cell interior. (b) NIH/3T3 mouse fibroblast cells under 10V mm^{-1} and a 10 kHz electric field. (Inset) The blue color indicates a dead cell.

Most cells remain viable during the assembly process for up to 1 h [18]

1.1.2. Micropatterning

In recent years, micropatterning of cells and related biomaterials has become very popular due to its importance in the development of biosensors [10-23], tissue engineering [24] and cellular studies [25, 26]. Biosensors based on living cells can be used for environmental and chemical monitoring; accurate positioning of the cells used for sensing on these devices is critical for monitoring the status of the cells. Control over the positioning of cells is also important for cell-based screening, in which individual cells need to be accessed repeatedly to perturb them and to monitor their response. Tissue engineering may require that cells be placed in specific locations to create organized structures. Patterning techniques that control both the size and shape of the cell anchored to

a surface, and the chemistry and topology of the substrate to which the cell is attached, are also extremely crucial in understanding the influence of the cell-material interface on the behavior of cells [27, 28]. In this section, the techniques developed for cell micropatterning are briefly outlined.

1.1.2.1 Photolithography

Photolithography which is used in the semiconductor industry for metal patterning in electronic microcircuits has been applied to biomaterial and cell micropatterning. Photolithography is the process of transferring geometric shapes on a mask to the surface of a wafer or substrate. In this technique, micropatterns are generated using light, photoresist (light sensitive organic polymer) and mask as shown in Figure 1.4. A layer of photoresist is applied to the surface of the substrate and is selectively exposed to ultraviolet light through a mask containing the pattern. For positive photoresist, the exposed polymer becomes more soluble in a developer solution than the unexposed polymer, whereas for a negative photoresist, the exposed polymer becomes insoluble in the developer solution. The resulting photoresist pattern can then act as a mask for patterning the material of interest. A number of groups had used photoresist lithography to control protein attachment [29-30] and cell growth [31-32]. Researchers have made use of photolithography to generate many different chemical micropatterns to assist them in their patterning of biomolecules and cells. For instance, a layer-by-layer (LbL) technique was combined with photolithography for the construction of bioactive nanocomposite film [33]; a high density array of polyethylene glycol (PEG) hydrogel microwells was fabricated to control mammalian cell–surface interactions [34], and a simple and rapid method to create patterned surfaces using photocrosslinkable chitosan was developed onto which cardiac fibroblasts, cardiomyocytes and osteoblasts formed arrays and remained stable for up to 18 days [35].

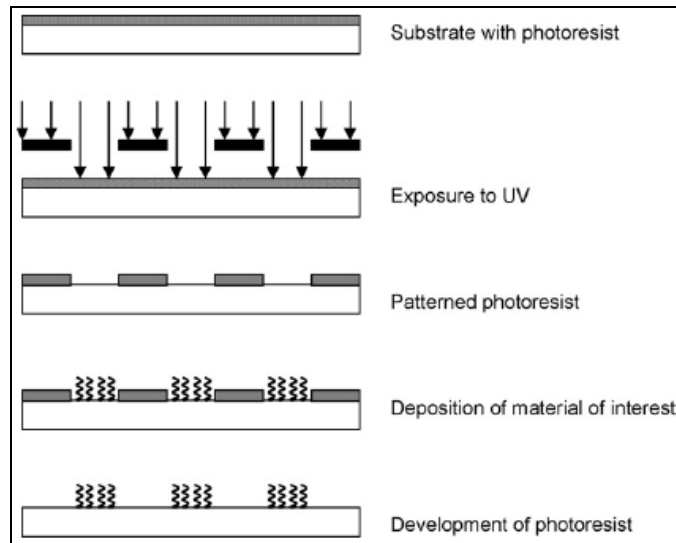


Figure 1.4. Micropatterning using photoresist lithography [36]

1.1.2.2. *Soft lithography*

Soft lithography is generally used to create patterns and structures on surfaces for controlling cell–substrate interactions [37, 38]. It does not include one specific method but rather a group of techniques with the common feature that at some stage of the process an elastomeric soft material ‘stamp’ is used to create the patterns and structures. The stamp is prepared by casting the liquid prepolymer of poly(dimethylsiloxane) (PDMS) against a master that has patterned structure as shown on Figure 1.5. Microcontact printing [39], microfluidic patterning [40] and stencil patterning [41] are the common soft lithography related techniques that are used for deposition and micropatterning of biomaterials and cells.

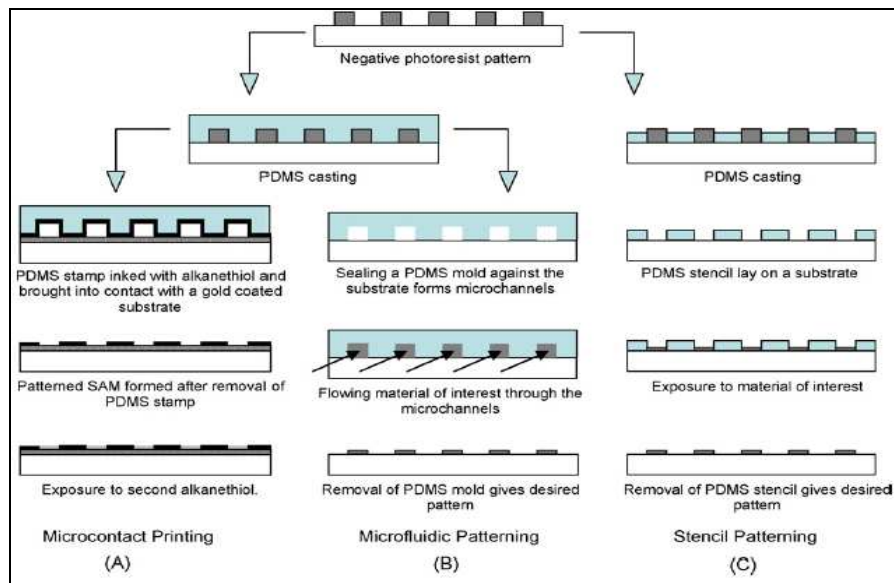


Figure 1.5. Schematic procedure for patterning using soft lithography related techniques. (A) Microcontact printing, (B) Microfluidic patterning, and (C) Stencil patterning [36]

Among the soft lithographic techniques, microcontact printing is the most widely used. The popularity of the technique originates from its simplicity, cost-effectiveness and flexibility, regarding both the choice of substrate and the material to be transferred during imprinting. Patterning cells on surfaces [42, 43] and influence of patterning on cell physiology [26, 44] has been studied by several groups. The most popular method to achieve controlled cell growth is to pattern specific cell adhesion molecules such as the RGD peptide [45] onto surfaces, which can also be used in association with patterns of protein-repellent PEG molecules [46]. Applications in patterned neural growth [47, 48] open up possibilities for viable neuronal networks. In a recent study, Krol *et al.* reported deposition of polyelectrolyte coated yeast cells onto defined areas formed by microcontact printing of polyelectrolytes which may help to find new ways to develop biosensors based on the use of whole living cells [49].

1.1.3. Convective Assembly

In 1992, Denkov and his colleagues proposed a mechanism for the self-assembly of colloidal particle suspensions in thin films and named it as ‘convective assembly’ [50]. They stated that the main factors governing the ordering were the attractive capillary forces due to the menisci form around the particles and the convective transport of the particles toward the ordered region. Dimitrov and Nagayama proposed an equation balancing the volumetric fluxes of the solvent and the accumulation of the particles in the drying region [51]

$$v_c = \frac{\beta j_e l \phi}{h(1-\varepsilon)(1-\phi)} \quad (1.3)$$

where β is an interaction parameter that relates the mean solvent velocity to the mean particle speed before entering the drying region, ε and h are the porosity and height of the deposited colloidal crystal, ϕ is the volume fraction of the particles in suspension, j_e is the rate of evaporation, and v_c is the crystal growth rate. Figure 1.6 represents the self-assembly of the particles by convective assembly.

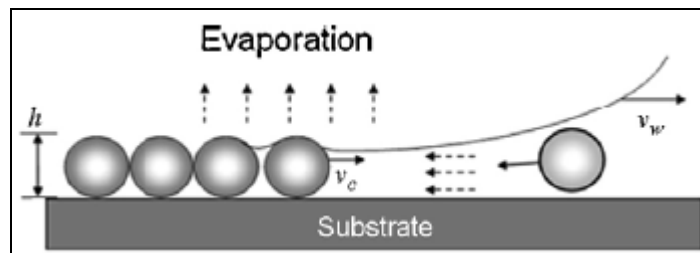


Figure 1.6. Schematic of the drying region of a thin wetting film being dragged at a rate, v_w , on a substrate [52]

Later, Prevo and Velev reported a modified convective assembly technique which increases process speed and reduce material consumption [53]. Since that time this deposition technique has been used to fabricate a wide variety of different coatings including ferritin protein films [54], large-scale nanocoating from tobacco mosaic virus

[55], latex crystals [53, 6], antireflective silica coatings [57], surface-enhanced Raman scattering (SERS) substrates [58, 59], and cell coating [60].

1.1.4. Droplet Templating

What is the simplest way to deposit anything in suspension onto a surface? Everyone replies this question saying “evaporative deposition”, because deposition of material onto surface just needs evaporation of the fluid part of the suspension. Due to the simplicity of the technique, researchers have investigated the ways to create novel structured materials, and to coat patterned and unpatterned surfaces with functional particles and biomolecules.

Deposition of materials on surfaces via drying of a sessile drop of a colloidal suspension has been used for self-assembly of polystyrene latex particles [61-65], silica microspheres [66], oligodeoxynucleotides [67-69], and cells [70-71]. While this deposition is simple and no complex equipment or microfabrication steps are required, it has been shown that by varying parameters, such as particle and surfactant concentration, and hydrophilicity/hydrophobicity of the surface, it is possible to produce a variety of architectures.

On the other hand, in order to use this technique efficiently, controllable distribution of particles in suspensions during drying has severe importance. However, it is hard task to obtain desired pattern due to three convective mechanisms inside the drying droplets. First one is the radial outward flow carrying particles toward the pinned wetting line [72]. During drying of the droplets, in many cases, solvent loss due to evaporation occurs at the highest rate at the perimeter of the droplets, and in order to compensate this loss, an outward flow from the central part to the perimeter occurs. This flow of the solvent also carries dispersed particles to the wedge resulting in a ring formation as seen on Figure 1.7.

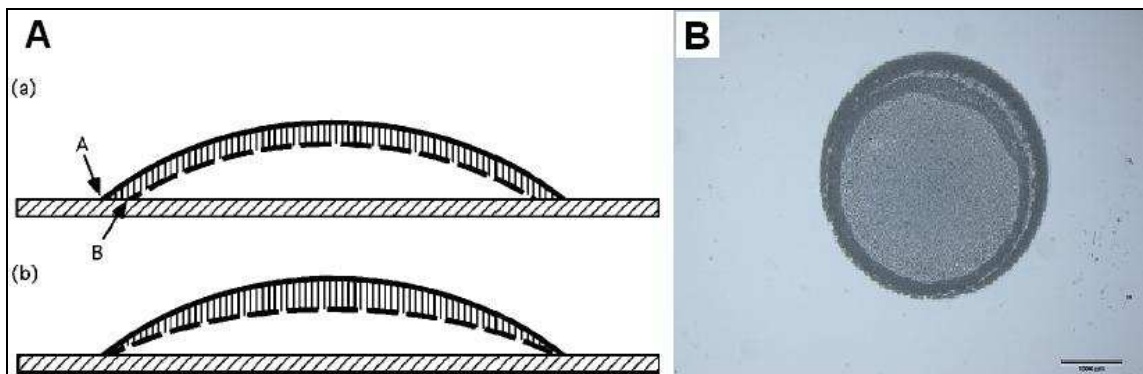


Figure 1.7. (A) When the contact line is not pinned, droplet interface moves from the solid line to the dashed line, and the contact line moves from A to B (a). However, if the contact line is pinned, then the motion from A to B is prevented by an outflow to replenish the liquid removed from the edge (b). (B) Bright-field image of evaporation pattern from droplet of *Saccharomyces cerevisiae*.

Deegan *et al.* was the first to propose a physical model for this phenomenon [72]. In their model, capillary flow, induced by droplet evaporation at a pinned contact line, is the main cause for the coffee ring. Since that time, many others have investigated the mechanism of this capillary flow within drying droplets and described it using different theories and numerical methods, and in most of these studies, polystyrene latex particles at varying sizes and concentrations have been chosen as model particles due to their small size, availability in various sizes, and surface uniformity.

The other mechanism which affects the distribution of particles on surfaces after evaporative deposition is Marangoni flow which is generated due to a surface tension gradient caused either by concentration gradient or by a temperature gradient. In their report, Hu and Larson stated that the coffee-ring phenomenon requires not only a pinned contact line, particles that adhere to the substrate, and high evaporation rate near the droplet's edge but also that the Marangoni effect resulting from the latent heat of evaporation be suppressed [73]. Marangoni flow reverses the coffee-ring phenomenon and produces deposition at the droplet center rather than the edge. For water droplets, Deegan *et al.* observed that the Marangoni flow is weak [65]. However, for solvents such as octane and other alkanes, a strong recirculating flow is observed in droplets [73].

The third mechanism involves DLVO (named after Derjaguin and Landau, Verwey and Overbeek) interactions which include the force between charged surfaces interacting through a liquid medium. In classical DLVO theory, the total force between two interacting particles is the sum of electrostatic and van der Waals forces [74]. When attractive DLVO forces between particles and substrate predominate over radially outward flow and Marangoni flow, the pattern is a uniform deposit.

Figure 1.8 represents the three convective mechanisms compete to form the deposit.

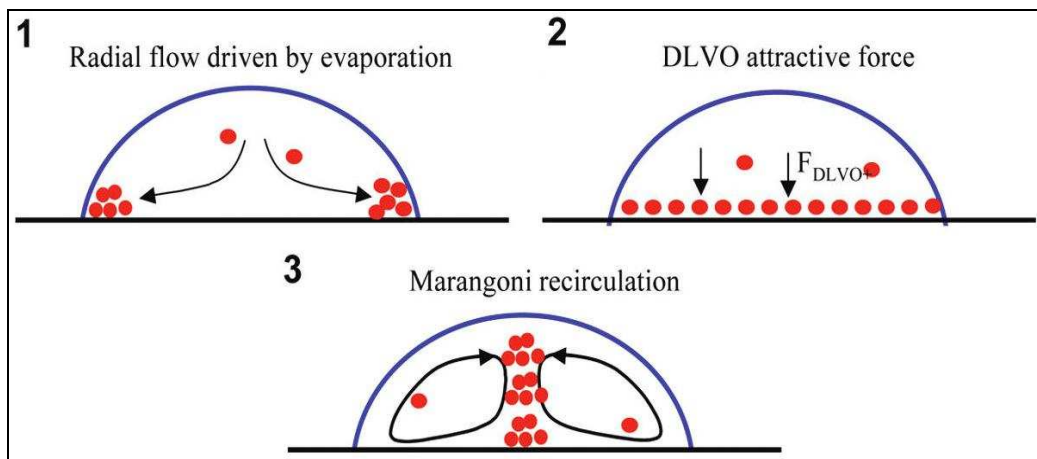


Figure 1.8. The three convective mechanisms in a drying droplet [75]

Regarding from the biological perspective, evaporative deposition of cells onto surfaces in controlled way may have a wide variety of potential applications. Uniform cell coatings on bioreactor surfaces may enhance bioreactor's efficiency. They may also be used for biosensors, gradient bioassays, implant coatings, and toxicity studies. By the help of occurring ring structures, some bioelectronic devices may also be developed. Furthermore, deposition of microorganisms by this way may open up some possibilities for further understanding of cell-cell and cell-substrate interactions which play key roles in biofilm formation.

Although deposition of microorganisms by this technique has many potential uses in biotechnological and biomedical applications, related reports in literature are very few. In a recent report about evaporative deposition of bacteria on glass, it was observed that motile

bacteria create uniform deposits and nonmotile bacteria produce ring structures [70]. In another report, by using motile bacteria, it was shown that creations of various deposition patterns by changes in the surface wettability were possible [71].

In this study, a simple approach for uniform assembly of yeast cells on surfaces was investigated. *Saccharomyces cerevisiae* yeast cells, which are one of the most robust and intensively studied eukaryotic model organisms in cell biology and biotechnology, are used. Since evaporative deposition from a sessile drop is a simple and appealing way to deposit materials on a surface, yeast cells are deposited by the droplet templating technique. The influence of experimental parameters such as surface hydrophobicity, pH of the suspension, droplet size, number of yeast cells in suspension on the behavior of the living cells and their assembly on surfaces was investigated. Lastly, the results of this technique were compared to the previously reported method [60] which involves the use of convective assembly approach to deposit yeast cells.

2. MATERIALS and METHODS

2.1. PREPARATION OF HYDROPHILIC and HYDROPHOBIC SURFACES

Glass slides (Pearl, China) were cleaned in H_2CrO_4 solution by overnight immersion which was prepared by dissolving 10 g of $\text{K}_2\text{Cr}_2\text{O}_7$ (Fluka, Switzerland) in enough H_2SO_4 (Riedel de Haen, Germany). The slides were carefully rinsed with deionized water and dried in laminar flow. After chemical treatment of surfaces, they were found as highly hydrophilic substrates. Water droplets spotted on these slides had vanishing contact angles.

Hydrophobic surfaces were prepared by PDMS casting and peeling method. PDMS was prepared using Sylgard elastomer kit (Dow Corning, USA) which consists of curing agent and silicone elastomer. They were mixed in a 1:10 mass ratio and resulting air bubbles were removed by placing PDMS mixture into the desiccator for 10-15 minutes. Then, PDMS mixture was decanted onto the glass substrates, cured in a 70°C oven for two hours and subsequently peeled to yield hydrophobic glass surface (Figure 1.8). Hydrophobicity of the resulting surfaces was verified by measuring the contact angle of $4\ \mu\text{l}$ of deionized water spotted on the slide. Side view photograph of the droplet was taken using Nikon D5000 digital camera. The ImageJ 1.43u software (NIH, USA) was used to measure contact angle.

The morphologies of the prepared hydrophilic and hydrophobic surfaces were characterized by using atomic force microscopy (AFM) (model XE-100, Park Scientific). The surface imaging was operated in non-contact mode with a standard silicone cantilever. For determination of topography properties, randomly selected regions ($5\ \mu\text{m} \times 5\ \mu\text{m}$) on both surfaces were visualized.

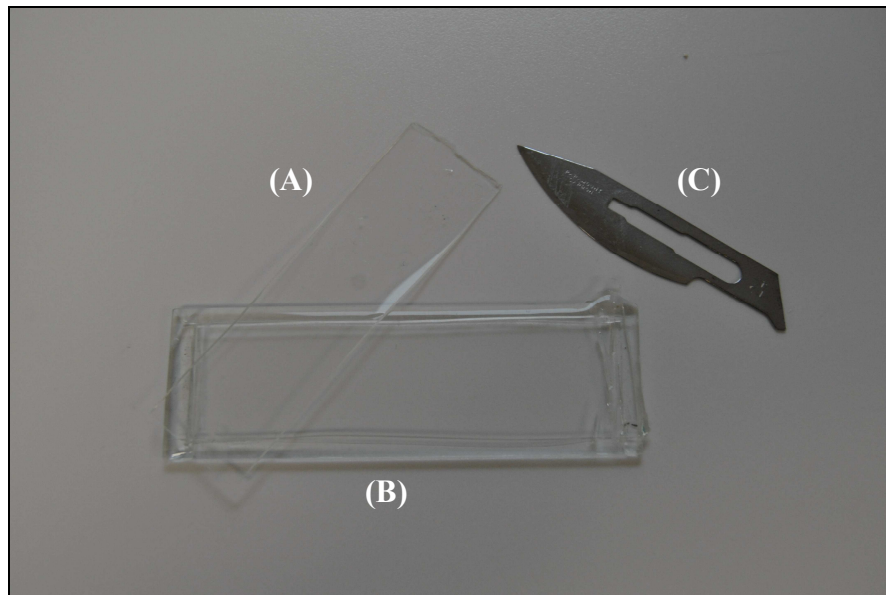


Figure 2.1. The images of peeled PDMS (A), PDMS peeled glass slide (B), scalpel blade (C)

2.2 PREPARATION OF YEAST CELL SUSPENSIONS

10 weight per cent suspensions of yeast cells were prepared by dispersing 0.5 g of active dry baker's yeast (Pakmaya Inc., Turkey), which is the granulated form of *Saccharomyces cerevisiae* as seen on seen on Figure 2.2, in 4.5 ml of deionized water, in five separate 50 ml Eppendorf tubes. The tubes were then manually agitated to suspend the yeast cells in the water and were allowed to sit for 30 minutes.



Figure 2.2. Active dried yeast in granulated form

The pH of suspensions in five tubes was measured using a pH meter (Mettler Toledo, USA), and each of them was adjusted to different pH values (2.0, 4.0, 6.0, 8.0, 10.0) using 1.0 N NaOH (Merck, Germany) and 1.0 N HCl (Riedel de Haen, Germany). The pH values were then adjusted every 30 minutes for several hours using small aliquots of NaOH and HCl until they were stabilized at desired pH values.

2.3. DEPOSITION OF CELL COATINGS

Firstly, serial dilutions of the stock suspensions were prepared by decreasing the number of the yeast cells by two fold in each dilution step until reaching 1:256 dilutions of the stock solutions. Each dilution was made using water at its own pH; that is to say, dilutions of the stock suspension at pH 2 were made using water adjusted to pH 2, and so on. Prior to deposition, the cell suspensions were sonicated gently for 20 seconds to break up aggregates. Then, the procedure continued in two ways; deposition of yeast cells onto substrates by droplet templating, and by the convective assembly technique.

2.3.1. Droplet Templating

In this part of the experiment, firstly, in order to understand the effect of pH on the deposition patterns after evaporation of the solvent, 4 μl of each suspension was spotted on both hydrophilic and hydrophobic glass substrates. Afterwards, in order to understand how the deposition patterns would be by spotting different volumes on hydrophobic surface, 200 μl , 100 μl , 50 μl , 10 μl , 5 μl , and 1 μl of all suspensions were spotted on PDMS coated glass slides and were allowed to dry. Onto hydrophilic surfaces, only 50 μl and 5 μl of all suspensions were spotted. All processes were performed at 22 ± 2 °C and 30-60 per cent relative humidity.

2.3.2. Convective Assembly

Experimental setup for convective assembly was a slight modification of the method reported by Prevo and Velez [53]. A hydrophilic glass slide was fixed on the moving stage and the other hydrophilic slide, held by a clamp, was placed on the top of the fixed slide with an angle of 24°. 12 μl from the stock cell suspension was then injected between the

two slides and spread to form uniform meniscus as shown in the Figure 2.3. The velocity of the bottom stage was set to 21 $\mu\text{m/s}$ and cells were deposited onto the substrate in 20-30 minutes. This procedure was applied for all five cell suspensions having different pH values. All processes were performed at 22 ± 2 °C and 30-60 per cent relative humidity. Figure 2.4 demonstrates the convective assembly process.

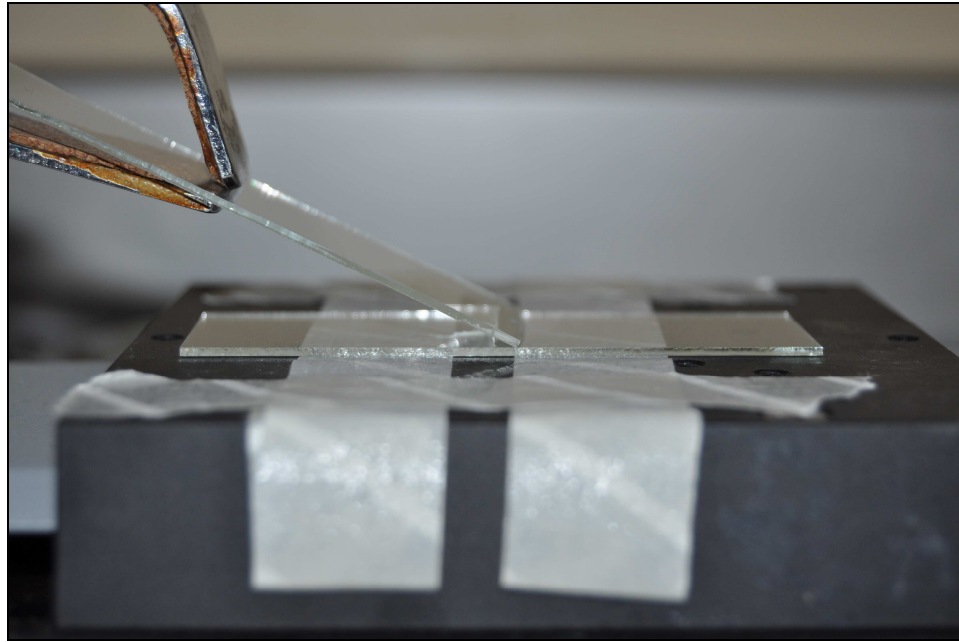


Figure 2.3. Convective assembly setup

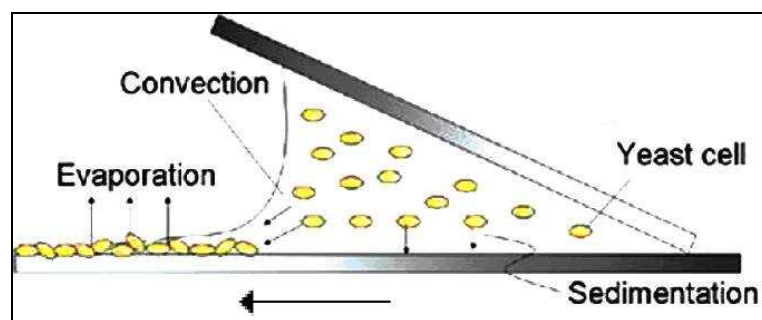


Figure 2.4. Schematic of the convective assembly process. The top slide remains in place while the bottom slide is moved to the left

2.4. COATING CHARACTERIZATION

Optical images of the dried patterns of 4 μ l droplets were taken using an inverted microscope with an attached camera. Contact angles of the droplets were measured by taking and processing side view photographs of the droplets using Nikon D5000 digital camera and ImageJ 1.43u software (NIH, USA), respectively. The samples obtained from drying of droplets on hydrophobic and hydrophilic surfaces and from convective assembly were imaged using Leica MZ16FA stereoscope. Further magnified images of the samples were obtained by using Carl Zeiss Evo 40 scanning electron microscope (SEM).

3. RESULTS and DISCUSSION

Evaporative deposition of cells is a simple way and may have a wide variety of potential applications as explained in introduction. On the other hand, due to the rarity of the reports, further investigation and exploration in this area were being required, and in this study, it was realized by evaporative deposition of *Saccharomyces cerevisiae* yeast cells on hydrophilic and hydrophobic surfaces. Regular glass slides have hydroxyl groups on their surfaces making them hydrophilic. However, their hydrophilicity varies with manufacturing. After chemical treatment of the slides with chromic acid, they became highly hydrophilic. A 4 μ l of water droplet had vanishing contact angle on these surfaces as seen on Figure 3.1. In order to obtain hydrophobic surfaces, PDMS was cast on slides and peeled after drying, and contact angle of the resulting surface was found to be 98°.



Figure 3.1. Photographs of water droplets on a slide prepared by PDMS cast and peel (A) and on a regular glass slide (B)

Figure 3.2 shows AFM images of a regular glass slide before and after PDMS treatment. As seen on the figure, surface pattern of the glass surface completely changes after PDMS treatment. After peeling, some PDMS remains stuck to the glass surface creating micropatches giving glass surface a hydrophobic character.

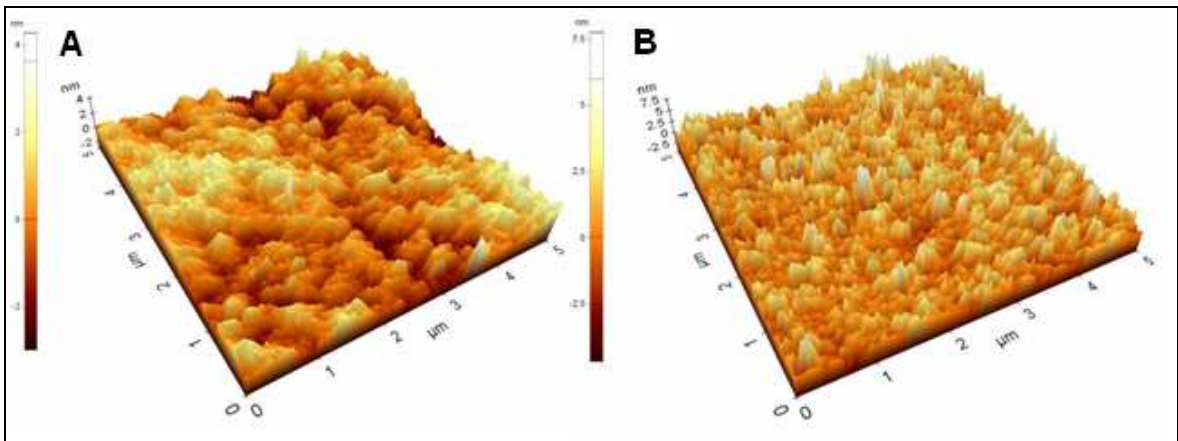


Figure 3.2. AFM images of regular glass slide (A) and glass slide prepared by PDMS cast and peel (B)

After preparation of the surfaces, next step was the preparation of yeast cell suspensions. The commercial dry powder of yeast consists of the rod-shaped particles containing mostly yeast and some small amount of additives. Since cells were in dried form, they had to be hydrated first.

Evaporative deposition mechanism of yeast cells would be completely different from that of latex particles and any other particles reported in literature. Since cells are much larger than the other types of particles, deposition process would be highly affected by the presence of sedimentation. In addition, being living organisms, surface of yeast cells are not uniform. Cells interact with other cells via many specific and nonspecific interaction mechanisms, and most of these interactions lead to aggregation of the cells.

3.1. pH EFFECT

In *Saccharomyces cerevisiae*, the cell wall makes up 15 to 30% of the dry weight of the cell. The walls are composed mostly of mannoprotein and fibrous $\beta_{1,3}$ glucan. There is also branched $\beta_{1,6}$ glucan that links the other components of the wall. An important minor component is chitin, which contributes to the insolubility of the fibers. The $\beta_{1,3}$ glucan-chitin complex is the major constituent of the inner wall. $\beta_{1,6}$ glucan links the components of the inner and outer walls. On the outer surface of the wall, there are mannoproteins,

which are extensively O and N glycosylated [76, 77]. The organization of general composition of yeast cells walls is represented in Figure 3.3.

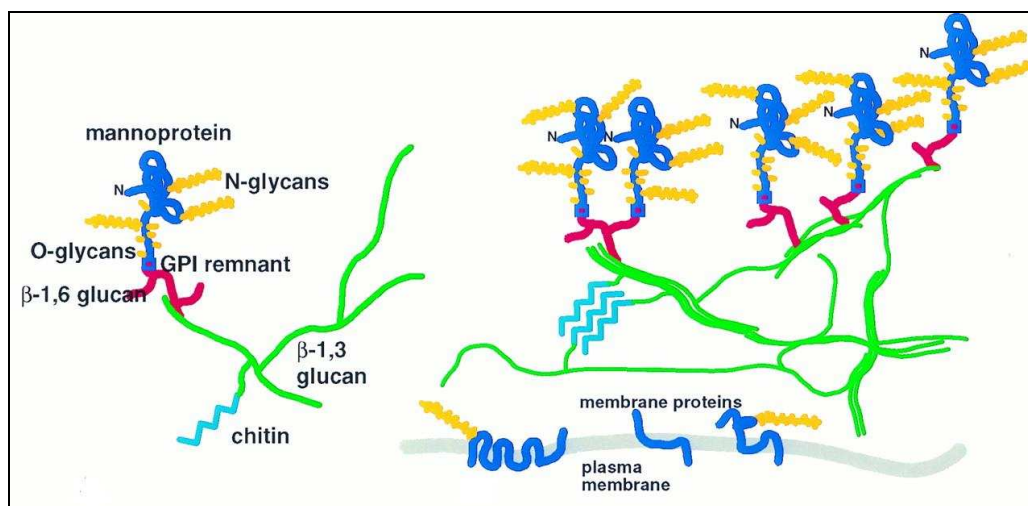


Figure 3.3. General components of yeast cell walls [77]

The surface macromolecules of yeast cells, i.e., glucans and mannoproteins, contain three main types of ionized groups: phosphodiester, carboxyl, and amino groups. At pH values lower than the isoelectric point of 4 [78], the surface is positively charged due to the presence of NH_3^+ groups. On the other hand, at pH values above the isoelectric point, the surface of the cells is negatively charged essentially due to the dissociation of the weakly acidic COOH groups.

Surface charges play an important role in interactions of cells with their environment, cell adhesion and aggregation. Yeast cells show some degree of aggregation as the cells resist changes in the pH of the suspension away from the isoelectric point of 4 because of the $-\text{COOH}$ groups and the other ionized macromolecules on their surface [79]. Since hydrophobic interactions between cells predominate, higher level of aggregation between cells is observed at pH values near their isoelectric point. As the pH of the suspension becomes lower or higher than this point, electrostatic repulsion forces predominate which, in turn, leads to decrease in aggregation level and single yeast cells start to become free to move alone in suspension [80].

First, the influence of pH on the cell on hydrophobic surfaces was investigated. The suspension volume spotted on hydrophobic surfaces was kept constant but the concentration of yeast cells in droplet was gradually decreased by dilution. The original suspension containing about 3×10^9 yeast cells per ml was diluted up to 1:256 by a factor of 2^n .

Hydrophobic surfaces can influence the behavior of the cells in two ways. One is that they affect the attachment of cells on the surface through several weak interactions. Second, since the droplet profile is different compared to the droplet profiles on hydrophilic surfaces, the drying time of a droplet on hydrophobic surfaces may be significantly higher than the same volume of droplet left on hydrophilic surfaces.

On hydrophobic surfaces, the drying times of the droplets take longer times due to the smaller droplet surface area, which diminishes the solvent evaporation rate, yeast cells can find more time to interact influencing the aggregation pattern.

Figures 3.4 to 3.12 show the pH and dilution effects on the assembly of yeast cells on hydrophobic surfaces.

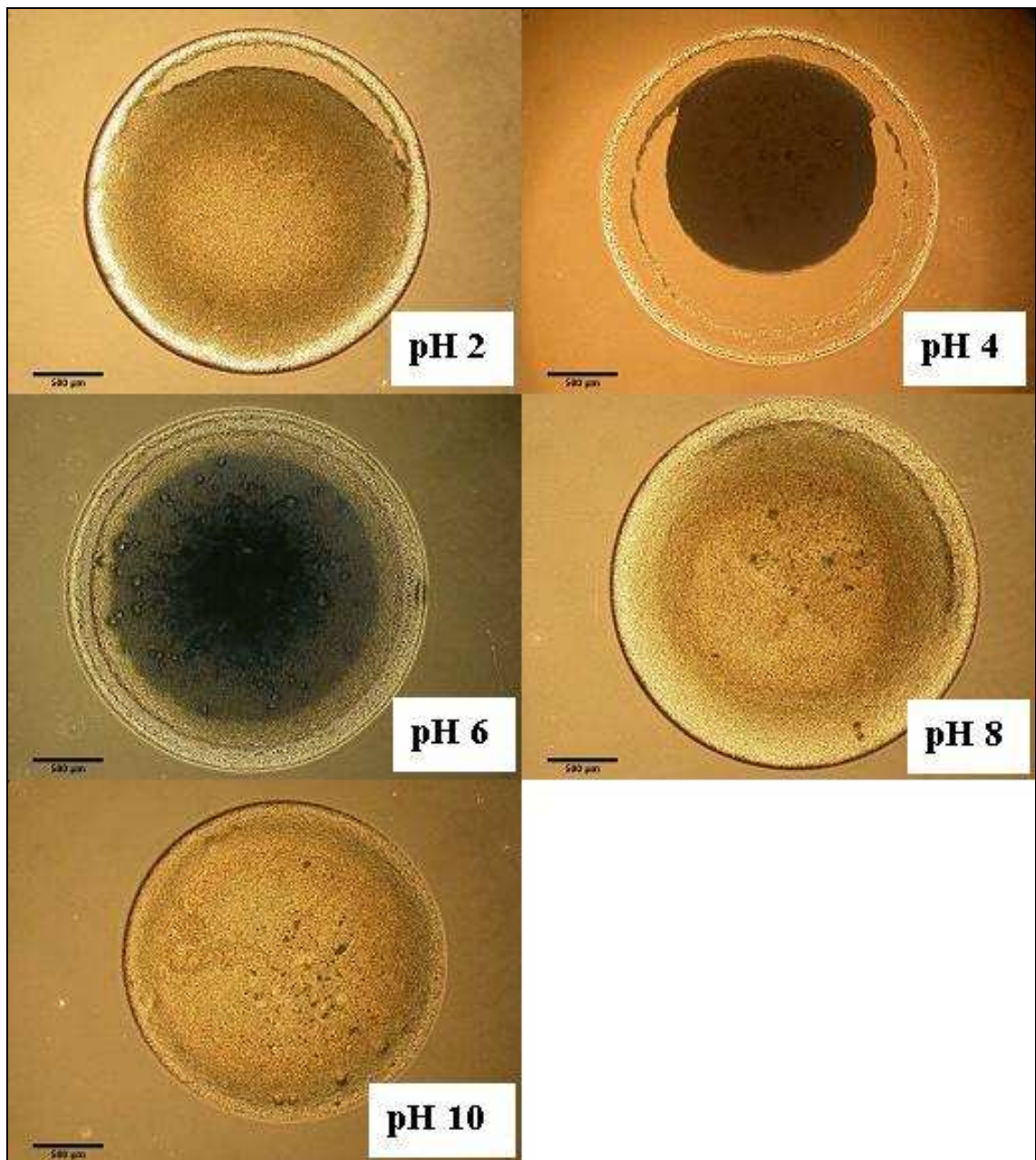


Figure 3.4. Patterns obtained from evaporative deposition of 4 μl of stock suspensions at five different pH values. The scale bars correspond to 500 μm .

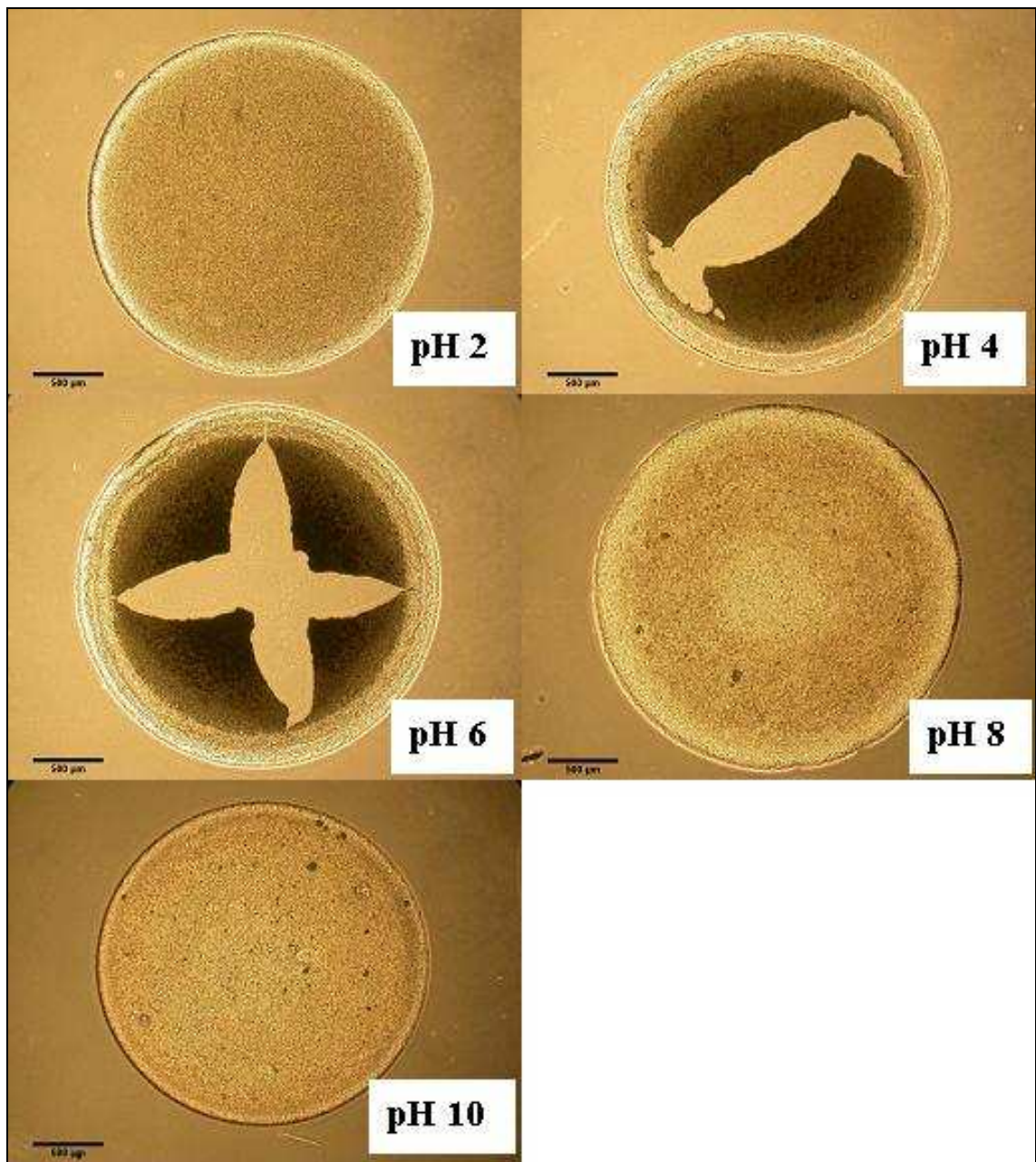


Figure 3.5. Patterns obtained from evaporative deposition of 4 μl of 1:2 diluted suspensions at five different pH values. The scale bars correspond to 500 μm .

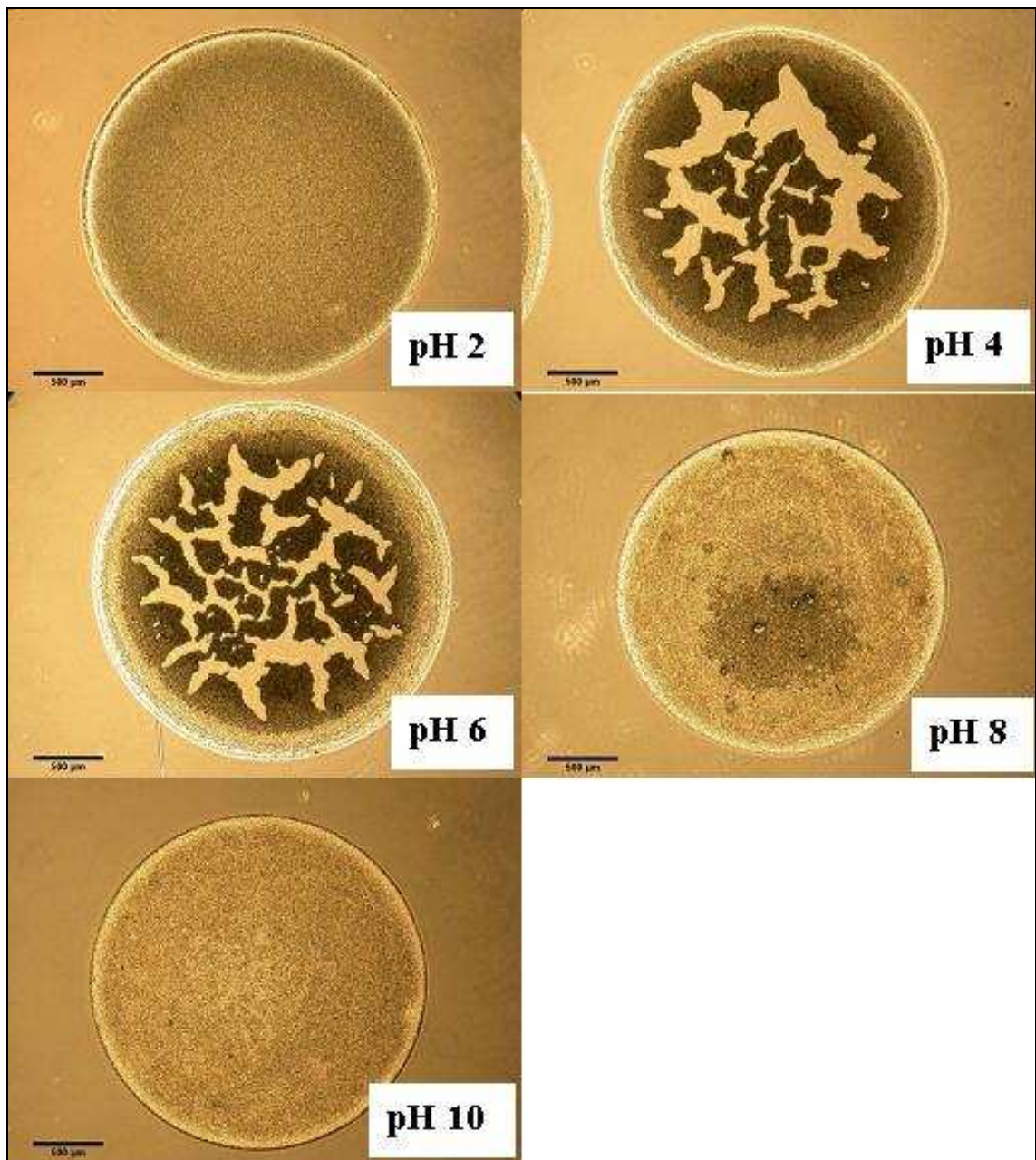


Figure 3.6. Patterns obtained from evaporative deposition of 4 μl of 1:4 diluted suspensions at five different pH values. The scale bars correspond to 500 μm .

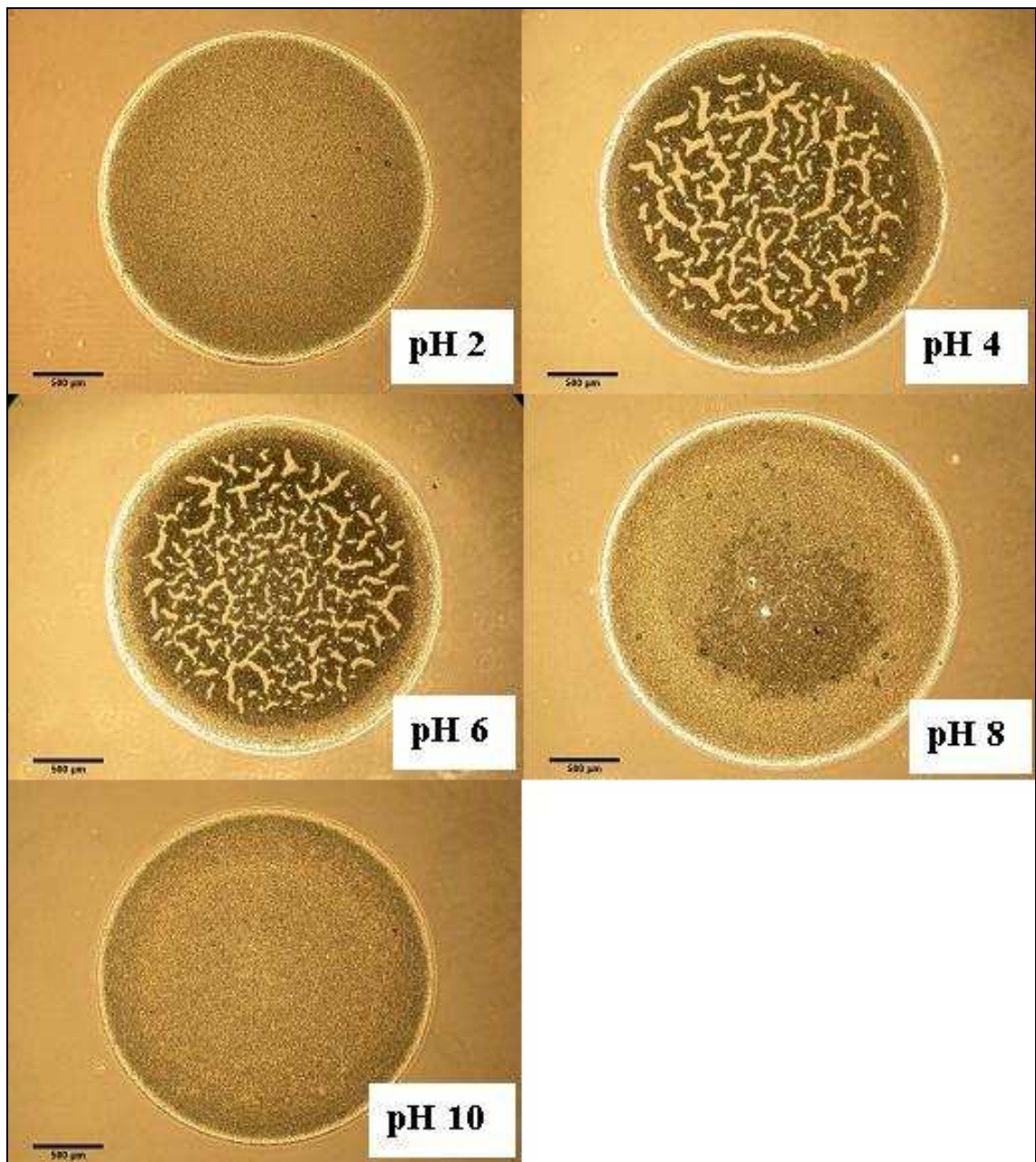


Figure 3.7. Patterns obtained from evaporative deposition of 4 μl of 1:8 diluted suspensions at five different pH values. The scale bars correspond to 500 μm .

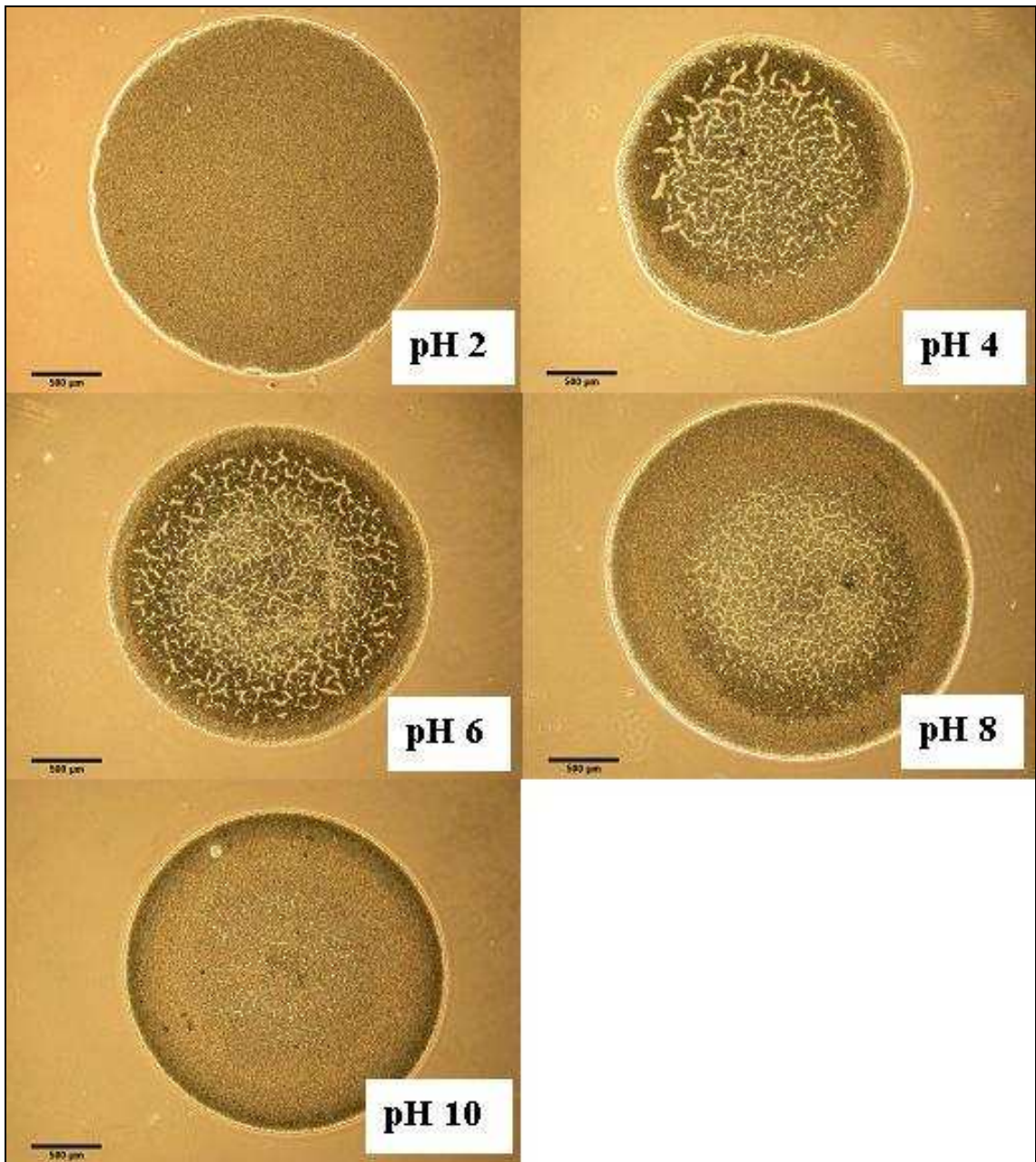


Figure 3.8. Patterns obtained from evaporative deposition of 4 μl of 1:16 diluted suspensions at five different pH values. The scale bars correspond to 500 μm .

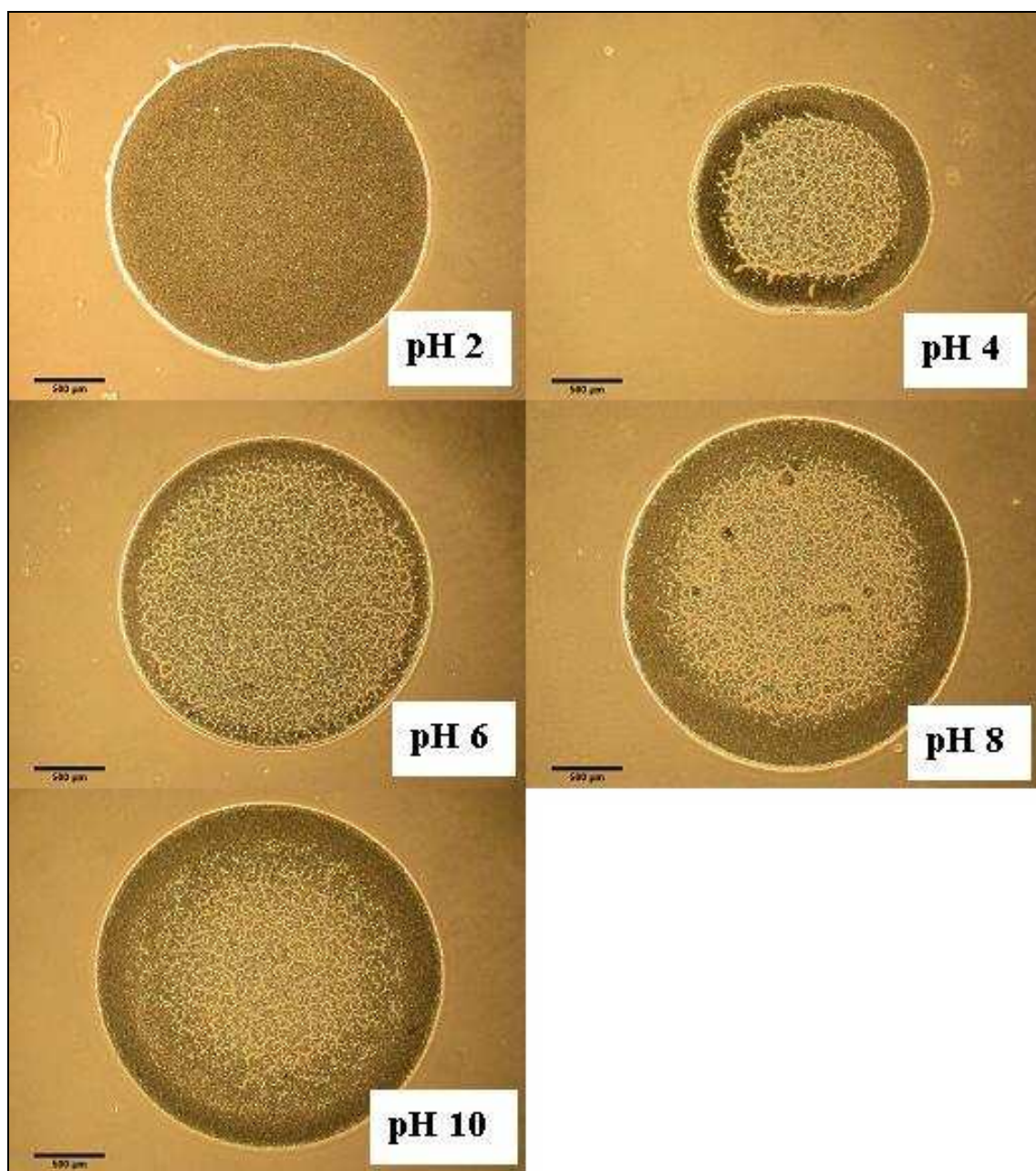


Figure 3.9. Patterns obtained from evaporative deposition of 4 μl of 1:32 diluted suspensions at five different pH values. The scale bars correspond to 500 μm .

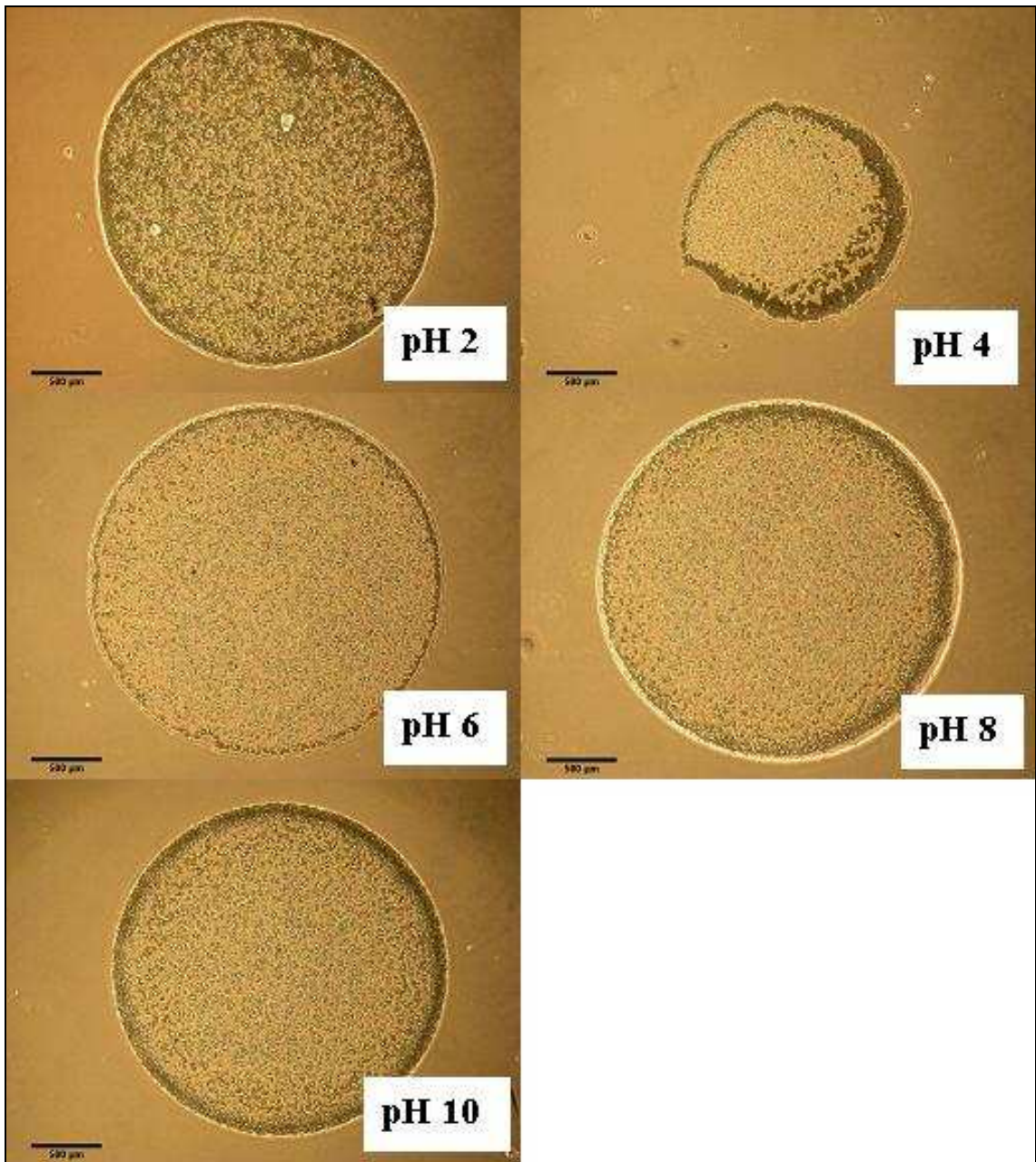


Figure 3.10. Patterns obtained from evaporative deposition of 4 μl of 1:64 diluted suspensions at five different pH values. The scale bars correspond to 500 μm .

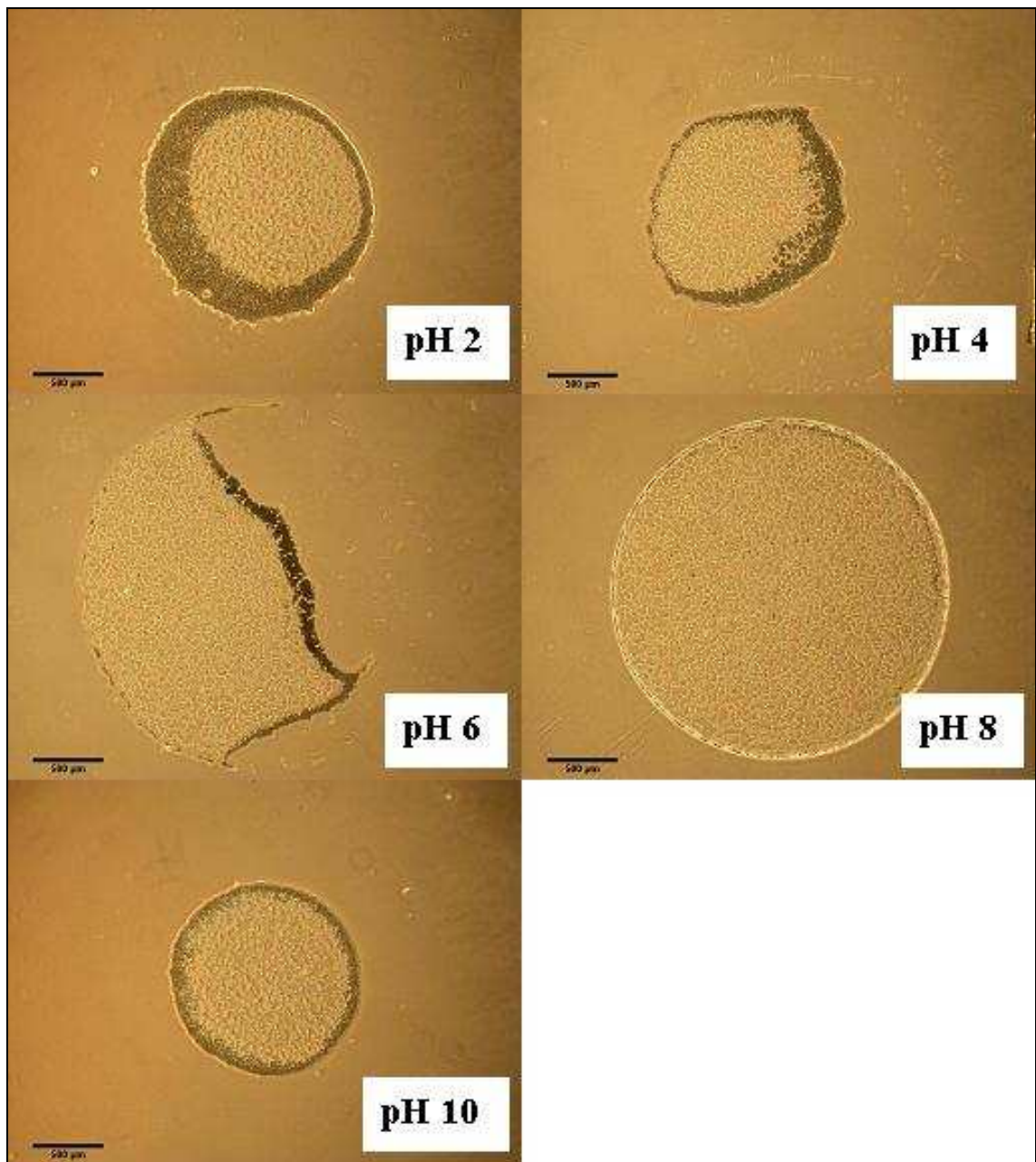


Figure 3.11. Patterns obtained from evaporative deposition of 4 μl of 1:128 diluted suspensions at five different pH values. The scale bars correspond to 500 μm.

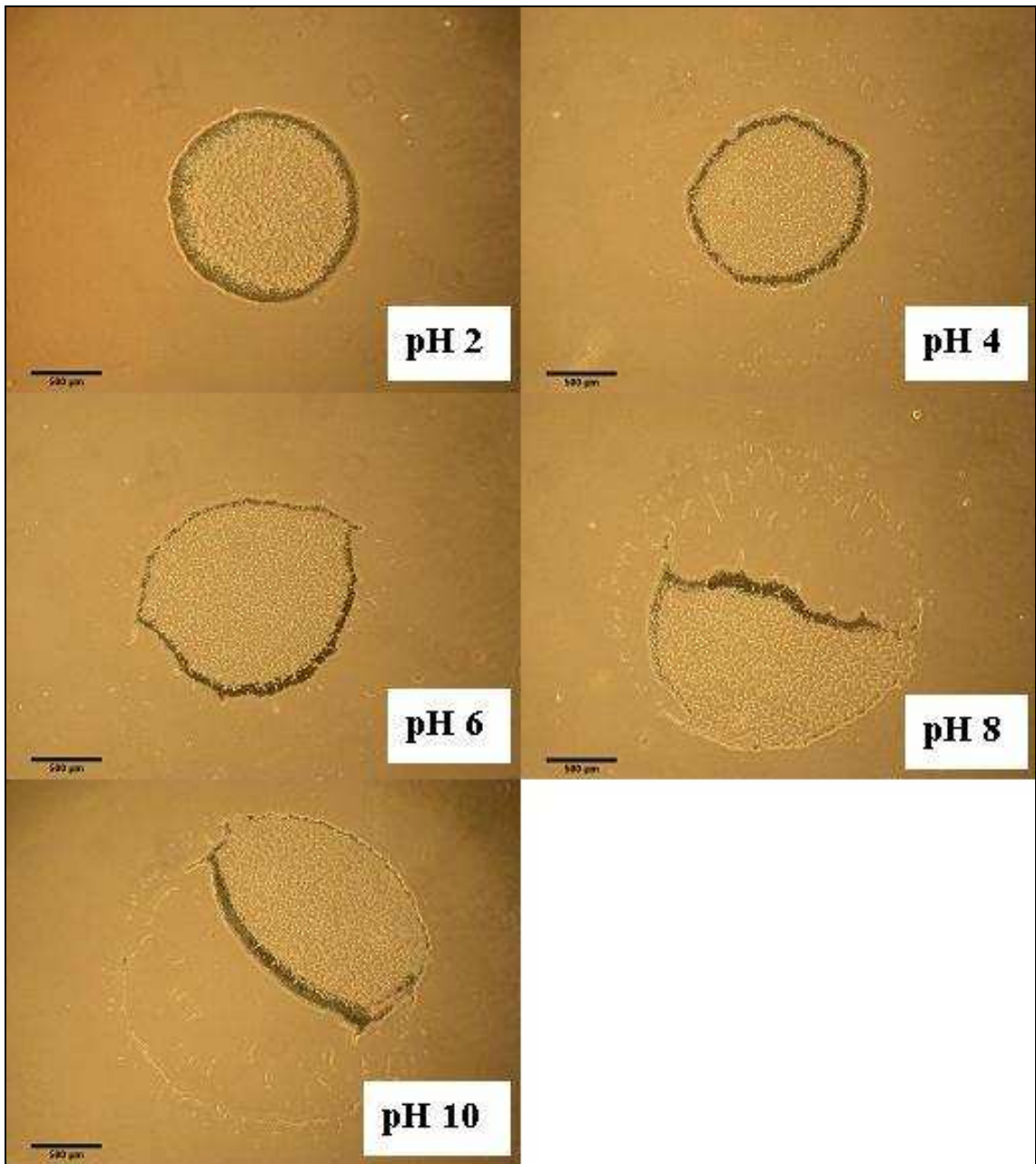


Figure 3.12. Patterns obtained from evaporative deposition of 4 μl of 1:256 diluted suspensions at five different pH values. The scale bars correspond to 500 μm .

Figure 3.4 shows not only distinct deposition patterns of cells at different pH values but also different drying modes of droplets. There are two distinct drying modes reported in the literature [81]. The droplets can dry with a constant contact area and decreasing contact angle or with a constant contact angle with decreasing contact area. The first mode is commonly observed on hydrophilic surfaces. In this mode, three-phase contact line pins due to both surface properties and flow of particles in suspension into the wedge region. Then, contact angle decreases in time due to evaporation of the solvent. On the other hand, the latter mode is commonly observed on hydrophobic surfaces. During drying, contact line recedes while contact angle is preserved. Figure 3.13 demonstrates the two modes of drying.

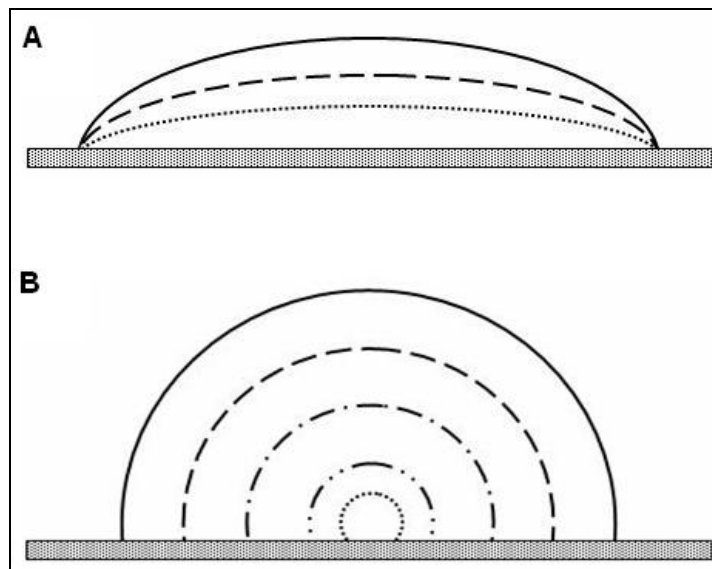


Figure 3.13. Two modes of drying

In many cases, both of the drying modes work during drying of a sessile droplet. As seen on Figure 3.4, on the deposition pattern of the suspension at pH 4, after the droplet was spotted on slide, contact line pinned initially. Then, some yeast cells accumulated at the wedge of the droplet forming a ring pattern due to aforementioned evaporation compensating flow. After some time, contact line could not remain pinned and got depinned. Droplet started to shrink and then pinned again. However, duration of this pinned stage of the contact line was shorter than the initial one; therefore, there were less yeast cells in the formed second ring. Later, some part of the contact line got depinned

again while some part remained in pinned state. As a result, contact line started to recede toward the pinned side. After drying, middle part of the deposited pattern detached from the surface and that situation can also be seen on Figure 3.5 (deposition patterns of suspensions at pH 4 and pH 6).

Since the aggregation behaviors of cells near the isoelectric point of 4 is in the highest level, at higher concentrations, the deposition patterns of the droplets at pH 2, pH 8, and pH 10 were more uniform than that of the droplets at pH 4 and pH 6 as can be seen throughout the Figures 3.4-3.7.

What is further, with a quick glance on the first seven figures, it was easy to comment that the areas occupied by the deposition patterns of the droplets at pH 4 decreased in size as the number of the cells in those droplets decreased. However, at the other pH values, deposition patterns preserved the contact areas of the initially spotted droplets. A logical explanation for these phenomena could be that at pH 4, the aggregation events become much more, and therefore, more clumps of cells form. The evaporation compensating flow inside the droplets can not carry these huge clumps to the wedges. Therefore, cells can not help for the pinning, and the contact area of the droplets becomes smaller during evaporation, which in turn, results in cellular deposits having smaller surface areas.

Figure 3.12 depicts another aspect of evaporation driven assembly. When the numbers of cells in suspensions were quite low, all parts of the contact lines could not pinned equally well. As some part of the contact lines remained pinned, the rest of the lines moved inward during evaporation and this receding part also swept cells to the inward regions. On the figure (especially on the deposition patterns at pH 8 and pH 10), some remnant cells of the sweeping process at the periphery can be observed. This situation suggests that cells in suspensions help contact line pinning. When sufficient number of cells can not reach to the edge of the droplet, the contact line can not remain pinned.

The major drawback of the evaporative deposition technique is the formation of coffee rings. Since Marangoni flow in aqueous droplets is weak, cells accumulated mostly at the perimeters due to the evaporation compensating outward flow inside droplets, which

restrained uniformity of the coatings. The coffee ring effects on coatings can be seen on Figure 3.9, 3.10, 3.11, and 3.12.

For further analysis of the phenomenon, SEM images of some of the deposition patterns were acquired. Figure 3.14 demonstrates the distribution of the cells on the pattern obtained with 32 times diluted form of the stock suspension at pH 2. Although thickness of the coating increased at the perimeter meaning multilayer deposition of the cells, most of the coating was uniform and monolayer deposition of the cells was obtained.

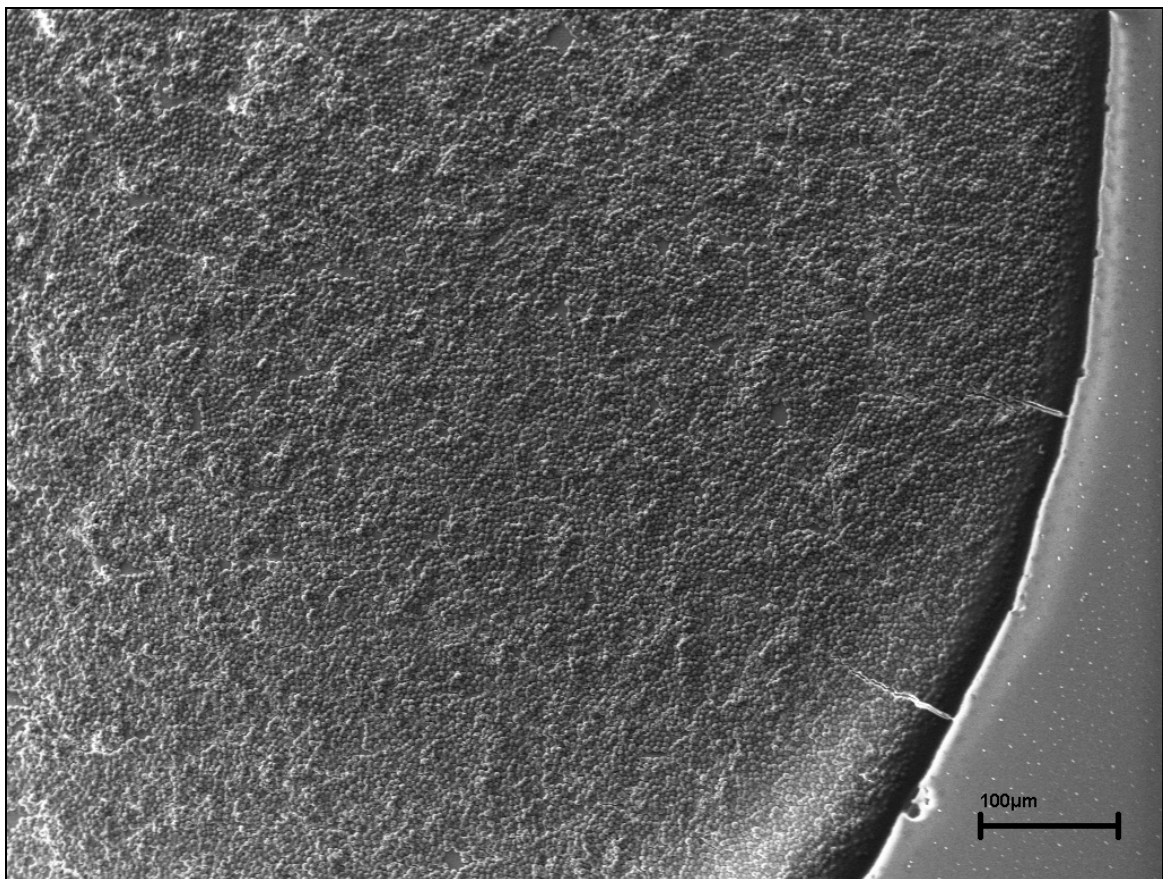


Figure 3.14. SEM image of a part of the deposition pattern obtained with 32 times diluted form of the stock solution at pH 2

Pattern generated by 64 times diluted form of the stock suspension was as seen on Figure 3.15. Since the number of the cells decreased two fold, resulting deposition was an incomplete monolayer.

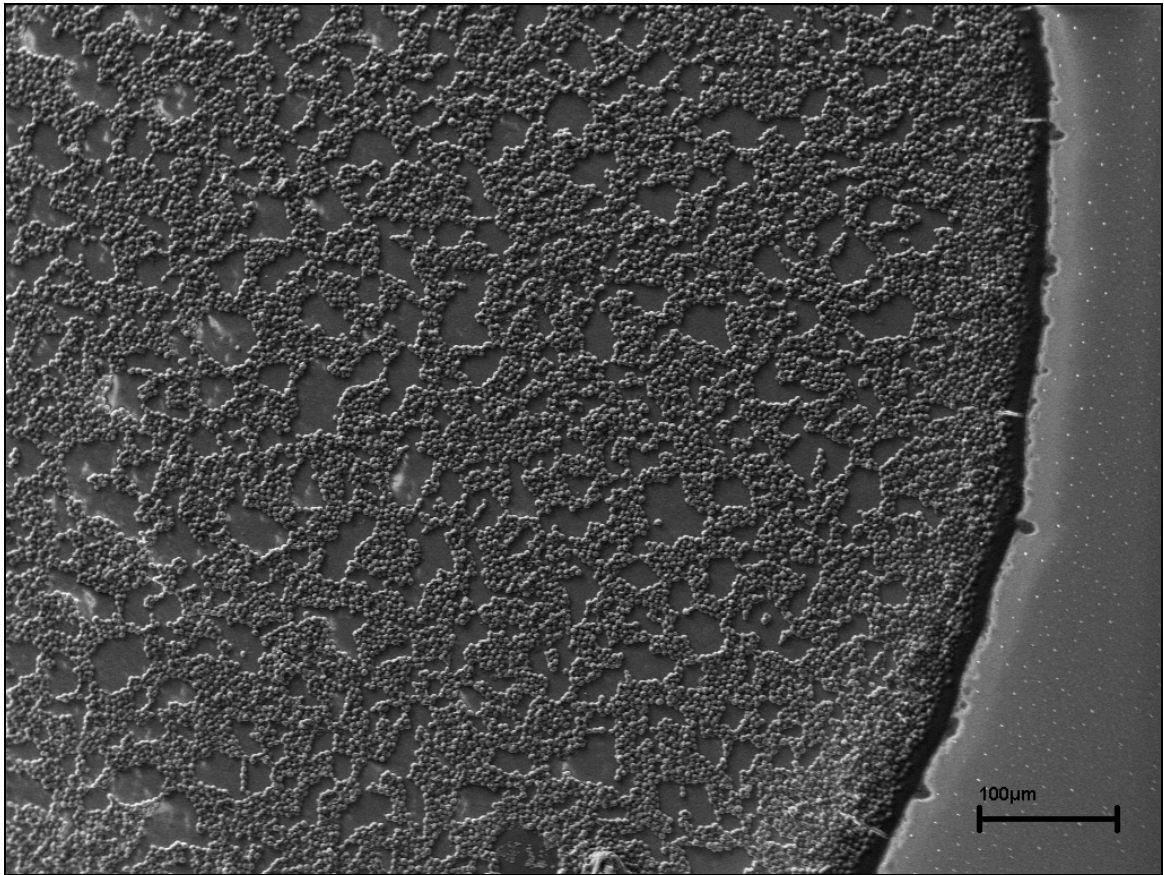


Figure 3.15. SEM image of a part of the deposition pattern obtained with 64 times diluted form of the stock solution at pH 2

In addition, at the subsequent dilution (128 times), most of the cells accumulated at the wedge of the deposition pattern due to so called ring phenomenon and the SEM image of a part of this pattern can be seen on Figure 3.16.

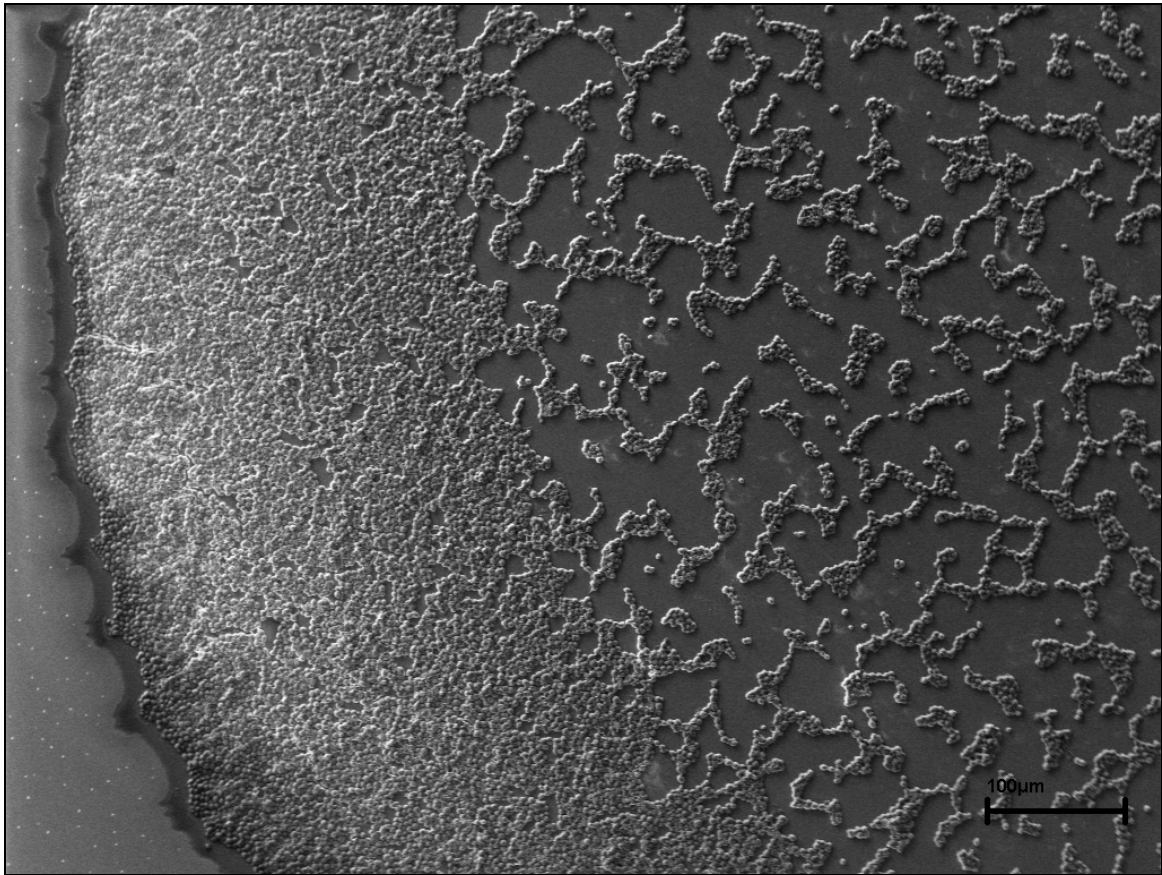


Figure 3.16. SEM image of a part of the deposition pattern obtained with 128 times diluted form of the stock solution at pH 2

3.2. EFFECTS of SURFACE HYDROPHOBICITY and HYDROPHILICITY on the BEHAVIOUR of CELL COATINGS

After having a proper understanding about the effect of pH and cell concentration on the droplet templating of cells, next steps were to investigate the effects of surface hydrophobicity and hydrophilicity on the evaporative deposition of the cells. In addition, suspensions were spotted on these surfaces in various volumes in order to observe the effect of droplet size.

3.2.1. Effects of Surface Hydrophobicity

Since it is closer to physiological pH and single yeast cells can move more freely being independent from other cells at that pH value, i.e., the aggregation of cells in suspensions at that pH are in a lesser degree, suspensions at pH 8 were selected for this part of the study. The droplets of suspensions in 200 μl , 100 μl , 50 μl , 10 μl , 5 μl , and 1 μl volumes, prepared as explained as in materials and methods, were spotted on the hydrophobic surfaces and the resulting patterns are presented on Figure 3.17, 3.18, 3.19, 3.20, 3.21, and 3.22.

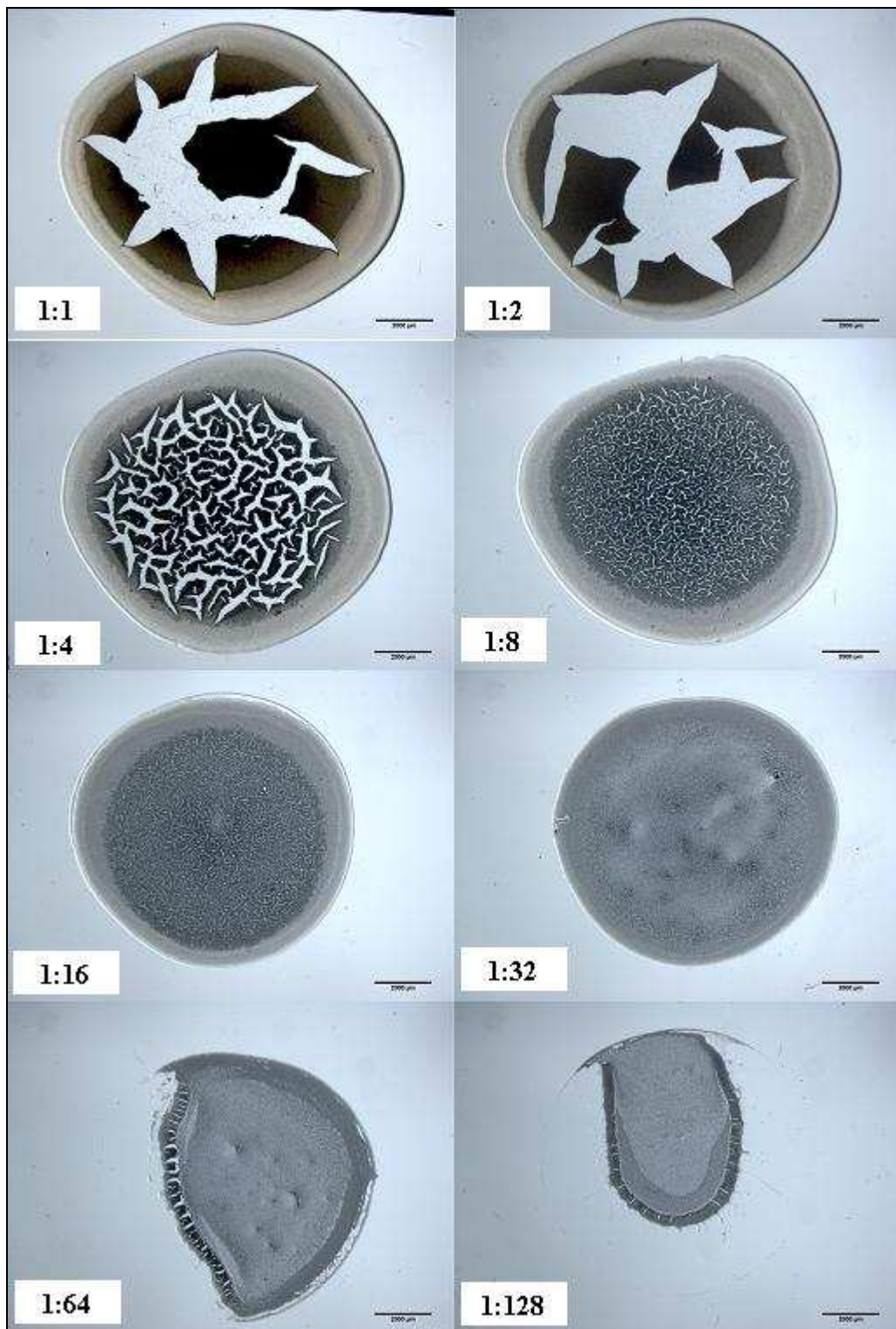


Figure 3.17. Deposition patterns obtained from evaporation of 200 μl of suspensions. The scale bars correspond to 2 mm.

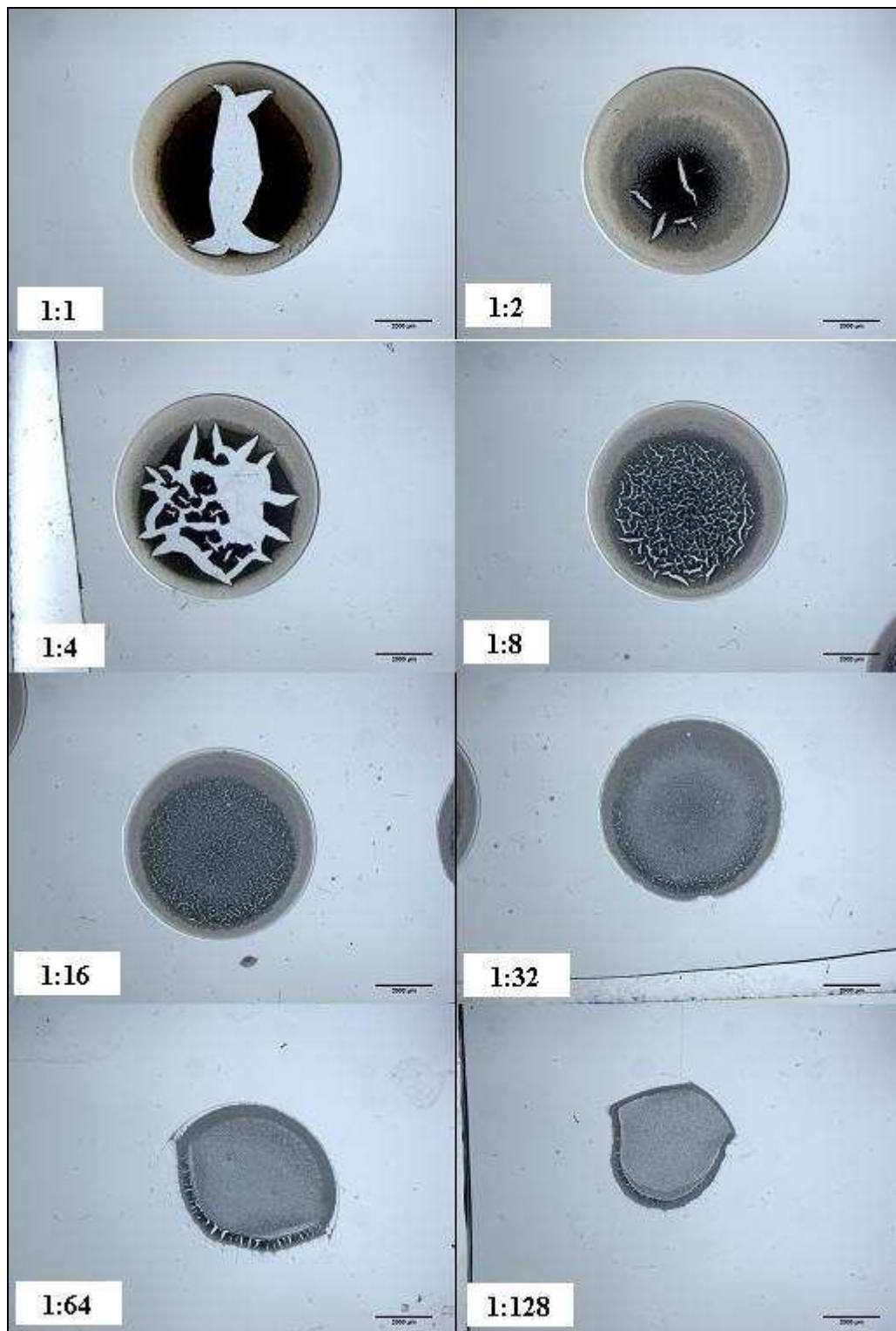


Figure 3.18. Deposition patterns obtained from evaporation of 100 μl of suspensions. The scale bars correspond to 2mm.

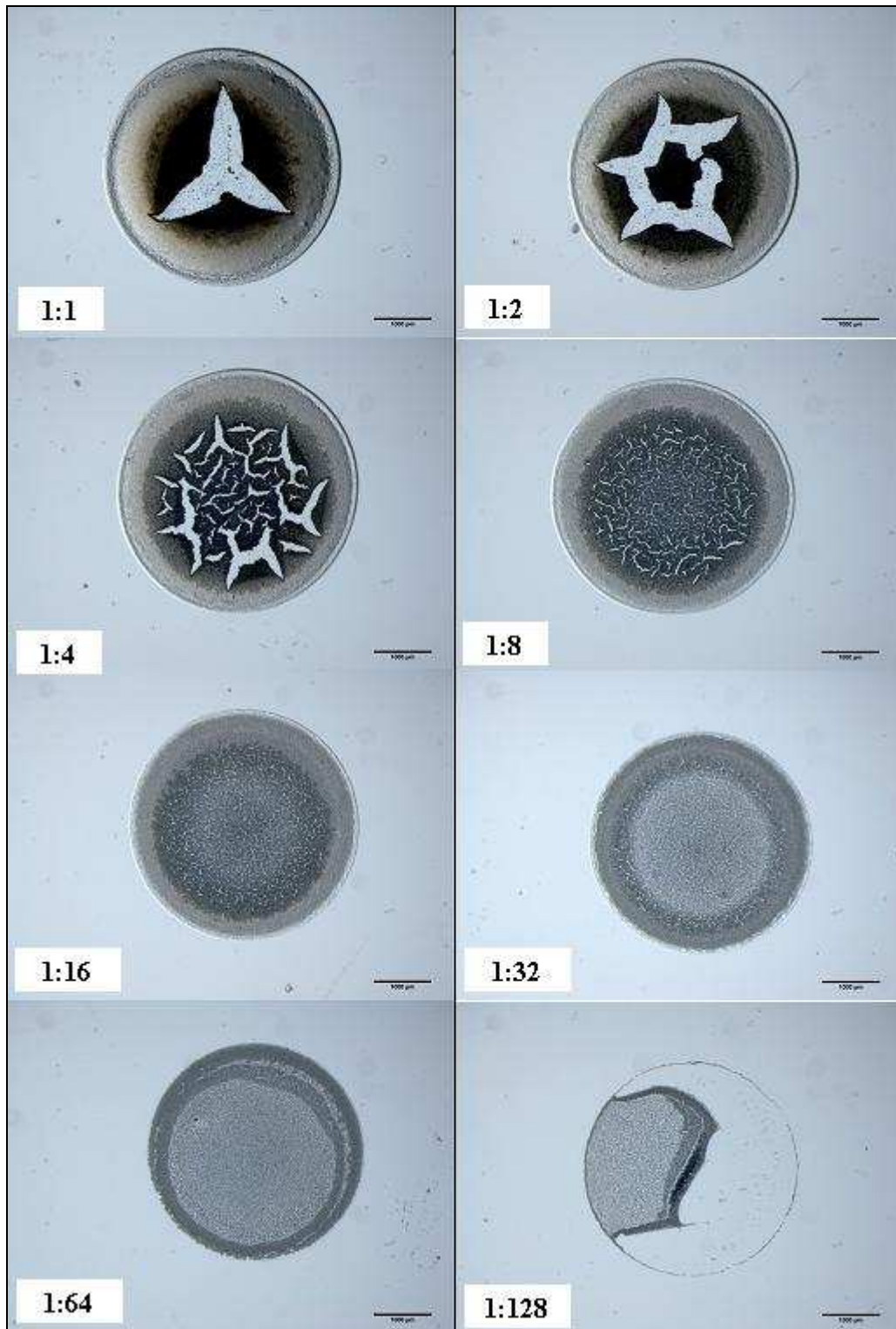


Figure 3.19. Deposition patterns obtained from evaporation of 50 μl of suspensions. The scale bars correspond to 1mm.

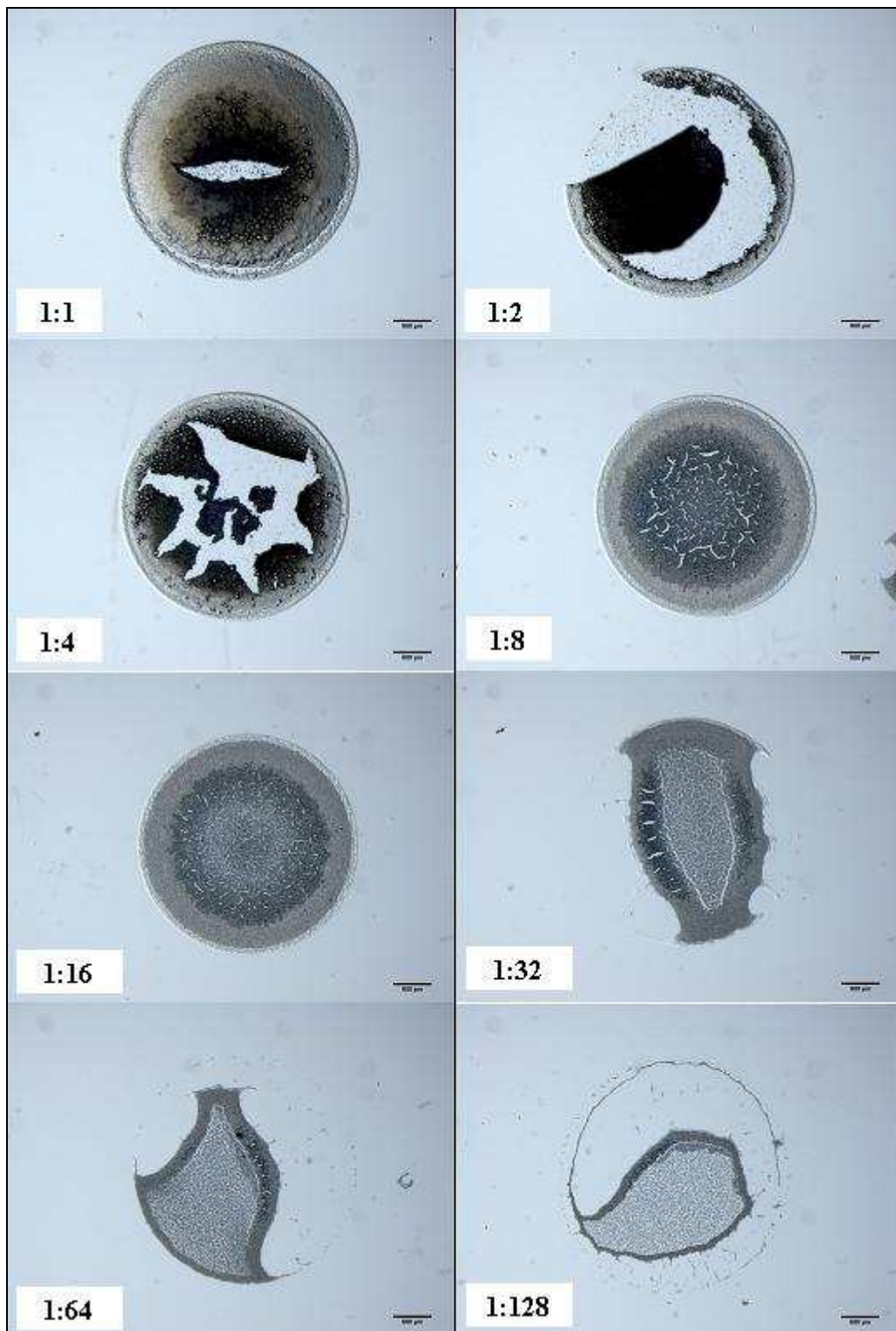


Figure 3.20. Deposition patterns obtained from evaporation of 10 µl of suspensions. The scale bars correspond to 500 µm.

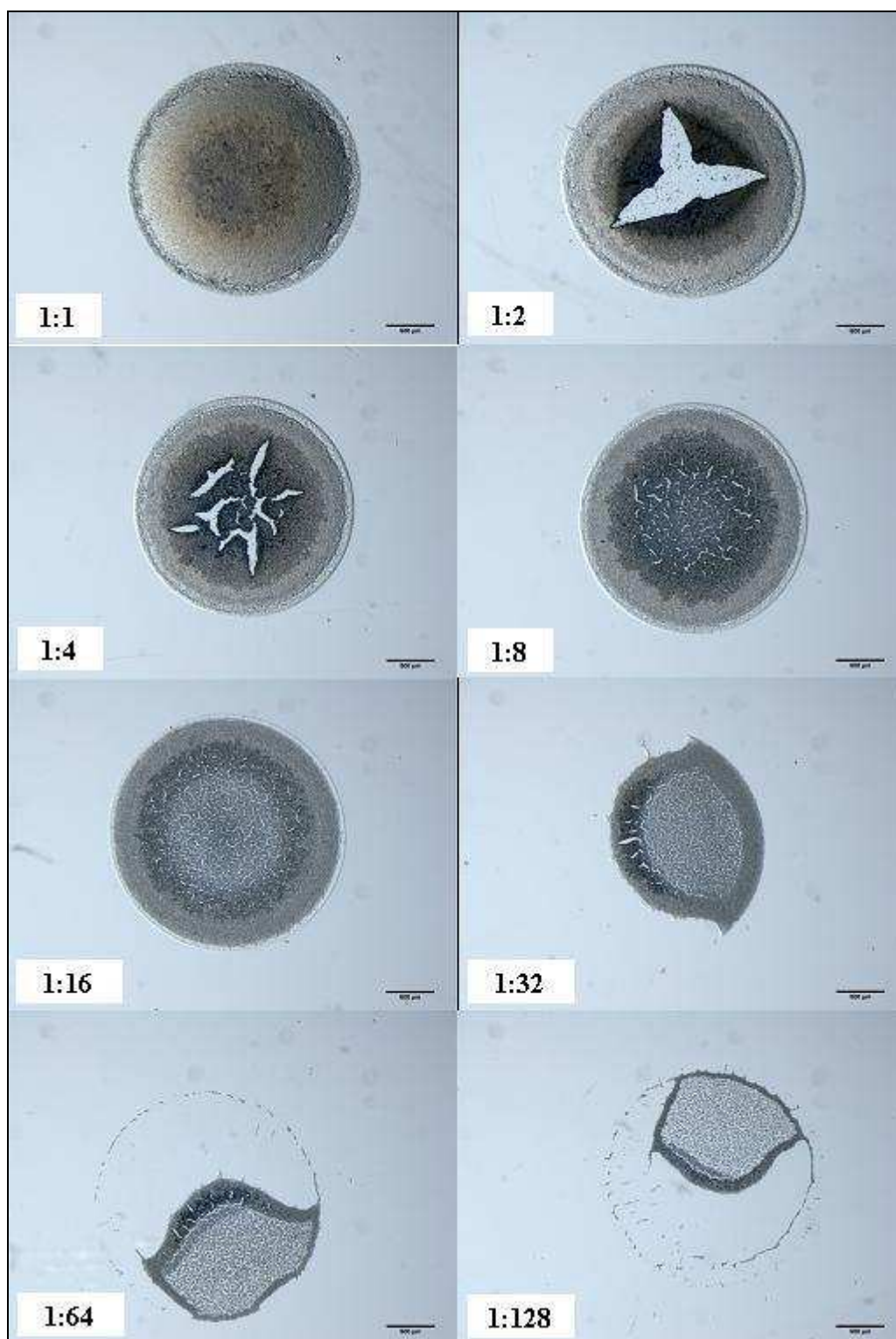


Figure 3.21. Deposition patterns obtained from evaporation of 5 µl of suspensions. The scale bars correspond to 500 µm.

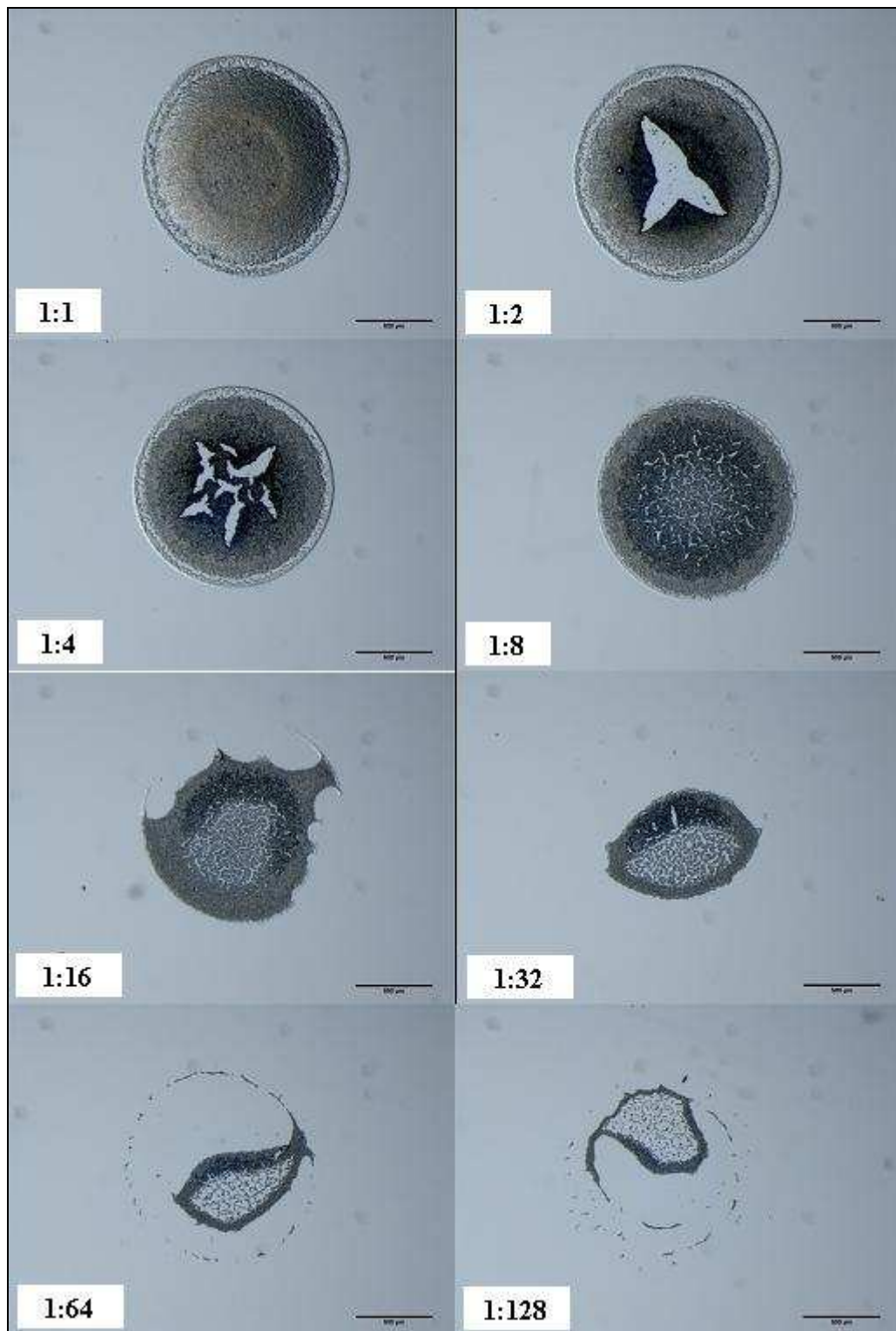


Figure 3.22. Deposition patterns obtained from evaporation of 1 μl of suspensions. The scale bars correspond to 500 μm .

The figures above show us that changing droplet volume on hydrophobic surfaces do not create distinct patterns. Evaporative deposition of cells ranging from 200 μl to 1 μl droplet volumes generated more or less similar patterns which resembled the patterns analyzed in the previous section. At high concentrations of cell depositions, the pattern was detached from the middle of the droplet area. At intermediate concentrations ring patterns formed as less cells remained in the middle part of the patterns. Since evaporation of the liquid parts of the droplets took longer times, cells had more chance to accumulate at the perimeters due to evaporation compensating convective outward flow.

To conclude, it is hard task to generate uniform cellular patterns on hydrophobic surfaces. On the other hand, it could be possible by using different liquids to suspend cells in it which may affect the flow of particles inside the droplets, as well as with appropriate cell concentrations and humidity.

3.2.2. Effects of Surface Hydrophilicity

In this part of the study, the effect of surface hydrophilicity was investigated. All suspensions at five different pH values and their diluted forms (except 1:256 dilution) prepared as explained in materials and methods section were spotted on hydrophilic glass slides in 5 μl and 50 μl volumes.

Before applying the procedure, it was known that since droplets spread widely and cover larger areas on hydrophilic surfaces, it was expected that at some suspension concentrations, nearly uniform cell coatings could be obtained. As seen on Figure 3.23, 3.24, 3.25 (patterns obtained from droplets 5 μl in volume), 3.31, 3.32, and 3.33 (patterns obtained from droplets 50 μl in volume), it was realized at high cell concentrations. At the other pH values, the aggregation of cells and sedimentation related to aggregation prevented uniformity of the cell coatings. At those pH values, some cells were carried to the perimeter of the droplets during drying by convective flow resulting in a nearly uniform packaging of cells. On the other hand, aggregation and related sedimentation of cells resulted in non-uniform patterns at the middle region of the coatings.

At low concentrations, it was clearly evident that deposition patterns were quite different than the patterns obtained on hydrophobic surfaces, that is to say, wide ring patterns were not observed on these patterns. Due to high wettability properties of the hydrophilic surfaces, droplets spread widely on the surface and as result, have small contact angles. In this study, droplets had vanishing contact angles on glass surfaces as shown on Figure 4.1. Therefore, sedimentation of the cells took less time, and because of this, convective flow could not carry the cells to the wedge.

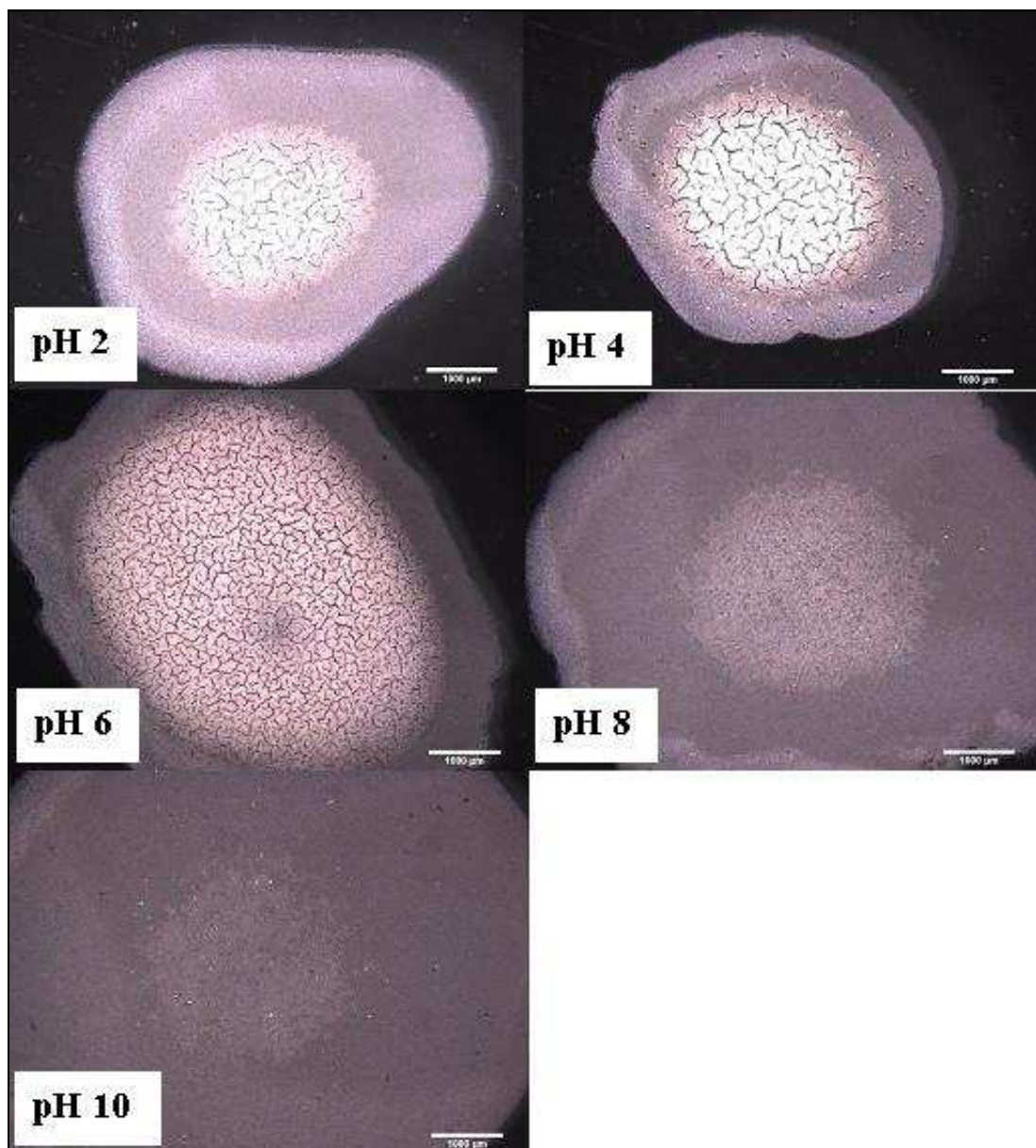


Figure 3.23. Patterns obtained from evaporative deposition of 5 µl of stock suspensions at five different pH values. The scale bars correspond to 1mm

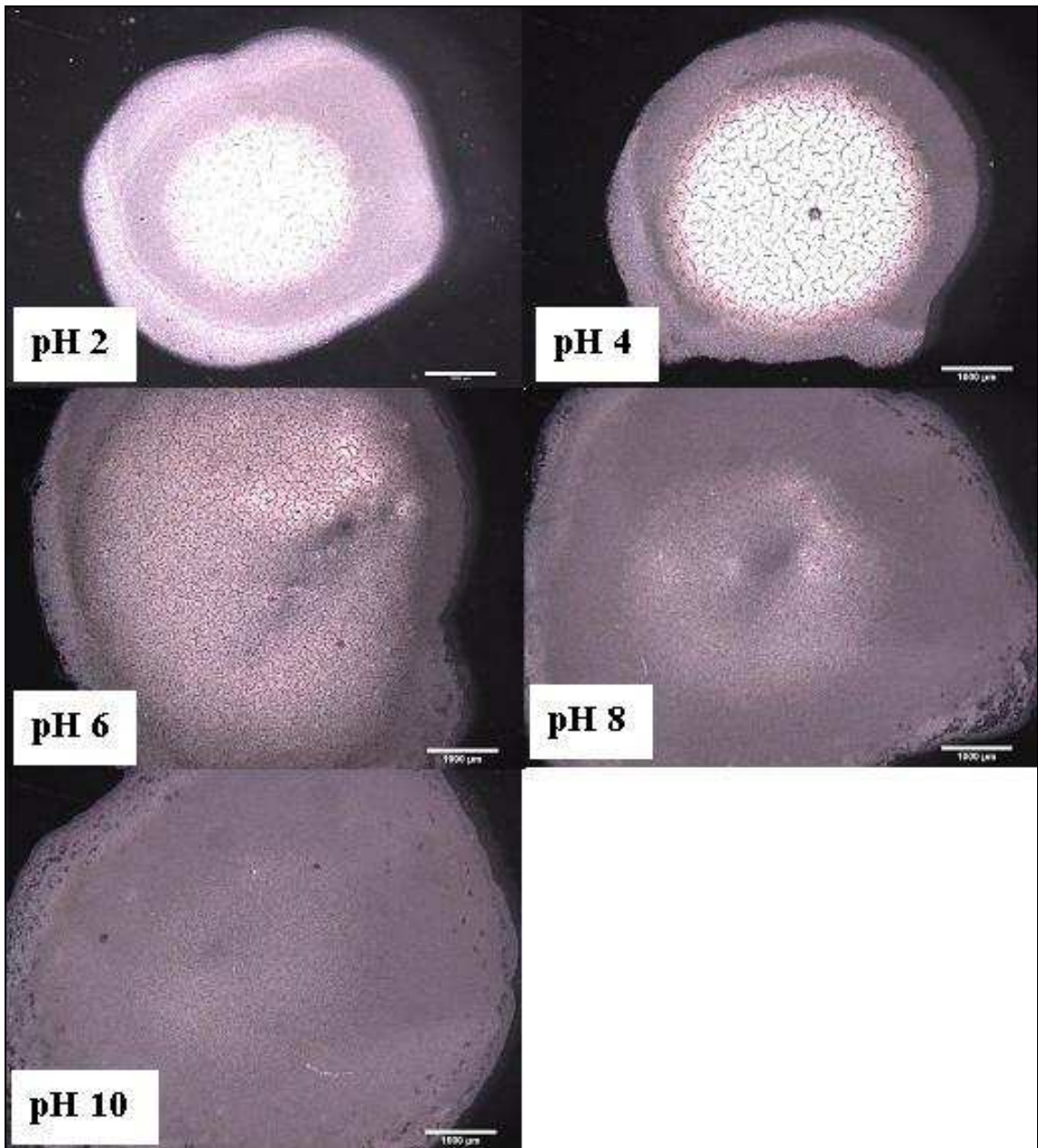


Figure 3.24. Patterns obtained from evaporative deposition of 5 μl of 1:2 diluted suspensions at five different pH values. The scale bars correspond to 1mm.

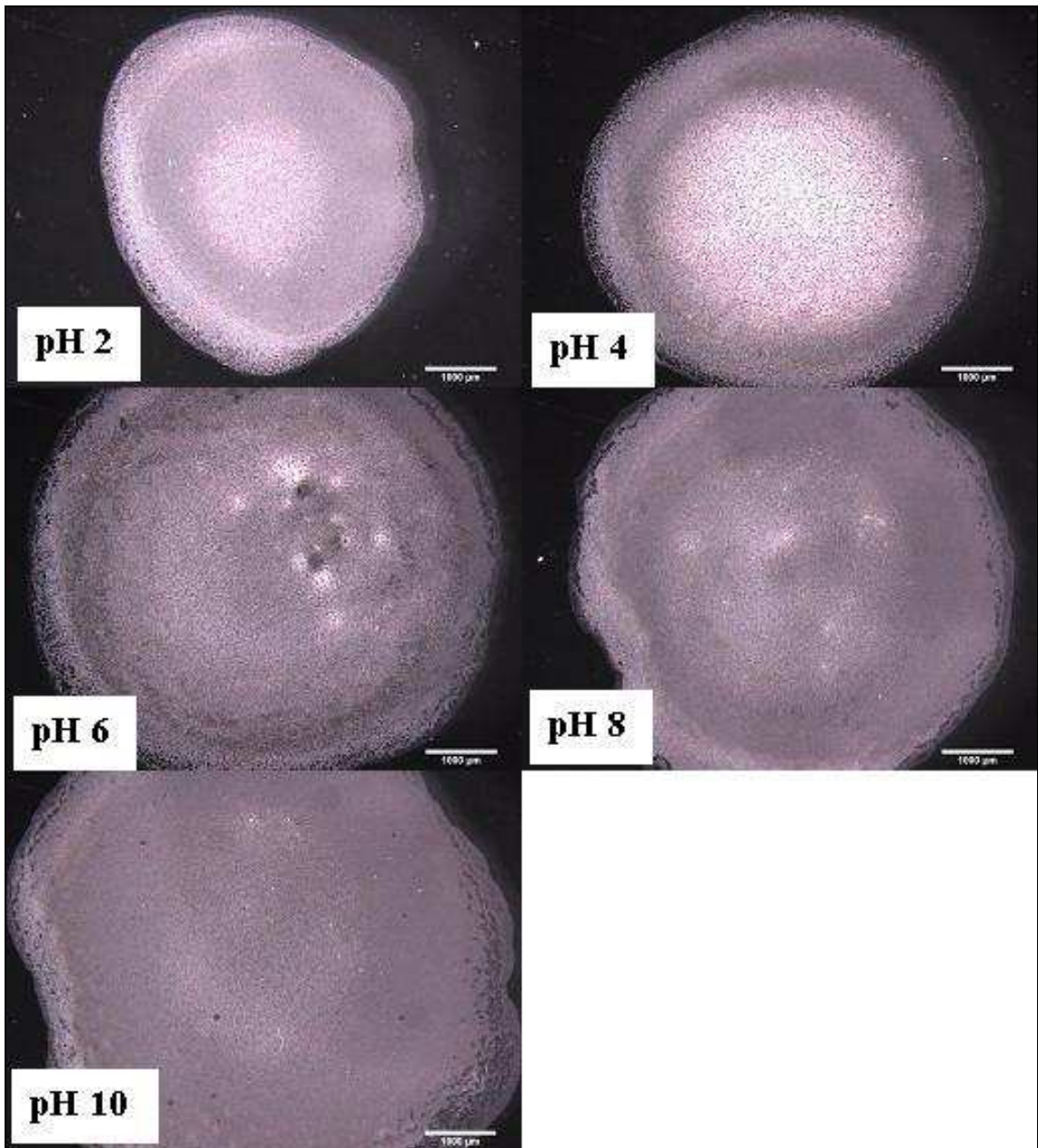


Figure 3.25. Patterns obtained from evaporative deposition of 4 μl of 1:4 diluted suspensions at five different pH values. The scale bars correspond to 1mm.

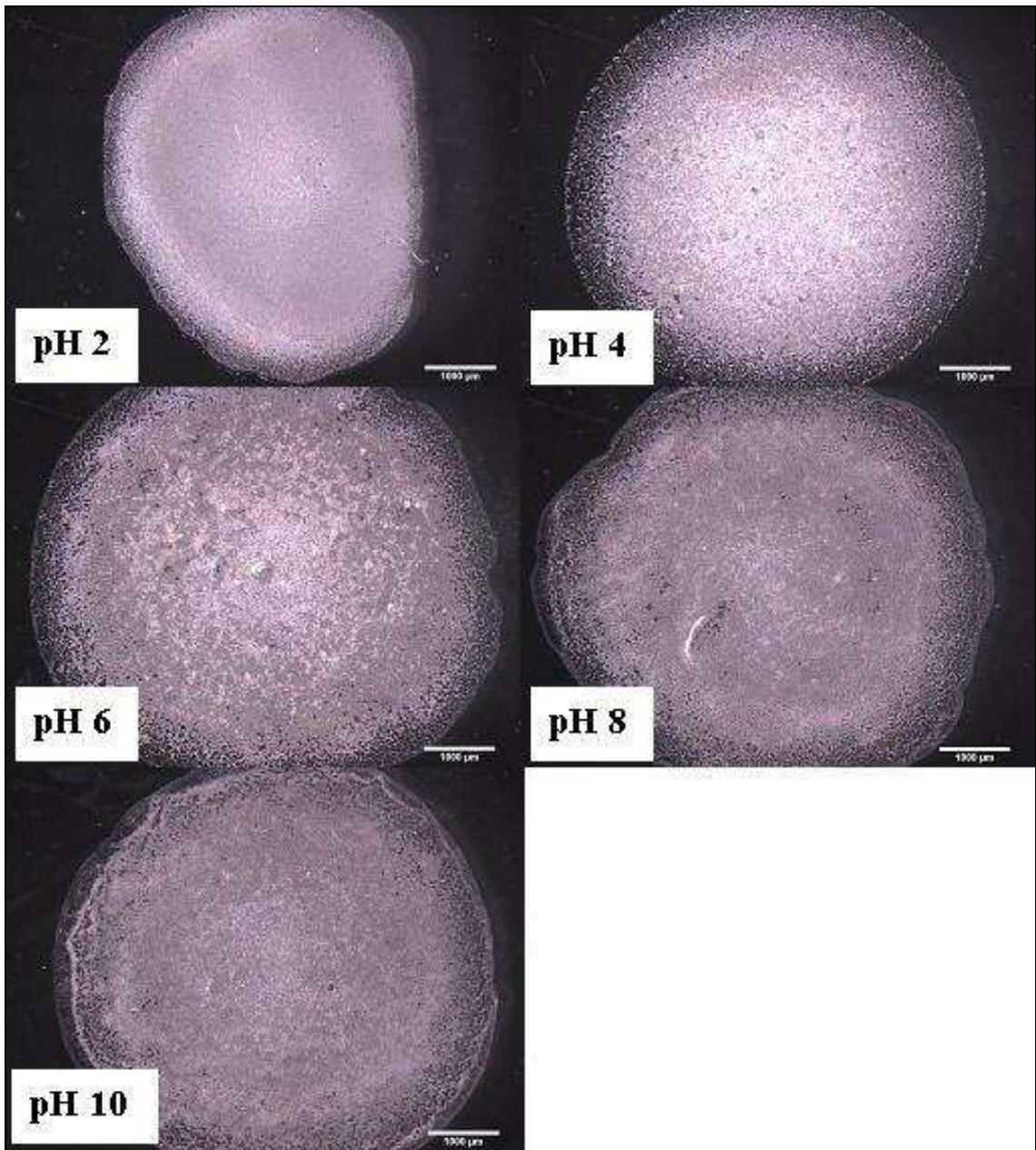


Figure 3.26. Patterns obtained from evaporative deposition of 5 μl of 1:8 diluted suspensions at five different pH values. The scale bars correspond to 500 μm .

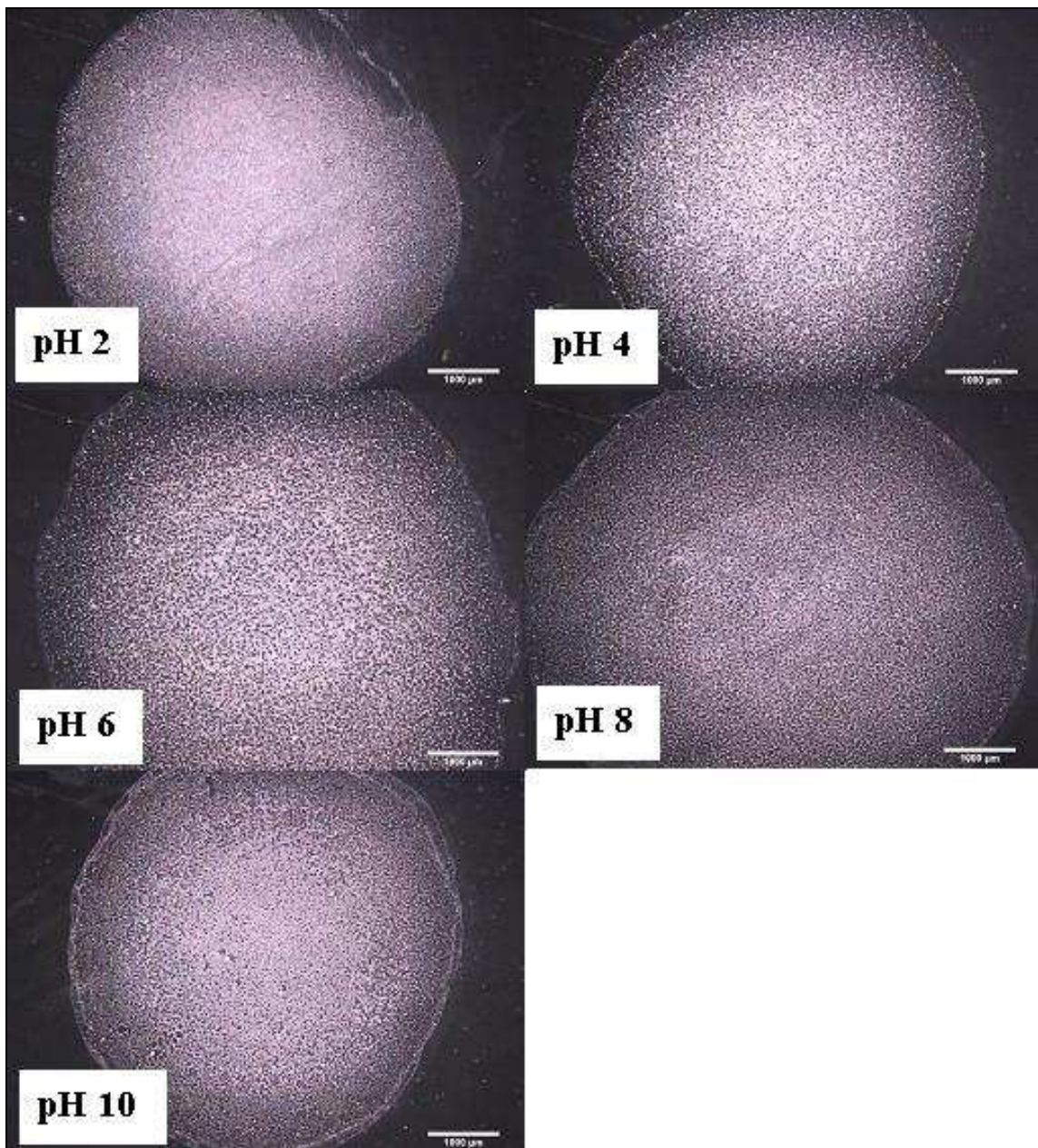


Figure 3.27. Patterns obtained from evaporative deposition of 5 μl of 1:16 diluted suspensions at five different pH values. The scale bars correspond to 500 μm .

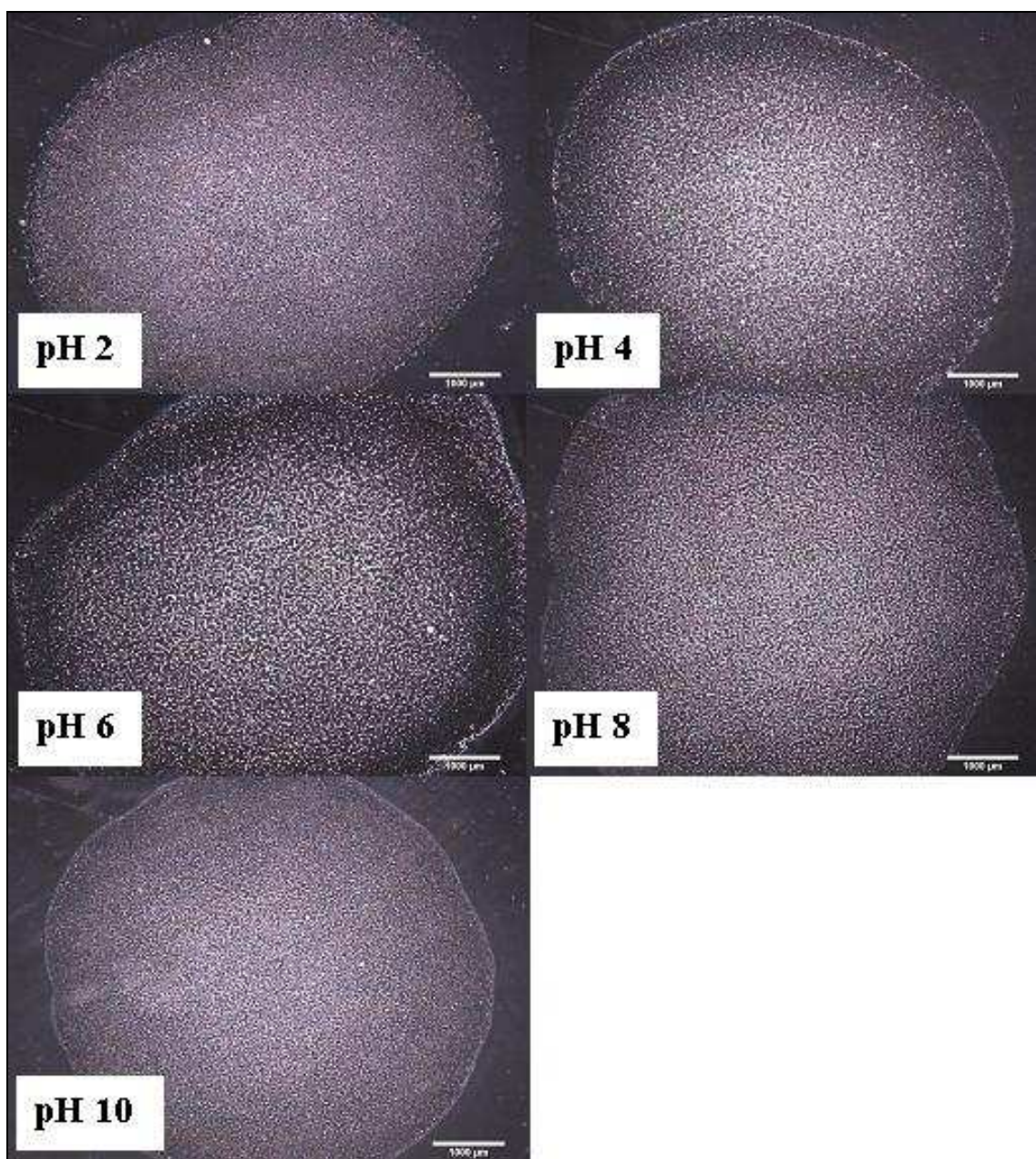


Figure 3.28. Patterns obtained from evaporative deposition of 5 μl of 1:32 diluted suspensions at five different pH values. The scale bars correspond to 1 mm.

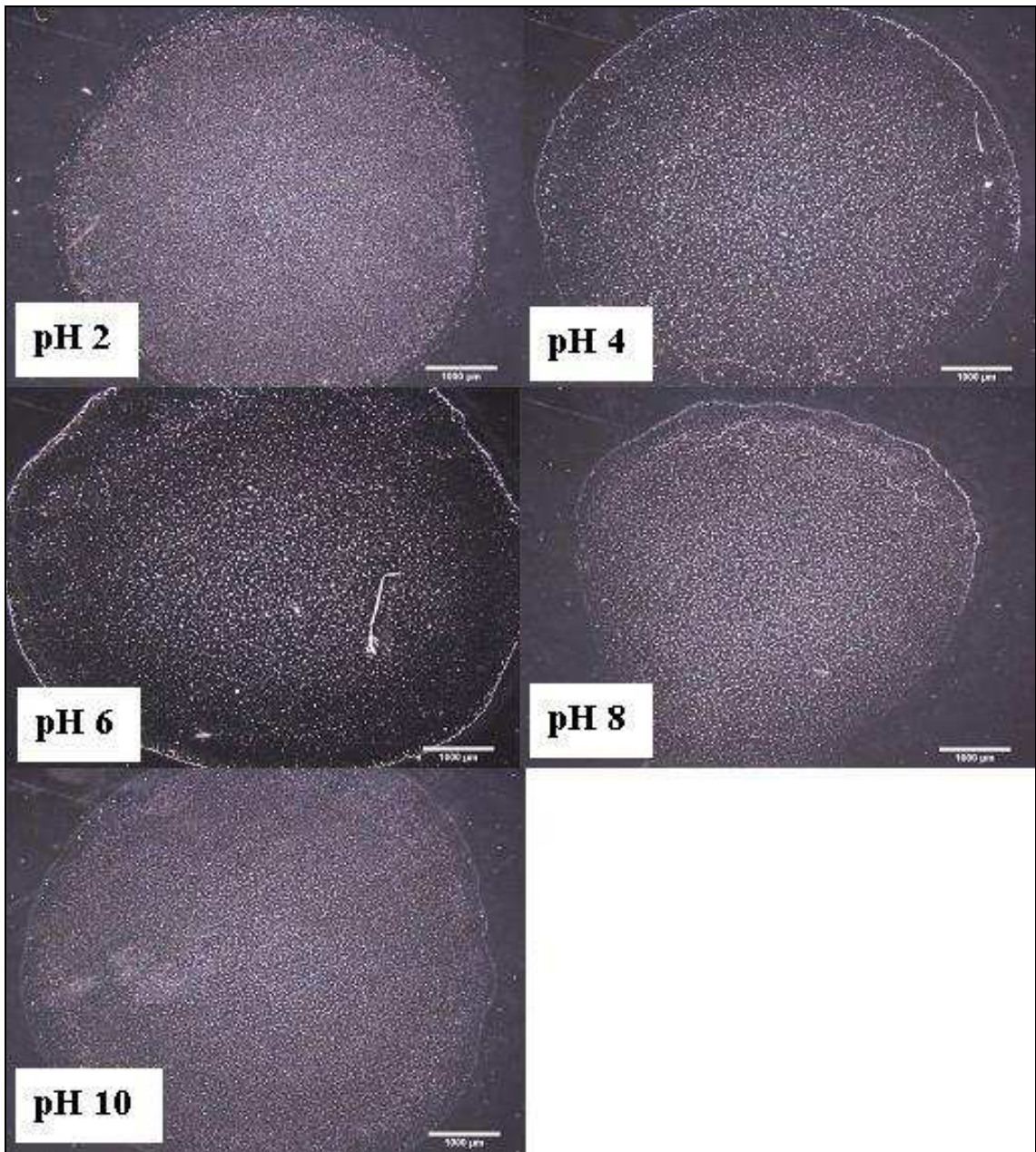


Figure 3.29. Patterns obtained from evaporative deposition of 5 μl of 1:64 diluted suspensions at five different pH values. The scale bars correspond to 1 mm.

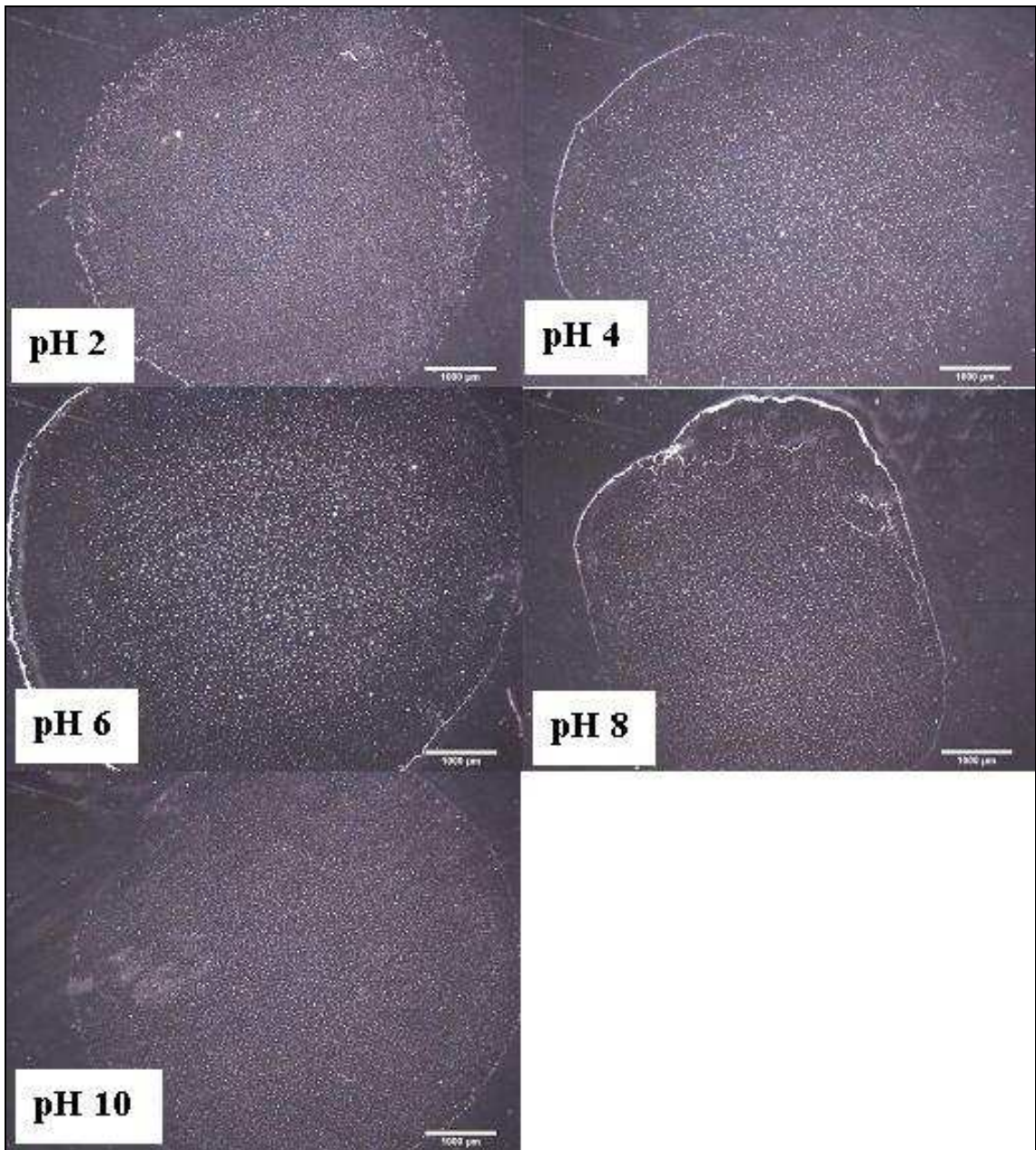


Figure 3.30. Patterns obtained from evaporative deposition of 5 μl of 1:128 diluted suspensions at five different pH values. The scale bars correspond to 1 mm.

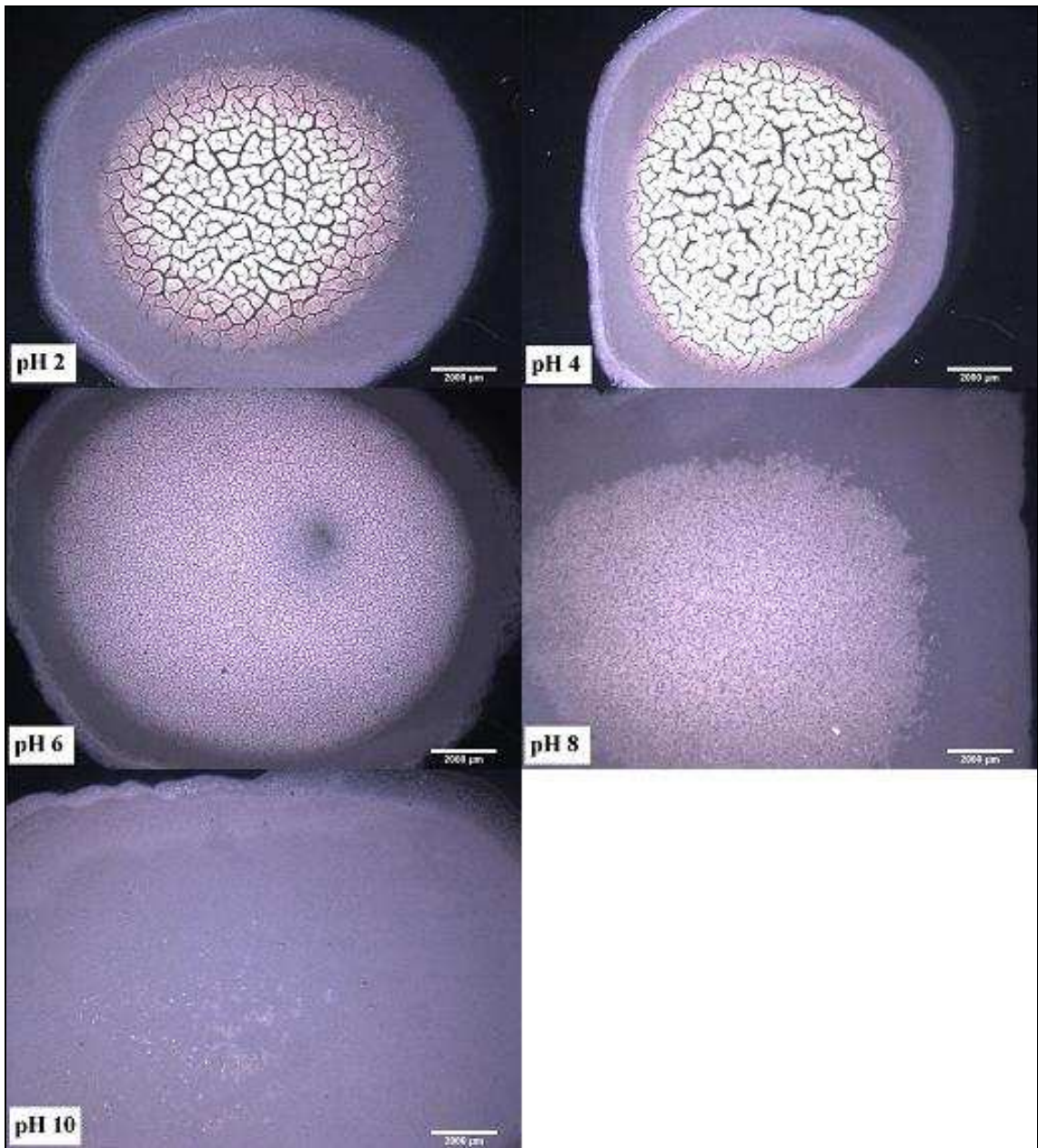


Figure 3.31. Patterns obtained from evaporative deposition of 50 μl of stock suspensions at five different pH values. The scale bars correspond to 2 mm.

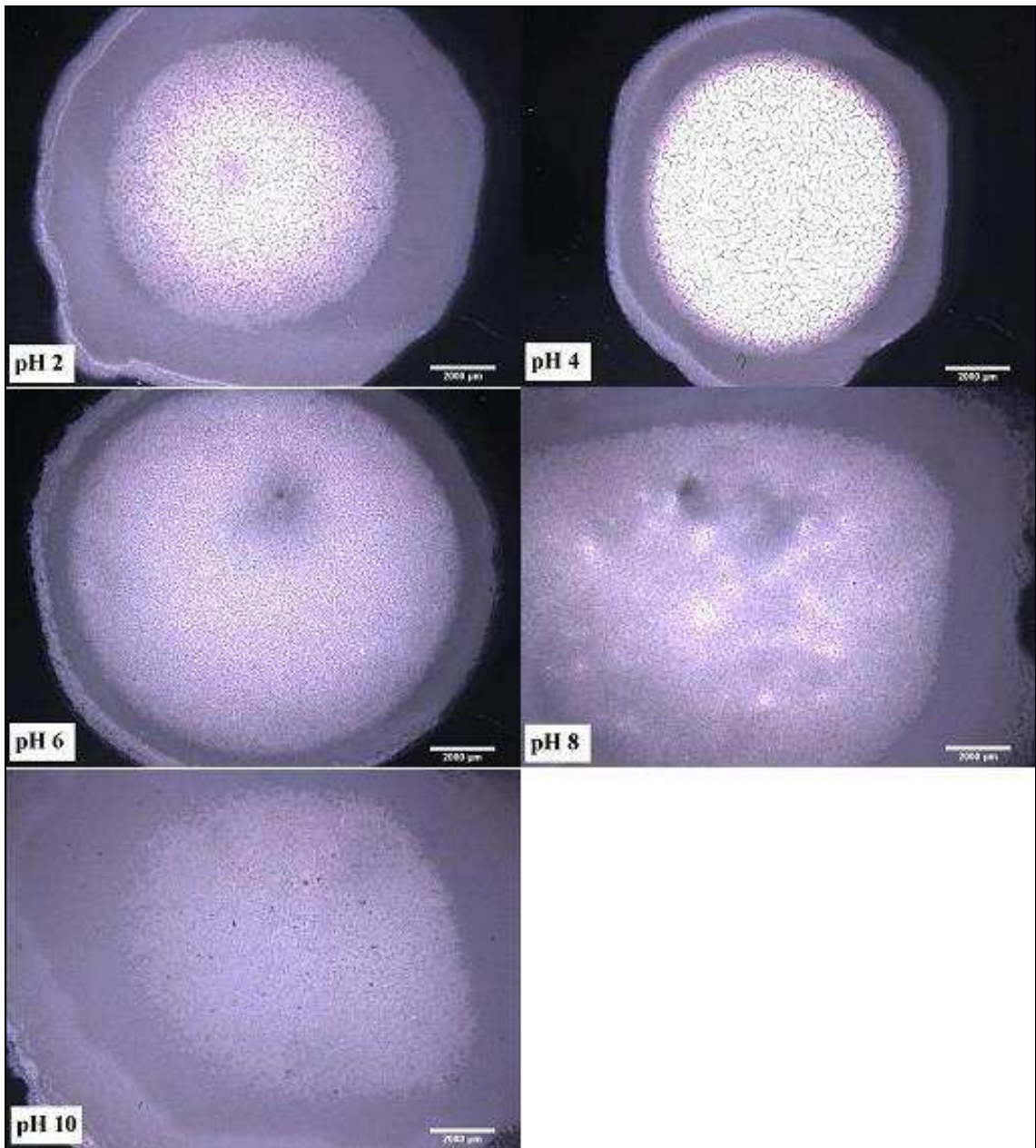


Figure 3.32. Patterns obtained from evaporative deposition of 50 μ l of 1:2 diluted suspensions at five different pH values. The scale bars correspond to 2 mm.

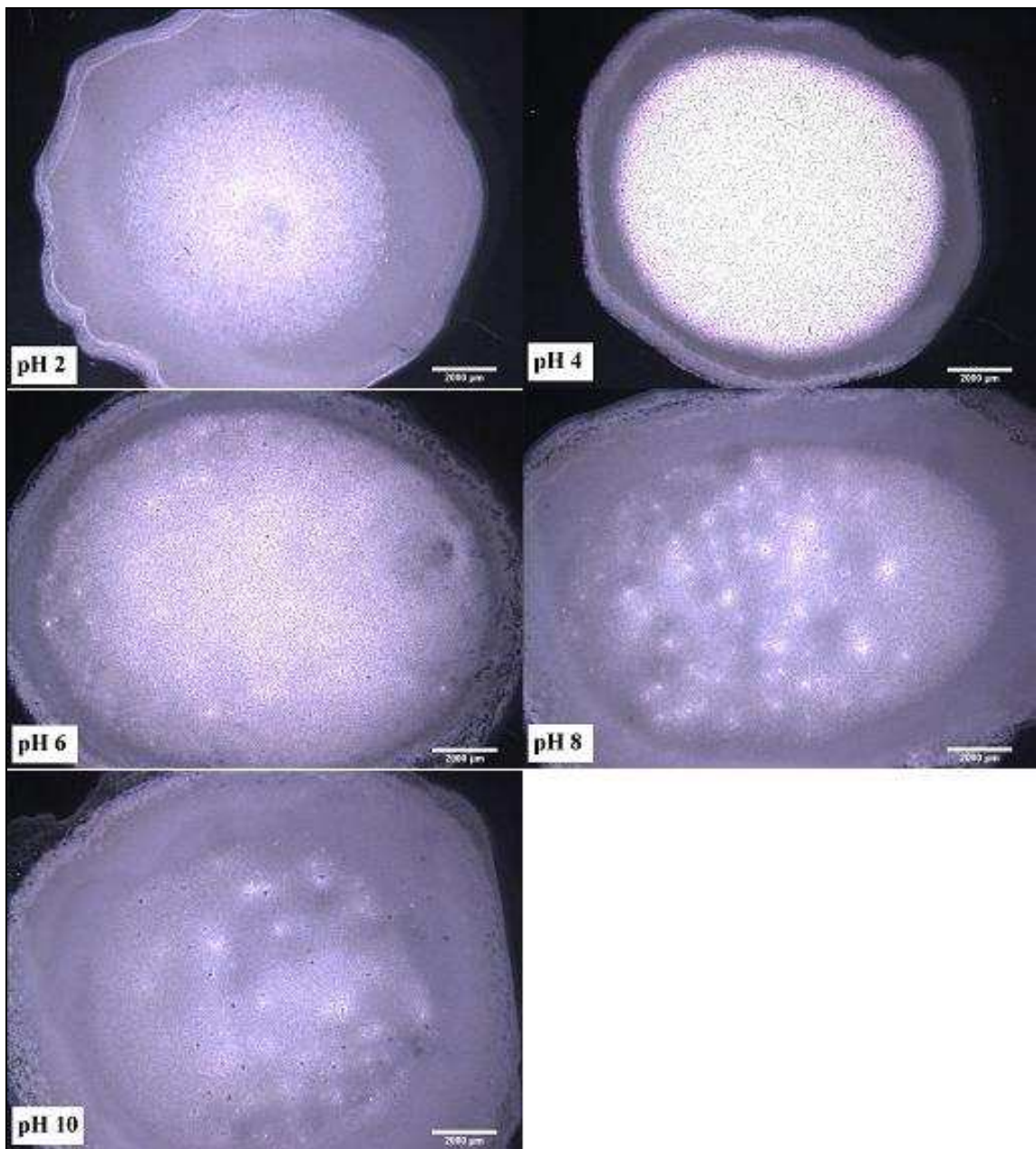


Figure 3.33. Patterns obtained from evaporative deposition of 50 μ l of 1:4 diluted suspensions at five different pH values. The scale bars correspond to 2 mm.

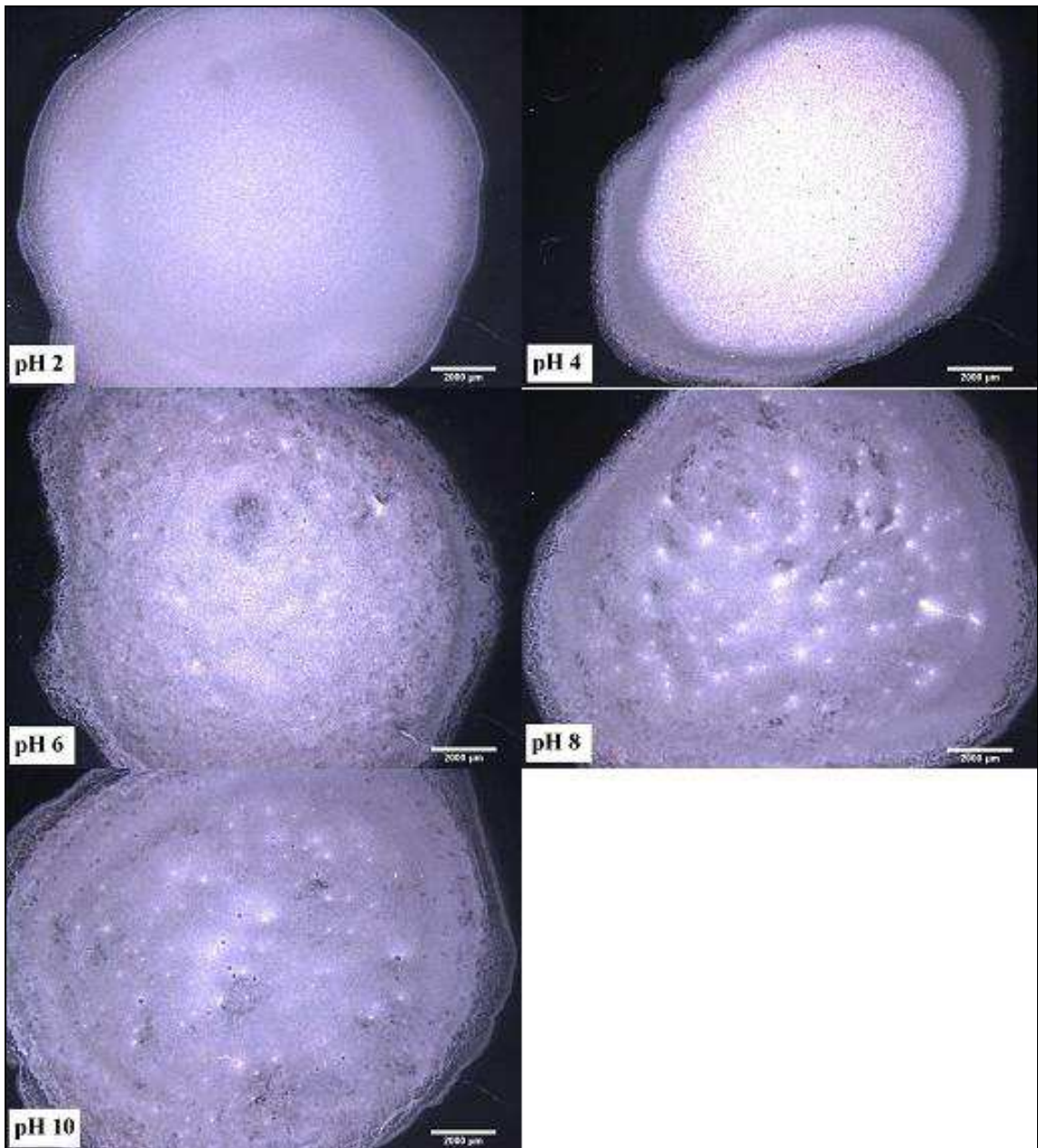


Figure 3.34. Patterns obtained from evaporative deposition of 50 μl of 1:8 diluted suspensions at five different pH values. The scale bars correspond to 2 mm.

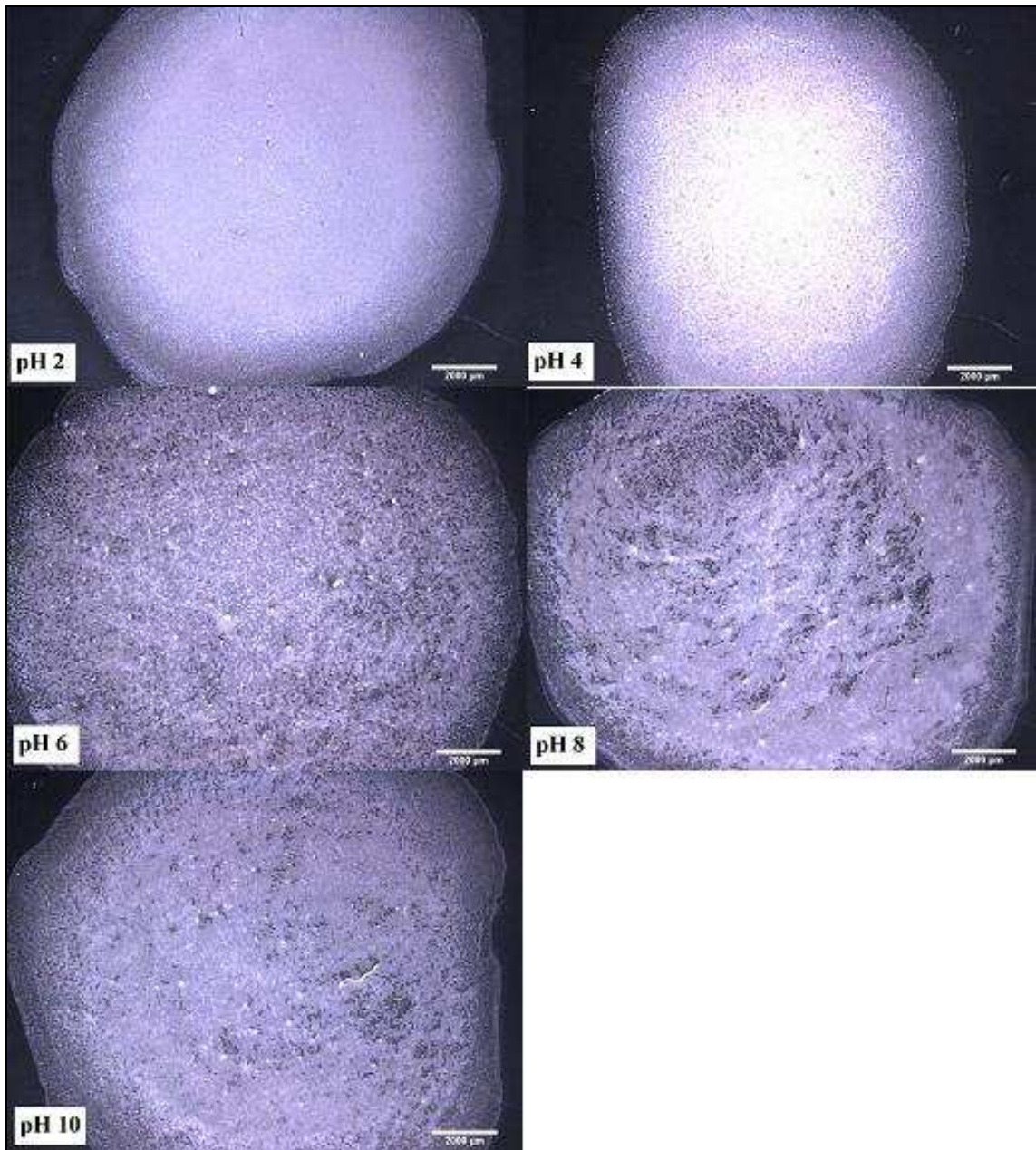


Figure 3.35. Patterns obtained from evaporative deposition of 50 μl of 1:16 diluted suspensions at five different pH values. The scale bars correspond to 2 mm.

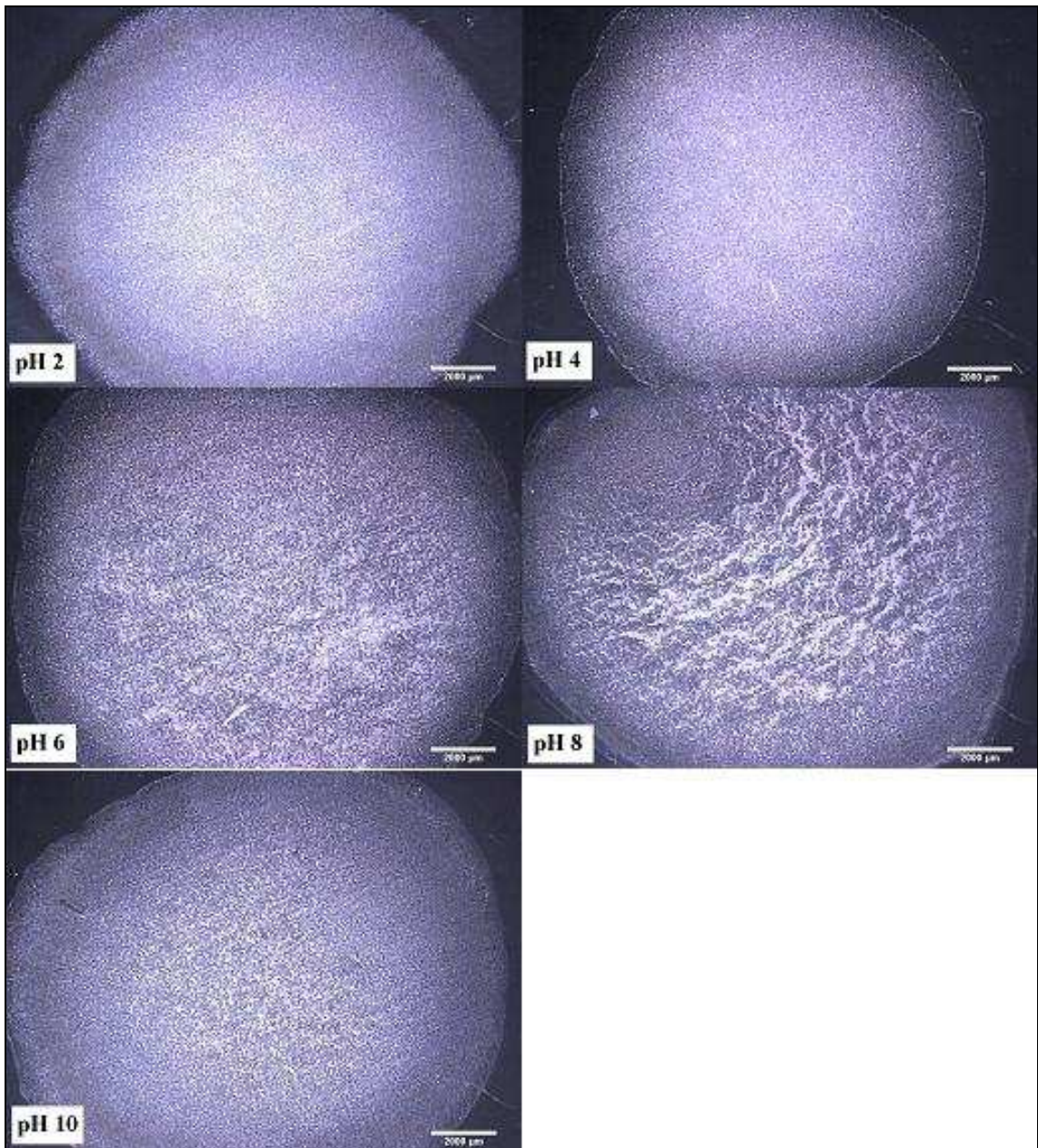


Figure 3.36. Patterns obtained from evaporative deposition of 50 μl of 1:32 diluted suspensions at five different pH values. The scale bars correspond to 2 mm.

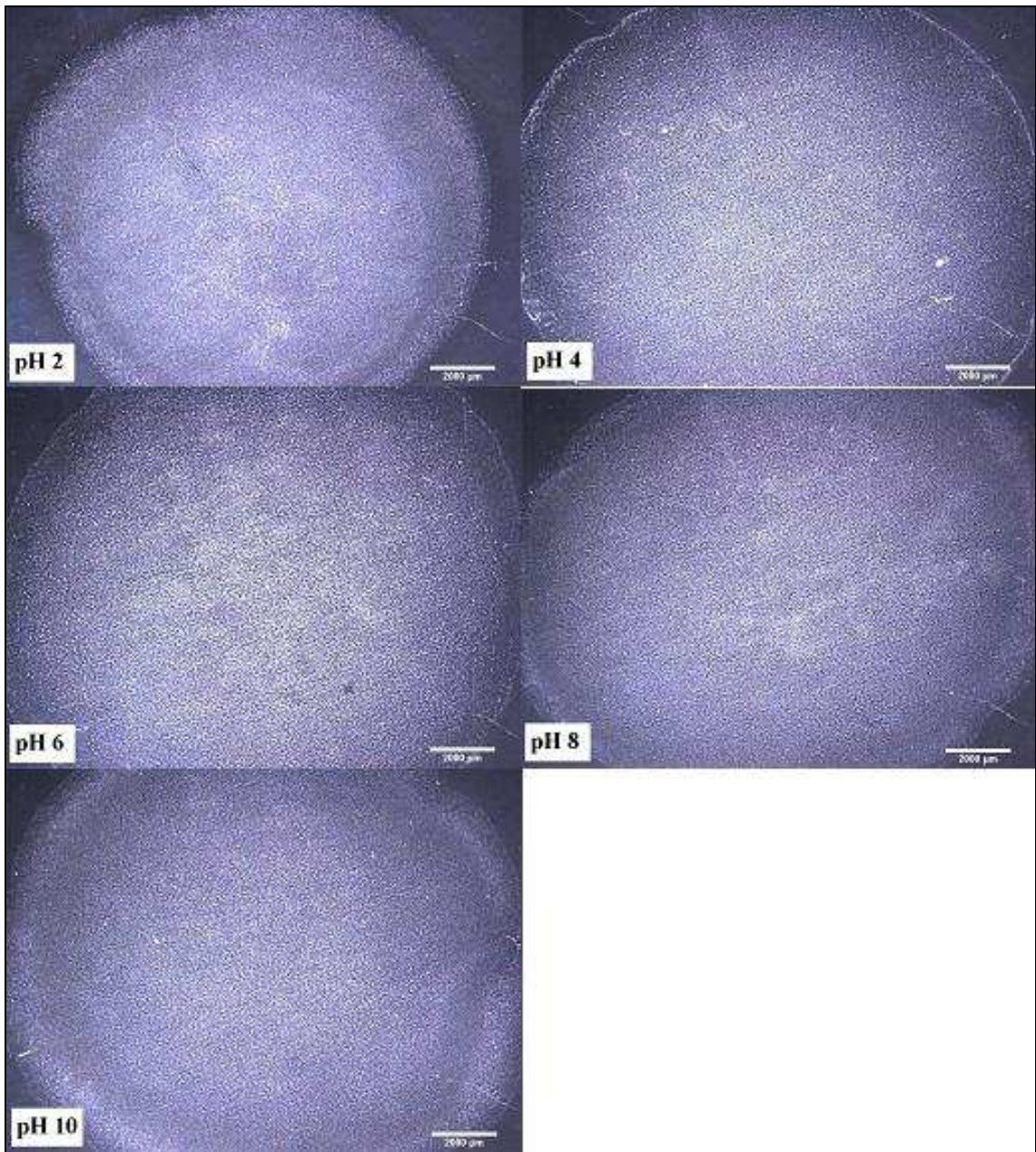


Figure 3.37. Patterns obtained from evaporative deposition of 50 μl of 1:64 diluted suspensions at five different pH values. The scale bars correspond to 2 mm.

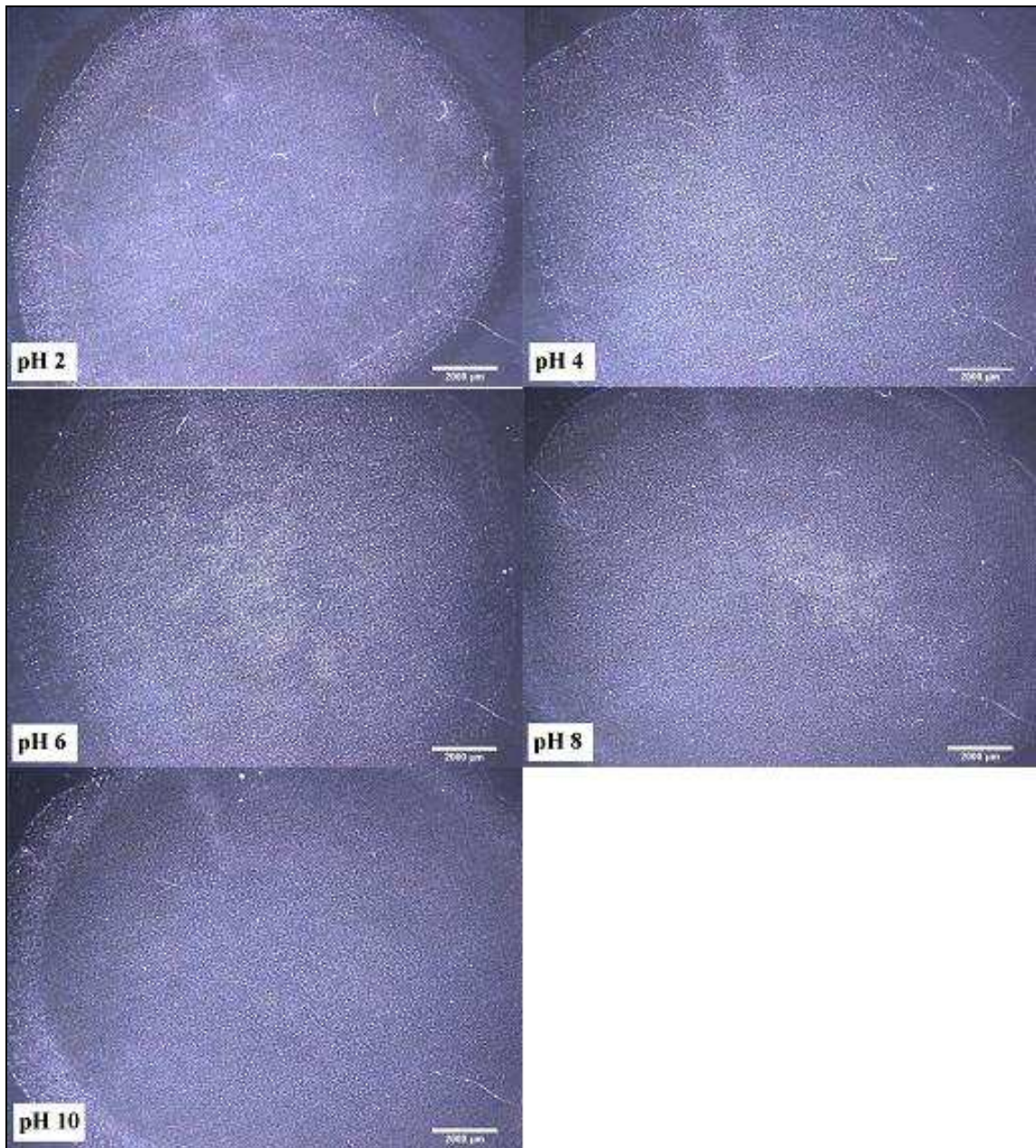


Figure 3.38. Patterns obtained from evaporative deposition of 50 μl of 1:128 diluted suspensions at five different pH values. The scale bars correspond to 2 mm.

3.3. CONVECTIVE ASSEMBLY

Deposition of yeast cells on surfaces by convective assembly had already been reported by Jerrim and Velev [73]. In their work, they reported the optimum operating stage velocity and optimum volume and concentration of the suspension of yeast cells injected between the slides to be able to obtain uniform cell coatings. Their suspension was at pH 8. In this part of the study, that reported work was repeated with some additions. In order to observe the effects of aggregation on cell coatings, convective assembly of the suspensions having pH values at 2, 4, 6, and 10 was also done along with that of suspension at pH 8.

Figure 3.39 demonstrates the results. At pH 2, 4, and 6, uniformity of the coatings were largely affected by aggregation and sedimentation. While the cells were pulled forward and deposited at the front of the meniscus by the help of convective flow, cells found enough time to aggregate at the back resulting in non-uniform coatings. On the other hand, at pH 8 and 10, electrostatic repulsion forces predominated between cells causing less aggregation, and this situation led to obtain relatively uniform coatings.

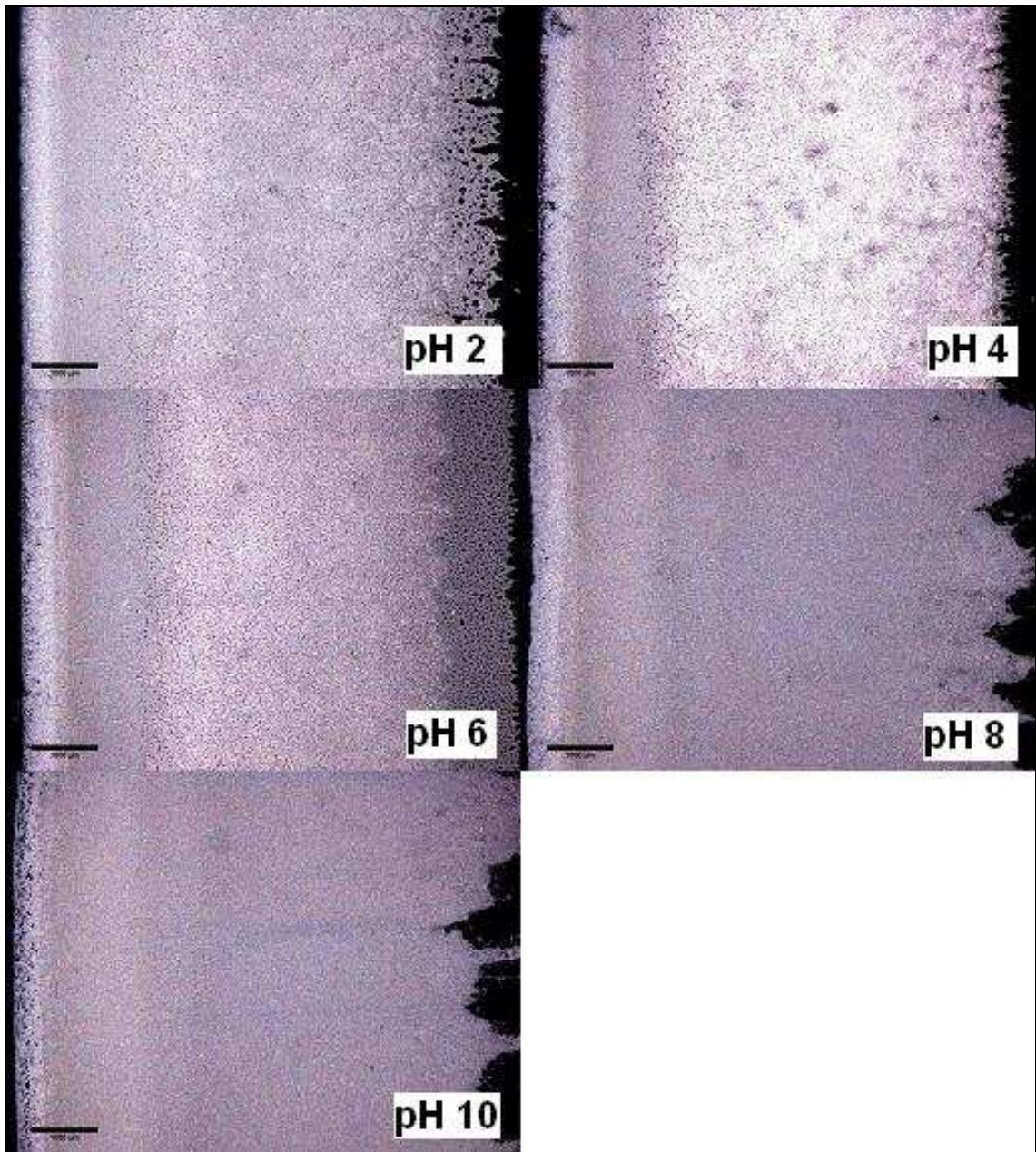


Figure 3.39. Coatings of the yeast cells by convective assembly at pH 2, 4, 6, 8, and 10

4. CONCLUSION and RECOMMENDATIONS

4.1. CONCLUSION

Being the simplest technique to deposit anything in suspensions onto surfaces, evaporative deposition of cells on surfaces in controllable ways has a wide variety of applications. By generating uniform cell coatings, efficiency of bioreactors may be improved. Biosensors obtained by this way offer new ways for further understanding of cell-cell, cell-environment, and cell-substrate interactions. Some toxicity studies may also be developed based on these coatings. Furthermore, with further study, it may open up some possibilities to get more information about biofilm initiation and formation.

In this study, *Saccharomyces cerevisiae* yeast cells were used as model eukaryotic organisms to obtain uniform cell coatings by droplet templating on hydrophobic and hydrophilic surfaces. Initially, the effects of pH on the formation of cell coatings were investigated by spotting 4 μ l of cell suspensions in a variety of concentration at five different pH values. It was found that suspensions at pH 2, 8, and 10 could be candidates for yielding uniform cell coatings. Since it is closer to physiological pH than the other pH values, for studies on hydrophobic surfaces, suspensions at pH 8 were used. It was observed that it was a hard task to obtain uniform cell coatings on such surfaces due to either detachment of coatings from surfaces at high concentrations and so called ring phenomena at intermediate and low concentrations. For studies on hydrophilic surfaces, suspensions at all pH values were used. It was found that since droplets spread widely on such surfaces having vanishing contact angles, uniform cell coatings at pH 8 and 10 could be obtained at higher cell concentrations. In the last part of the study, the coatings obtained by convective assembly process. By comparing the two techniques, it can be said that with proper experimentation, droplet templating of cells can be more powerful than convective assembly method to obtain uniform cell coatings on surfaces.

As a conclusion, the presented work offers a simple way with no complex instrumentation to deposit cells uniformly on surfaces which have possible uses in biotechnological and biomedical areas.

4.2. RECOMMENDATIONS

As a future work, in order to obtain uniform cell coatings, different kind of liquids having stronger Marangoni forces than water may be used. In addition, surfactant addition and changing the ionic strength of the suspensions by adding salts may alter the surface tension, and in turn, different patterns may be obtained.

Surfaces having intermediate contact angles between 10° and 98° may also result in distinct evaporation patterns.

REFERENCES

1. Velev, O. D. and K. H. Bhatt, "On-chip micromanipulation and assembly of colloidal particles by electric fields", *Soft Matter*, Vol. 2, No. 9, pp. 738-750, 2006.
2. Alp, B., G. M. Stephens and G. H. Markx, "Formation of artificial, structured microbial consortia (ASMC) by dielectrophoresis", *Enzyme and Microbial Technology*, Vol. 31, No. 1-1, pp. 35-43, 2002.
3. Chiou, P. Y., A. T. Ohta and M. C. Wu, "Massively parallel manipulation of single cells and microparticles using optical images", *Nature*, Vol. 436, No. 7049, pp. 370-372, 2005.
4. Pethig, R. and G. H. Markx, "Applications of dielectrophoresis in biotechnology", *Trends in Biotechnology*, Vol. 15, No. 10, pp. 426-432, 1997.
5. Pethig, R., Y. Huang, X. Wang and J. P. H. Burt, "Positive and negative dielectrophoretic collection of colloidal particles using interdigitated castellated microelectrodes" *Journal of Physics D: Applied Physics*, Vol. 25, No. 5, pp. 881-888, 1992.
6. Gong, T., D. T. Wu and D. W. M. Marr, "Electric Field-Reversible Three-Dimensional Colloidal Crystals", *Langmuir*, Vol. 19, No. 15, pp. 5967-5970, 2003.
7. Gong, T. and D. W. M. Marr, "Electrically Switchable Colloidal Ordering in Confined Geometries", *Langmuir*, Vol. 17, No. 8, pp. 2301-2304, 2001.
8. Sung, J. M., *Dielectrophoresis and Optoelectronic Tweezers for Nanomanipulation*, <http://large.stanford.edu/courses/2007/ph210/sung2.html>, 2007.
9. Jones, T. B., *Electromechanics of Particles*, Cambridge University Press, Cambridge, 1995.

10. Pohl, H. A., *Dielectrophoresis*, Cambridge University Press, Cambridge, 1978.
11. Markx, G. H. and R. Pethig, "Dielectrophoretic separation of cells: Continuous separation, *Biotechnology and Bioengineering*", Vol. 45, No. 4, pp. 337-343, 1995.
12. Markx, G. H., X. F. Zhou and R. Pethig, "Dielectrophoretic manipulation of micro-organisms in microelectrode arrays", *Proceedings of the 9th International Conference*, York, 2-5 April 1995, Vol. 143, pp. 145-148, Institute of Physics Publishing, Bristol, 1991.
13. Markx, G. H., Y. Huang, X. F. Zhou and R. Pethig, "Dielectrophoretic characterisation and separation of micro-organisms", *Microbiology*, Vol. 140, No. 3, pp. 585-591, 1994.
14. Markx, G. H., M. S. Talary and R. Pethig, "Separation of viable and non-viable yeast using dielectrophoresis", *Journal of Biotechnology*, Vol. 32, No. 1, pp. 29-37, 1994.
15. Burt, J. P. H., T. A. K. Al-Ameen and R. Pethig, "An optical dielectrophoresis spectrometer for low-frequency measurements on colloidal suspensions", *Journal of Physics E: Scientific Instruments*, Vol. 22, No. 11, pp. 952-557, 1989.
16. Price, J. A. R., J. H. Burt and R. Pethig, "Applications of a new optical technique for measuring the dielectrophoretic behaviour of micro-organisms. *Biochimica et Biophysica Acta*, Vol. 964, No. 2, pp. 221-230, 1988.
17. Markx, G. H., P. A. Dyda and R. Pethig, "Dielectrophoretic separation of bacteria using a conductivity gradient", *Journal of Biotechnology*, Vol. 51, No. 2, pp. 175-180, 1996.
18. Gupta, S., R. G. Alargova, P. K. Kilpatrick and O. D. Velev, "On-Chip Dielectrophoretic Coassembly of Live Cells and Particles into Responsive Biomaterials", *Langmuir*, Vol. 26, No. 5, pp. 3441-3452, 2010.

19. Gross, G. W., B. K. Rhoades, H. M. E. Azzazy and M. C. Wu, "The use of neuronal networks on multielectrode arrays as biosensors", *Biosensors and Bioelectronics*, Vol. 10, No. 6-7, pp. 553-557, 1995.
20. D. R. Jung, D. S. Cuttino, J. J. Pancrazio, P. Manos, T. Cluster, R. S. Sathanoori, L. E. Aloï and M. G. Coulombe, "Cell-based sensor microelectrode array characterized by imaging X-ray photoelectron spectroscopy, scanning electron microscopy, impedance measurements, and extracellular recordings", *Journal of Vacuum Science and Technology A*, Vol. 16, No. 3, pp. 1183-1188, 1998.
21. Mrksich, M and G. M. Whitesides, "Patterning self-assembled monolayers using microcontact printing: A new technology for biosensors?", *Trends in Biotechnology*, Vol. 13, No. 6, pp. 228-235, 1995.
22. Pacrazio, J. J., P. P. Bey, A. Loloee, S. Manne, H. C. Chao, L. L. Howard, W. M. Gosney, D. A. Borkholder, G. T. A. Kovacs, P. Manos, D. S. Cuttino and D. A. Stenger, "Description and demonstration of a CMOS amplifier-based-system with measurement and stimulation capability for bioelectrical signal transduction" *Biosensors and Bioelectronics*, Vol. 13, No. 9, pp. 971-979, 1998.
23. Kewley, D. T., M. D. Hills, D. A. Borkholder, I. E. Opris, N. I. Maluf, C. W. Storment, J. M. Bower and G. T. A. Kovacs, "Plasma-etched neural probes", *Sensors and Actuators A: Physical*, Vol. 58, No. 1, pp. 27-35, 1997.
24. Folch, A. and M. Toner, "Cellular Micropatterns on Biocompatible Materials", *Biotechnology Progress*, Vol. 14, No. 3, pp. 388-392, 2008.
25. Singhvi, R., A. Kumar, G. P. Lopez, G. N. Stephanopoulos, D. I. Wang, G. M. Whitesides and D. E. Ingber, "Engineering cell shape and function", *Science*, Vol. 264, No. 5159, pp. 696-698, 1994.

26. Chen, C. S., M. Mrksich, S. Huang, G. M. Whitesides and D. E. Ingber, "Geometric control of cell life and death", *Science*, Vol. 276, No. 5317, pp. 1425-1428, 1997.
27. Lopez, G. P., M. W. Albers, S. L. Schreiber, R. Carroll, E. Peralta and G. M. Whitesides, "Convenient methods for patterning the adhesion of mammalian cells to surfaces using self-assembled monolayers of alkanethiolates on gold", *Journal of the American Chemical Society*, Vol. 115, No. 13, pp. 5877-5878, 1993.
28. Mrksich, M., C. S. Chen, Y. Xia, L. E. Dike, D. E. Ingber and G. M. Whitesides, "Controlling cell attachment on contoured surfaces with self-assembled monolayers of alkanethiolates on gold", *Proceedings of the National Academy of Sciences*, Vol. 93, No. 20, pp. 10775-10778, 1996.
29. Britland, S., E. Perezarnaud, P. Clark, B. McGinn, P. Connolly and G. Moores, "Micropatterning Proteins and Synthetic Peptides on Solid Supports: A Novel Application for Microelectronics Fabrication Technology", *Biotechnology Progress*, Vol. 8, No. 2, pp. 155-160, 1992.
30. Lom, B., K. E. Healy and P. E. Hockberger, "A versatile technique for patterning biomolecules onto glass coverslips", *Journal of Neuroscience Methods*, Vol. 50, No. 3, pp. 385-397, 1993.
31. Healy, K. E., C. H. Thomas, A. Rezania, J. E. Kim, P. J. McKeown, B. Lom and P. E. Hockberger, "Kinetics of bone cell organization and mineralization on materials with patterned surface chemistry", *Biomaterials*, Vol. 17, No. 2, pp. 195-208, 1996.
32. Kleinfeld, D., K. H. Kahler and P. E. Hockberger, , "Controlled outgrowth of dissociated neurons on patterned substrates", *The Journal of Neuroscience*, Vol. 8, No. 11, pp. 4098-4120, 1988.

33. Mohammed, J. S., M. A. DeCoster and M. J. McShane, "Micropatterning of Nanoengineered Surfaces to Study Neuronal Cell Attachment in Vitro", *Biomacromolecules*, Vol. 5, No. 5, pp. 1745-1755, 2004.
34. Revzin, A., R. G. Tompkins and M. Toner, "Surface Engineering with Poly(ethylene glycol) Photolithography to Create High-Density Cell Arrays on Glass", *Langmuir*, Vol. 19, No. 23, pp. 9855-9862, 2003.
35. Karp, J. M., Y. Yeo, W. Geng, C. Cannizarro, K. Yan, D. S. Kohane, G. Vunjak-Novakovic, R. S. Langer and M. Radisic, "A photolithographic method to create cellular micropatterns", *Biomaterials*, Vol. 27, No. 27, pp. 4755-4764, 2006.
36. Yap, F. L. and Y. Zhang, "Protein and cell micropatterning and its integration with micro/nanoparticles assembly", *Biosensors and Bioelectronics*, Vol. 22, No. 6 pp. 775-788, 2007.
37. Xia, Y. N. and G. M. Whitesides, "Soft lithography", *Annual Review of Materials Science*, Vol. 28, pp. 153-184, 1998.
38. Kane, R. S., S. Takayama, E. Ostuni, D. E. Ingber and G. M. Whitesides, "Patterning proteins and cells using soft lithography", *Biomaterials*, Vol. 20, No. 23-24, pp. 2363-2376, 1999.
39. Kam, L. and S. G. Boxer, "Cell adhesion to protein-micropatterned-supported lipid bilayer membranes", *Journal of Biomedical Materials Research*, Vol. 55, No. 4, pp. 487-945, 2001.
40. Cuvelier, D., O. Rossier, P. Bassereau and P. Nassoy, "Micropatterned "adherent/repellent" glass surfaces for studying the spreading kinetics of individual red blood cells onto protein-decorated substrates", *European Biophysics Journal with Biophysics Letters*, Vol. 32, No. 4, pp. 342-354, 2003.

41. Folch, A., B. H. Jo, O. Hurtado, D. J. Beebe and M. Toner, "Microfabricated elastomeric stencils for micropatterning cell cultures", *Journal of Biomedical Materials Research*, Vol. 52, No. 2, pp. 346-353, 2000.
42. John, P. M. S., L. Kam, S. W. Turner, H.G. Craighead, M. Issacson, J. N. Turner and W. J. Shain, "Preferential glial cell attachment to microcontact printed surfaces", *Journal of Neuroscience Methods*, Vol. 75, No. 2, pp. 171-177, 1997.
43. Bhatia, S. N., U. J. Balis, M. L. Yarmush and M. Toner, "Microfabrication of Hepatocyte/Fibroblast Co-cultures: Role of Homotypic Cell Interactions", *Biotechnology Progress*, Vol. 14, No. 3, pp. 378-387, 1998.
44. Mrksich, M., L. E. Dike, J. Tien, D. E. Ingber and G. M. Whitesides, "Using microcontact printing to pattern the attachment of mammalian cells to self-assembled monolayers of alkanethiolates on transparent films of gold and silver", *Experimental Cell Research*, Vol. 235, No. 2, pp. 305-313, 1997.
45. Lee, K. B., D. J. Kim, Z. W. Lee, S. I. Woo and I. S. Choi, "Pattern Generation of Biological Ligands on a Biodegradable Poly(glycolic acid) Film", *Langmuir*, Vol. 20, No. 7, pp. 2531-2535, 2004.
46. Csucs, G., R. Michel, J. W. Lussi, M. Textor and G. Danuser, "Microcontact printing of novel co-polymers in combination with proteins for cell-biological applications", *Biomaterials*, Vol. 24, No. 10, pp. 1713-1720, 2003.
47. Yeung, C. K., L. Lauer, A. Offenhausser and W. Knoll, "Modulation of the growth and guidance of rat brain stem neurons using patterned extracellular matrix proteins", *Neuroscience Letters*, Vol. 301, No. 2, pp. 147-150, 2001.
48. Veiseh, M., B. T. Wickes, D. G. Castner and M. Zhang, "Guided cell patterning on gold-silicon dioxide substrates by surface molecular engineering", *Biomaterials*, Vol. 25, No. 16, pp. 3315-3324, 2004.

49. Krol, S., M. Nolte, A. Diaspro, D. Mazza, R. Magrassi, A. Gliozzi and A. Fery, "Encapsulated Living Cells on Microstructured Surfaces", *Langmuir*, Vol. 21, No. 2, pp. 705-709, 2005.
50. Denkov, N. D., O. D. Velev, P. A. Kralchevsky, I. B. Ivanov, H. Yoshimura and K. Nagayama, "Mechanism of formation of two-dimensional crystals from latex particles on substrates", *Langmuir*, Vol. 8, No. 12, pp. 3183-3190, 1992.
51. Dimitrov, A. S. and K. Nagayama, "Continuous Convective Assembling of Fine Particles into Two-Dimensional Arrays on Solid Surfaces", *Langmuir*, Vol. 12, No. 5, pp. 1303-1311, 1996.
52. Prevo, B. G., D. M. Kuncicky, O. D. Velev, "Engineered deposition of coatings from nano- and micro-particles: A brief review of convective assembly at high volume fraction", *Colloids and Surfaces A: Physicochemical and Engineering Aspects*, Vol. 311, No. 1-3, pp. 2-10, 2007.
53. Prevo, B. G. And O. D. Velev, "Controlled, Rapid Deposition of Structured Coatings from Micro- and Nanoparticle Suspensions", *Langmuir*, Vol. 20, No. 6, pp 2099-2107, 2004.
54. Yuan, Z., D. N. Petsev, B. G. Prevo, O. D. Velev and P. Atanassov, "Two-Dimensional Nanoparticle Arrays Derived from Ferritin Monolayers", *Langmuir*, Vol. 23, No. 10, pp. 5498-5504, 2007.
55. Kuncicky, D. M., R. R. Naik and O. D. Velev, "Rapid Deposition and Long-Range Alignment of Nanocoatings and Arrays of Electrically Conductive Wires from Tobacco Mosaic Virus", *Small*, Vol. 2, No.12, pp. 1462-1466, 2006.
56. Kitaev, V. and G. Ozin, "Self-Assembled Surface Patterns of Binary Colloidal Crystals" *Advanced Materials*, Vol. 15, No. 1, pp. 75-78, 2003.

57. Wang, Y., L. Chen, H. Yang, Q. Guo, W. Zhou and M. Tao, "Spherical antireflection coatings by large-area convective assembly of monolayer silica microspheres", *Solar Energy Materials and Solar Cells*, Vol. 93, No. 1, pp. 85-91, 2009.
58. Kuncicky, D. M., S. D. Christesen and O.D. Velev, "Role of the Micro- and Nanostructure in the Performance of Surface-Enhanced Raman Scattering Substrates Assembled from Gold Nanoparticles", *Applied Spectroscopy*, Vol. 59, No. 4, pp. 401-409, 2005.
59. Kahraman, M., M. M. Yazici, F. Sahin and M. Culha, "Convective Assembly of Bacteria for Surface-Enhanced Raman Scattering", *Langmuir*, Vol. 24, No. 3, pp. 894-901, 2008.
60. Jerrim, L. B. and O. D. Velev, "Deposition of Coatings from Live Yeast Cells and Large Particles by "Convective-Sedimentation" Assembly", *Langmuir*, Vol. 25, No. 10, pp. 5692-5702, 2009.
61. Shen, X., C-M. Ho and T-S. Wong, "Minimal Size of Coffee Ring Structure", *The Journal of Physical Chemistry B*, Vol. 114, No. 16, pp. 5269-5274, 2010.
62. Adachi, E., A. Dimitrov and K. Nagayama, "Stripe Patterns Formed on a Glass Surface during Droplet Evaporation", *Langmuir*, Vol. 11, No. 4, pp. 1057-1060, 1995.
63. Kuncicky, D. and O. D. Velev, "Surface-Guided Templating of Particle Assemblies Inside Drying Sessile Droplets", *Langmuir*, Vol. 24, No. 4, pp. 1371-1380, 2008.
64. Deegan, R. D., "Pattern formation in drying drops", *Physical Review E*, Vol.61, No. 1, pp. 475-485, 2000.
65. Deegan, R. D., O. Bakajin, T. F. Dupont, G. Huber, S. R. Nagel and T. A. Witten, "Contact line deposits in an evaporating drop", *Physical Review E*, Vol.62, No. 1, pp. 756-765, 2000.

66. Park, J. and J. Moon, "Control of Colloidal Particle Deposit Patterns within Picoliter Droplets Ejected by Ink-Jet Printing", *Langmuir*, Vol. 22, No. 8, pp. 3506-3513, 2006.
67. Smalyukh, I. I., O. V. Zribi, J. C. Butler, O. D. Lavrentovich and G. C. L. Wong, "Structure and Dynamics of Liquid Crystalline Pattern Formation in Drying Droplets of DNA", *Physical Review Letters*, Vol. 96, No. 17, pp. 177801, 2006.
68. Lockett, M. R. and L. M. Smith "Fabrication and Characterization of DNA Arrays Prepared on Carbon-on-Metal Substrates", *Analytical Chemistry*, Vol. 81, No. 15, pp. 6429-6437, 2009.
69. Heim, T., S. Preuss, B. Gerstmayer, A. Bosio and R. Blossey, "Deposition from a drop: morphologies of unspecifically bound DNA", *Journal of Physics: Condensed Matter*, Vol. 17, No. 9, pp. S703, 2005.
70. Nellimoottil, T. T., P. N. Rao, S. S. Ghosh and A. Chattopadhyay, "Evaporation-Induced Patterns from Droplets Containing Motile and Nonmotile Bacteria", *Langmuir*, Vol. 23, No. 17, pp. 8655-8658, 2007.
71. Baughman, K. F., R. M. Maier, T. A. Norris, B. M. Beam, A. Mudalige, J. E. Pemberton and J. E. Curry. "Evaporative Deposition Patterns of Bacteria from a Sessile Drop: Effect of Changes in Surface Wettability Due to Exposure to a Laboratory Atmosphere", *Langmuir*, Vol. 26, No. 10, pp 7293-7298, 2010.
72. Deegan, R. D., O. Bakajin, T. F. Dupont, G. Huber, S. R. Nagel and T. A. Witten, "Capillary flow as the cause of ring stains from dried liquid drops", *Nature*, Vol. 389, No. 6653, pp. 827-829, 1997.
73. Hu, H. and R. G. Larson, "Marangoni Effect Reverses Coffee-Ring Depositions", *The Journal of Physical Chemistry B*, Vol. 110, No.14, pp. 7090-7094, 2006.
74. Verwey, E. J. W. and J. Th. G. Overbeek, "Theory of the stability of Lyophobic Colloids", Elsevier, Amsterdam, 1948.

75. Bhardwaj, R., X. Fang, P. Somasundaran and D. Attinger, "Self-Assembly of colloidal particles from evaporating droplets: Role of DLVO interactions and proposition of a phase diagram", *Langmuir*, Vol. 26, No. 11, pp. 7833-7842, 2010.
76. Kollar, R., E. Petrakova, G. Ashwell, P. W. Robbins and E. Cabib, "Architecture of the yeast cell wall: The linkage between chitin and $\beta(1,3)$ -glucan", *The Journal of Biological Chemistry*, Vol. 207, No. 3, pp. 1170-1178, 1995.
77. Lipke, P. N. and R. Ovalle, "Cell Wall Architecture in Yeast: New Structure and New Challenges", *Journal of Bacteriology*, Vol. 180, No. 15, pp. 3735-3740, 1998.
78. Ahimou, F., F. A. Denis, A. Touhami and Y. F. Dufrene, "Probing Microbial Cell Surface Charges by Atomic Force Microscopy", *Langmuir*, Vol. 18, No. 25, pp. 9937-9941, 2002.
79. Narong, P. and A.E. James, "Effect of pH on the ζ -potential and turbidity of yeast suspensions", *Colloids and Surfaces A: Physicochemical and Engineering Aspects*, Vol. 274, No. 1-3, pp. 130-137, 2006.
80. Tazhibaeva, S. M., K. B. Musabekov, A. B. Orazymbetova and A. A. Zhubanova, "Surface Properties of Yeast Cells", *Colloid Journal*, Vol. 65, No. 1, pp. 122-124.
81. Picknett, R. G. and R. Bexon, "The evaporation of sessile or pendant drops in still air" *Journal of Colloid and Interface Science*, Vol. 61, No. 2, pp. 336-350, 1977.